Master Thesis

zur Erlangung des akademischen Grades eines

Master of Science

der Studienrichtung Earth Science
an der University of Graz

über das Thema

Morphological Evolution of the Gurktaler Alps

Betreuer: Kurt Stüwe

von

Thorsten Bartosch

Weizbergstraße 34/8
8160 Weiz

Graz, June 2018

Acknowledgement

In particular, I want to thank my supervisor Kürt Stüwe. Besides important discussions for my understanding of the local neotectonics, which took me some time to develop, we had inspiring trips in the Gurktaler regions, where we got to know each other on a private level. Thank you for that! I kindly thank Jochen Schlammberger from GIS Kärnten for his provision of the shape-file of the 1:200.000 geology from the Kärnten Atlas portal (GeoServies-KAGIS, 2017). This data was very helpful due to the scarcity of available resources. Beyond that, my special thanks are attributed to my partner Irmgard Reisinger. She patiently supported me during my studies for many years. In particular, she accompanied me during most of my field trips also facilitating my work by being my driver.

Abstract

Studies in the non-glaciated parts of the Eastern Alps have revealed the existence of Miocene relict landscapes in the Palaeozoic of Graz and the Koralpe. These relic landscapes provide proxies for uplift of the Eastern Alps that cannot be derived from the glacially overprinted majority of landforms in the range. In order to extend this dataset from the eastern end of the range toward the west, this thesis performs a geomorphic analysis of landforms in the Gurktaler Alps. The Gurktaler Alps are the westernmost never glaciated region of the Eastern Alps and lie in close proximity to the central alpine orogenic wedge. Topographic heights about 2000 m and above can be found. Therefore, information on surface uplift more close to the wedge building process can be obtained.

Four palaeo-surfaces were identified by geomorphological fieldwork and river profile analysis. All four levels lie below the well-known Nockfläche (at 1700-2200 m) and above present day base level (at 300 m). These planation levels are termed L1 - L4. They start with the lowest level at 750-850 m, followed by two intermediate levels at 800-950 m and 900-1300 m and finally end with the level above 1200 m, which is the highest level below the Nockfläche surface, that is unrelated to glacial processes. From the elevations of these planation levels above the present day base level uplift and associated incision is inferred to be 181 m for level L1, 337 m for level L2, 421 m for level L3 and 699 m for level L4. This result was interpreted as various stages of an uplift history in the region. Therefore, in total, a maximum uplift proxy of 700 m is measured.

Due to the Görschitztal and the Pöls-Lavanttal fault, a direct comparison with known planation levels from the eastern end of the Alps seems not possible. However, using a relative correlation technique, the lowermost levels L1 - L3 in the Gurktaler region show plausible relations with

the Stadelberg (3 Ma), the Hochstraden (3.4-4 Ma) and the Trahütten (4-5 Ma) levels in the Koralpe and the Styrian Basin. Therefore, an average uplift rate of approximately 84 m/Ma is estimated for the Gurktaler Alps since the Lower Pliocene.

Zusammenfassung

In nicht vergletscherten Teilen der Ostalpen haben Studien die Existenz von miozänen Reliktlandschaften im Grazer und Koralpe-Paläozoikum nachgewiesen. In diesen Reliktlandschaften lassen sich Proxys für die Anhebung der Ostalpen messen, die sich im Allgemeinen aus glazial überprägten Landschaftsformen nicht ableiten lassen. Um diesen Datensatz vom östlichen Ende des Verbreitungsgebiets Richtung Westen zu erweitern, wird in dieser Arbeit eine geomorphologische Analyse von Landformen in den Gurktaler Alpen durchgeführt. Die Gurktaler Alpen sind die westlichste, niemals vergletscherte Region der Ostalpen und liegen in unmittelbarer Nähe zum zentralalpinen Orogenkeil. Topographische Höhen um die 2000 m und darüber kommen vor. Daher können Informationen zur Hebungsgeschichte der Ostalpen in direkter Nähe zum Gebirgsbildungsprozeß gewonnen werden.

Durch geomorphologische Feldarbeit und Flussprofilanalyse konnten in Summe vier Paläoverebnungsflächen identifiziert werden. Alle vier Ebenen liegen unterhalb der bekannten Nockfläche (bei 1700-2200 m) und oberhalb des heutigen Basisniveaus (bei 300 m). Diese Ebenen werden als L1 - L4 bezeichnet und sind nicht durch glaziale Prozesse entstanden. Sie beginnen mit dem niedrigsten Niveau bei 750-850 m, gefolgt von zwei Zwischenebenen bei 800-950 m und 900-1300 m und enden schließlich bei dem Niveau über 1200 m, welches das höchste Niveau unterhalb der Nockfläche ist. Ausgehend von den Höhen dieser Verebnungsstufen in Bezug auf heutige Basishöhen, wird eine Anhebung und ein damit verbundener Taleinschnitt mit 180 m für das Niveau L1, 345 m für das Niveau L2, 427 m für das Niveau L3 und 699 m für das Niveau L4 ermittelt. Dieses Ergebnis wurde als sukzessive Phasen einer Hebungsgeschichte in der Region interpretiert. Daher wird insgesamt eine maximale Hebung der Oberfläche von 700 m interpretiert.

Aufgrund der Görschitztal- und der Pöls-Lavanttal-Verwerfung scheint ein direkter Vergleich mit bekannten Verebnungsniveaus vom östlichen Ende der Alpen nicht möglich. Die untersten Ebenen L1 - L3 in der Gurktalregion zeigen jedoch anhand relativer Höhenkorrelationen plausible Beziehungen, zu den in der Koralpe und im Steirischen Becken gelegenen Ebenen Stadelberg (3 Ma), Hochstraden (3.4-4 Ma) und Trahütten (4-5 Ma). Seit dem Untern Pliozän ergibt sich damit eine mittlere Hebungsrate von 84 m/Ma in den Gurktaler Alpen.

Contents

1. Introduction

In the Alps, there is an active debate on the question if some of the major morphological metrics of the topography are shaped by glacial processes during the glaciation periods of the last million years, or if they represent relics of Miocene landforms, that could then be interpreted in terms of the landscape evolution of the Alps since the Oligocene (Hergarten et al., 2010; Robl et al., 2017). In order to contribute to this debate, it is useful to study areas where glaciated and never glaciated mountains of otherwise similar climatic and geological characteristics exist in close spatial proximity, see Fig. 1.1. The Gurktaler region of the Eastern Alps is such a region and the documentation and interpretation of its geomorphology is the focus of this thesis.

During the Last Glacial Maximum (LGM), see e.g. Van Husen (2011), the Gurktaler region represented an ice-free oasis that was largely surrounded by glaciers. It is, therefore, an ideal region to document relics of the Miocene landscape. The Gurktaler region also has a second trait: It is the westernmost region of the eastern Alps that remained ice-free during the LGM and includes some of the highest never glaciated peaks of the entire mountain range as can be seen in Fig. 1.1. The region is therefore useful to trace Pre-Pleistocene uplift events that have recently been documented at the eastern end of the Alps (Legrain et al., 2014; Wagner et al., 2010) further toward the west. The purpose of this thesis is therefore twofold: Firstly, it is the aim to document morphological metrics in the Gurktaler region near the edge of the frontier of the LGM icecap in order to provide data that can be compared with glacial landforms further west. Secondly, it is the aim of this thesis to interpret the mapped landforms in terms of a Miocene landscape evolution of the region.

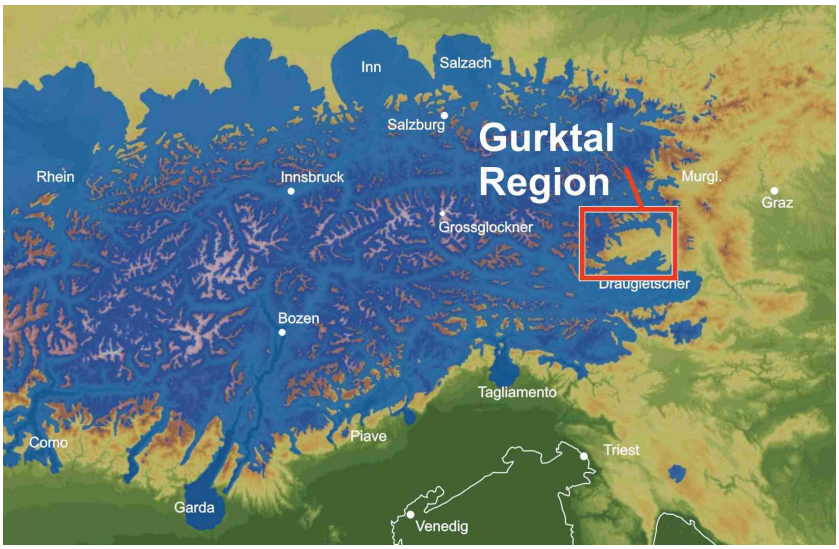

Figure 1.1.: Glaciation of the Eastern Alps during the last galcial maximum (LGM).

1.1. Landscape Evolution of the Eastern Alps

In general, the morphological evolution of the Eastern Alps is believed to have started in the Oligocene from a flat lowland topography and considered to have evolved more or less continuously according to Frisch et al. (1998). This interpretation is based on the age of the oldest sediments in the molasse foreland basins (Kuhlemann and Kempf, 2002; Kuhlemann et al., 2006), on abundant geo-chronological information from both detritus and basement studies (Spiegel et al., 2001; Wölfler et al., 2012) and on some indirect evidence from palaeo-surfaces, in particular, the elevated karst plateaus of the Northern Calcareous Alps at around 2000 m surface elevation (Tennengebirge, Dachstein, Hochschwab), where sedimentary remnants of a braided river system (Augenstein Formation) are still preserved (Frisch et al., 2001).

Besides the relic plateaus on top of the NCA about 1500 m above the current base levels, there is a series of other palaeo-surfaces that have been recognised in the basement parts of the Eastern Alps. In the never glaciated parts of the Alps these are the palaeo-surfaces of the Koralpe and the Grazer Bergland (Legrain et al., 2014; Wagner et al., 2010). In the glaciated parts of the Eastern Alps an example is the Nockalm surface (Exner, 1949). I begin with a summary of the state of knowledge of the landscape evolution of the Eastern Alps since the Miocene.

These elevated low relief areas are partly dissected by steep rivers flowing through narrow gorges and occur in many parts of the glaciated and the non-glaciated Eastern Alps (e.g. Ramsau near Schladming (Keil and Neubauer, 2011); Grazer Bergland; Salzach catchment. Today's topography is – at first sight – dramatically different between glaciated and unglaciated parts of the Eastern Alps. In the glaciated part of the Eastern Alps glacial landforms such as cirques, horns, glacial troughs and lakes mark the Pleistocene landscape transformation from a fluvial to a glacial appearance (Van Husen, 1987). Hanging valleys and associated knick points in channels are attributed to glacial lowering of the trunk valleys and the formation of cirques seems to be responsible for the observed hypsometric maximum at or above the LGM equilibrium line altitude (ELA) Robl et al. (2015). In the light of this intense landscape reconstruction, it appears to be fairly straightforward that researchers question the persistence of pre-glacial landscape characteristics. However, at the unglaciated eastern fringe of the Alps, elevated relict surfaces are common in many regions, for example, the Hochschwab- and Koralpe region. There, the lower set of palaeo-surfaces mentioned above has been interpreted as evidence for an uplift of the region by at least 500 m between ca. 4 Ma Wagner et al. (2010, 2011); Legrain et al. (2014, 2015). This uplift event correlates well with timing and magnitude of uplift and erosion reported from the surrounding basins north and east of the Eastern Alps (Ebner and Sachsenhofer, 1995; Genser et al., 2007). However, it is yet completely unknown if and how far this tectonic signal reaches to the glaciated realm of the Alps.

The Nockfläche palaeo-surface is in close vicinity to the north-west of the investigation area. Remnants of Tertiary conglomerates with a red matrix in the Tamsweger Basin were already described e.g. by Aigner (1924); Zeilinger et al. (1999) in detail as a facies, derived from lake sediments and from running waters possibly shed from the south by various smaller tributaries due to its grain sizes, spatially separated distribution and its mica-schist and phyllitic clasts, providing a first idea of a Miocene peneplane - the Nockfläche - in the region.

Geomorphological field observations of Aigner (1922) revealed that the Gurktaler Alps decent within several steps toward the Klagenfurter Basin, suggesting a descending Piedmont-step landscape, which levels developed during phases of tectonic stasis (Spreitzer, 1932). A mapping of the glacially overprinted Nockfläche plateau between 1700-2200 m was first given by Exner (1949). This planation surface stretches from the west of the Katschberg fault up to the

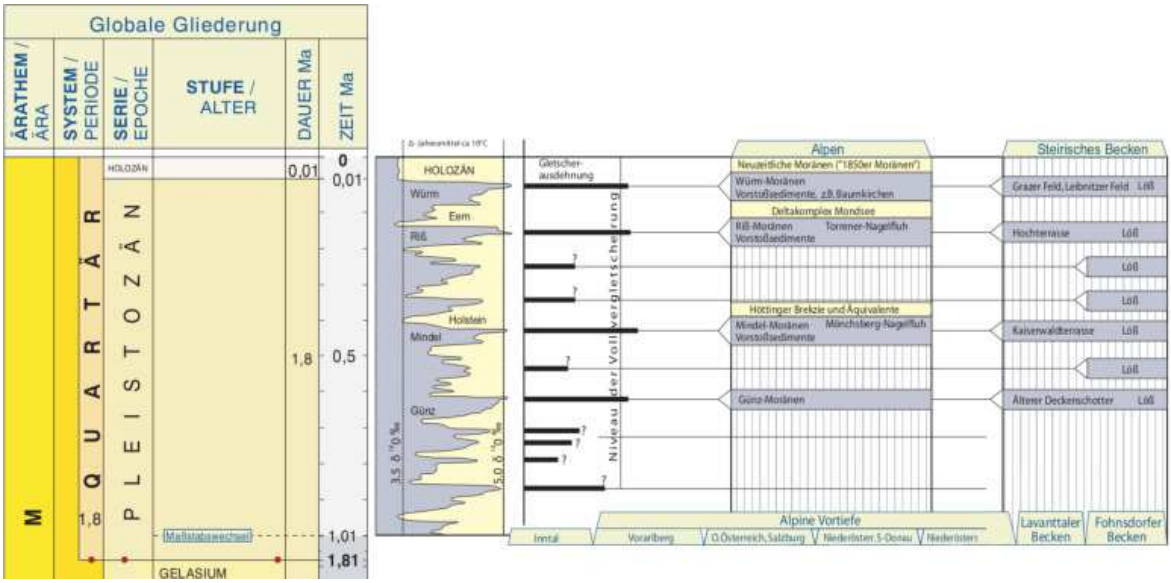

Figure 1.2.: Extraction of the Pleistocene part of the stratigraphic table of the Eastern Alps.

Flattnitz depression within the NW part of the Nockberge region. It consists out of hard-rock summit plateaus, e.g. the Aineck close to the Katschberg and large swampy peneplane with rarely preserved palaeo-soils (e.g. red loams) Exner (1989); Exner et al. (2005).

First Apatite fission-track thermochronology in the Gurktaler Alps provided landscape evolution models (Hejl, 1997, 1998; Reinecker, 2000). This studies touched the Gurktaler Alps on its northern (close to Turrach village) and western margin (close to Innerkrems village and Millstätter See), leaving out the core area of this investigation. Based on this thermochronological data a cooling history modelling suggests strong denudation with 87 m/Ma within the Early Miocene from 34-23 Ma, followed by a Mid Miocene phase of stasis, where probably the Nockfläche was denuded. Based on assumptions a final Plio- to Pleistocene uplift phase (≈4 Ma) is suggested.

1.1.1. Pleistocene Glaciation Events in the Alps

Much of the morphological evidence for the landscape forming events described above was overprinted by glacial carving during the glaciation periods (Fig. 1.2) in the Pleistocene to Quaternary. Within the last one million years four major cold periods with comparable extent

are depicted. These are the Würm, the Riß, the Mindl and the Günz glaciation events. For correlation of terraces the fluvioglacial stratigraphic sediment successions of the Alps and the Styrian basin are depicted. In general, fluvioglacial unconsolidated terrace sediments of the last two icing events, Würm and the Riß are correlated with the Niederterrasse and Hochterrasse.

The last glacial maximum (LGM) describes the maximum glaciation extent and was observed worldwide. It is of special interest in this work as non-glaciated river profiles need to be identified. From this profile segments, proxies for tectonic forcing are derived.

Van Husen (2011) provides an uncertain estimate for the beginning of the LGM about 21 ta before present, which is related to the climax of the Würm cold period. The first arrival of a glacier to the main longitudinal inner alpine drainage systems could be radiometrically dated to about 25-24 ta ago. Consequently, the valleys were overloaded by Vorstoßschotter out of unsorted coarse gravels. Van Husen (2011) estimates a period of stasis lasting about 4 ta before the retreat started about 17 ta ago.

The rather coarse LGM extent map in Van Husen (1987) and detailed maps from Van Husen (2012) were used as resources for a first overview of the glacial overprint in the investigated region of Gurktaler Alps. A modification based on morphometric and surface texture analysis in the region is suggested within this work.

1.1.2. The Gurktaler Block

The Tertiary orogeny of the Eastern Alps shows not only compressional processes between the European and the African plate. Gravitationally or tectonically controlled lateral extrusion in conjunction with normal faulting and strike-slip faulting is a dominating process observed in the Eastern Alps during the Miocene (Frisch et al., 1998; Neubauer and Genser, 1990; Ratschbacher et al., 1991; Linzer et al., 2002; Robl et al., 2008; Bartosch et al., 2017).

To the east of the Tauern Window, a set of conjugate strike-slip faults frame the so-called Gurktaler Block, which was normal faulted toward the SE in the Middle Miocene (Frisch et al., 1998; Reinecker, 2000; Wölfler et al., 2011). In Fig. 1.3A the DEM shows the area of relative subsidence, which is surrounded by the Prebersee and Seetaler faults (part of the

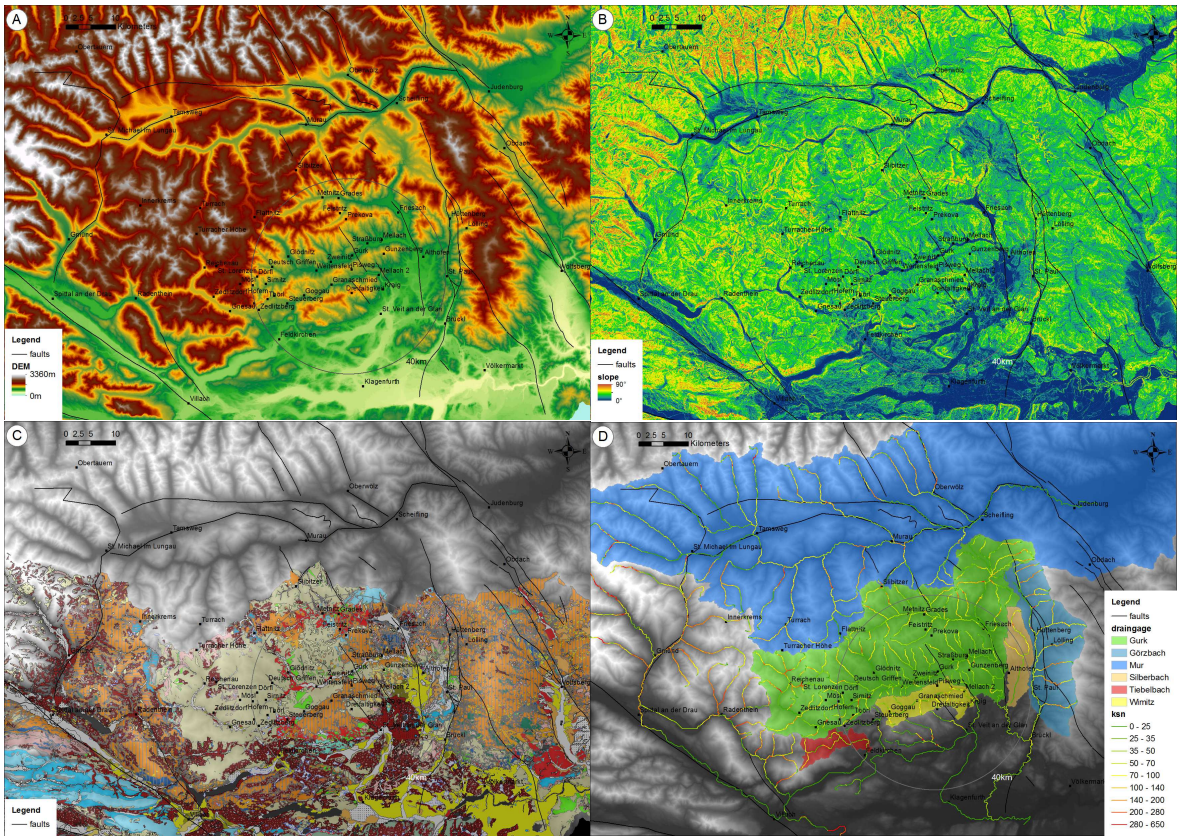

Figure 1.3.: Section of the Gurktaler Block. **A**: Shows the DEM of GeoServies-KAGIS (2015), **B**: Shows the slope map, **C**: Shows the geological map of Carinthia GeoServies-KAGIS (2017), **D**: Shows the drainage area of the important river systems based on pour point selection at 550 m altitude.

westernmost Mur-Mürz fault) to the north, the Radenthein and Katschberg fault to the west and the Görschitz and Pöls-Lavanttal fault to the east. Based on thermo-chronological and structural investigations Reinecker (2000) observed a change from strike-slip to normal faulting between Pre-Carpathian (17.2-16.5 Ma) leading to the uplift and high topography of the Niedere Tauern. Accordingly, a low topography within the Gurktaler Block developed. The calculated slope of the DEM in Fig. 1.3B shows an even more clear outline of the Gurktaler Block. Apparently, the slopes within the block are significantly lower indicating an erosion protected lower position, where lows might have been filled and steep slopes might have been prevented due to the lack of uplift. A lack of uplift was also detected by numerical thin viscous sheet modelling (England and McKenzie, 1983; England and Houseman, 1986) of the Eastern Alps in Klagenfurter Basin (Bartosch et al., 2017). This study reveals a basin build-

up since the Middle Miocene (20-15 Ma) in the Gurktaler Alps, despite the fact that fault systems, e.g. the Görschitztal fault were disregarded. This also coincides with apatite fission track cooling modelling by Hejl (1997, 1998) and Reinecker (2000) from the Western Gurktaler region, indicating the beginning of a stasis from Middle Miocene (24-16.5 M) until the Pliocene when uplift proceeded again.

In Fig. 1.3A in the SE side a strictly circular structure in the DEM of about 40 km diameter is observed. In the northern half, the height of this depression curbs down from approximately 1800-2200 m to 1200-1700 m in the Mödringberge, which is a mean delta of approximately 600 m height. To the west, the rim becomes visible between the SE Nockberge spanned by Mt. Kegel and Mt. Hochrindl and the Mödringberge. And to the east, the rim is defined by the Seetaler/Saualpe ridge. At the NE border, the elevation step is hardly visible due to the Mt. Dorferecken (1700 m) in the Obernhof window, which constitutes the highest summit within this circular Nockberge Senke. At the southern border, the rim disappears within the Klagenfurter basin. When the eastern border is excluded a comparison with the morphometric measures in Fig. 1.3A-D shows that the morphology correlates only with altitude. Interestingly the slop map, the lithology and fault systems are not defining this structure.

In particular, the slope map in Fig. 1.3B quite well identifies the Miocene normal faulting of the Gurktaler Block but not at all depicts structures of the Nockberge Senke. In addition, also morphometric proxies of river-profile analysis show no correlation with the pattern. In Fig. 1.3D, this is true for both the drainage areas and also $k_{sn}(\theta_{ref} = 0.45)$ values, showing differences in uplift or erosion. Therefore, the Nockberge Senke could not be explained with a different erosional/uplift history between the greater areas of the surrounding Gurktaler Block. It might be concluded, that this structure is older than the normal faulting of the Gurktaler Block and therefore older than Pre-Carpathian.

1.2. Geographical Setting

The Gurktaler Alps are a moderate mountainous area in the Eastern Alps in Central Carinthia. They are located between the Niedere Tauern and the Klagenfurter Basin in a north-south direction and between the Saualpe/Seetaler Alps and the eastern edge of the Tauern Window

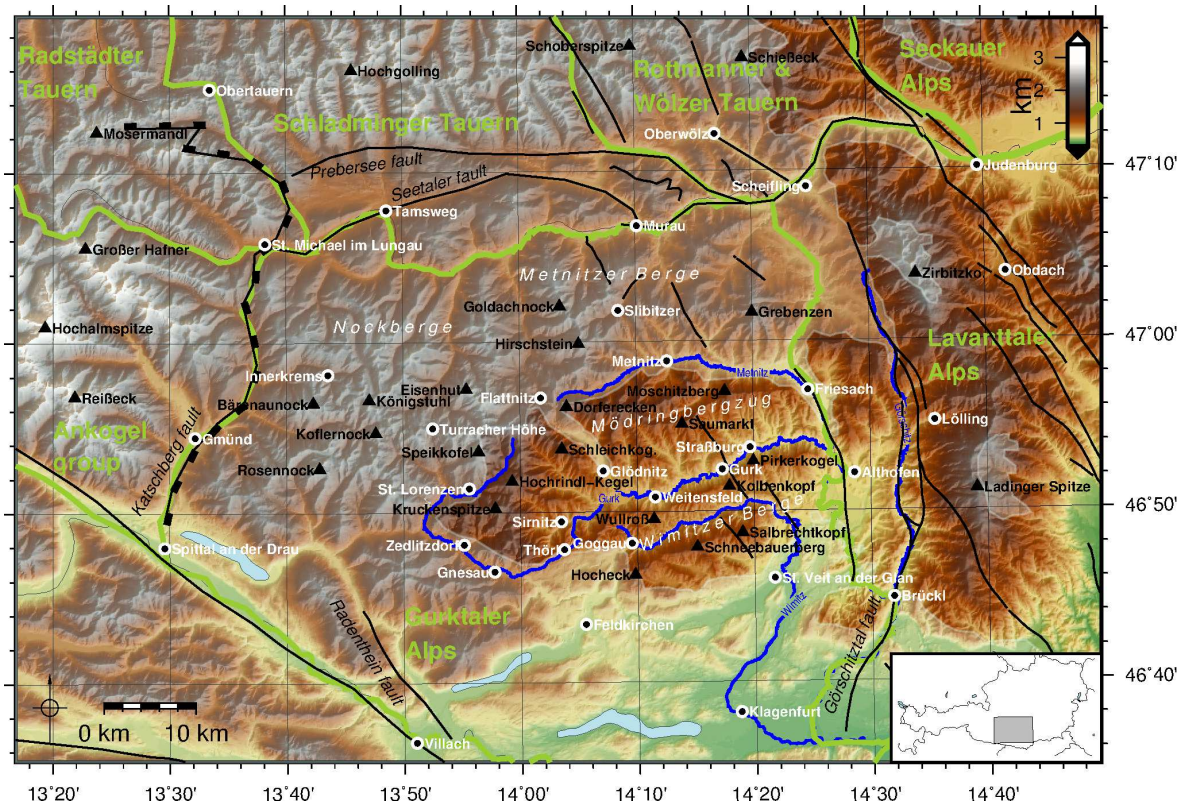

Figure 1.4.: Geographical overview of the Gurktaler Alps. Massif boundaries (green). Drainage systems (blue). Faults (black), LGM transparent polygon (Rocky Austria, Geologische Bundesanstalt, 2013).

in an east-west direction. The elevation in this region varies between 440 m at the Wörthersee and about 2400 m at the Mt. Rosennock and Mt. Eisenhut mountains in the NW of the region. Fig 1.4 show the topography based on GeoServies-KAGIS (2015) data and the approximate location within Austria in the inset map.

Major massifs are the Niedere Tauern to the north, consisting of the Radstädter, the Schladminger, the Rottmanner and Wölzer, and the Seckauer Tauern. The Tauern Window (Ankogel group) constitutes the margin to the west and the Lavanttaler Alps, consisting of the Saualpe and the Seetaler Alps to the east. To the souths the mountain heights curb down and vanish in the Klagenfurter Basin. The EW stretching Karawanken range at the Periadriatic suture line is bordering to the south.

The main trunks of the investigated river system (blue lines) and the maximum glaciation extent (LGM) after Rocky Austria, Geologische Bundesanstalt (2013) within the Pleistocene is mapped. In particular, the middle section of the Gurk River system, the upper Wimitz River

system and large parts of the Görschitz River systems belong to the non-glaciated areas.

In terms of drainage systems, the Gurktaler Alps are confined between the northern EW trending Mur River system with the cities Murau and Tamsweg in the catchment and the NW-SE to EW trending Drau River in the south, which passes the cities Villach and Klagenfurt. Both river systems were overprinted by large valley glaciers in the Pleistocene. To the west, the region is confined by the Lisa River, which drains through Gmünd in a southern direction, while the eastern margin is formed by the southward draining Görschitz River at the foot of the Seetaler/Saualpe ranges.

The Gurktaler Alps itself can be geographically divided into four distinct regions or sub-massifs. The western part of highest up to 2400 m high mountains from Mt. Rosennock to Mt. Eisenhut are called the Nockberge, which belong to the Biosphärenpark Nockberge. The term Nock is German slang and describes a rounded summit, which is a characteristic geomorphological feature of the whole region. Further to the east, the Gurktaler Alps are divided into three approximately EW trending massifs. The Metnitzberge in the north are symmetrically stretching for about 40 km perpendicular between the city Murau and the village Metnitz. The Mödringberge massif is extending for about 30 km between the villages Metnitz and Gurk and the southernmost Wimitzer Berge are formed by two ranges on the northern and southern side of the Wimitz River, namely the Zammelsberger Rücken and the Schneebauer Rücken. The southern part of the region up to the Drau River constitutes the Klagenfurter Basin.

1.3. Tectonic Evolution and Lithology

The alpine orogeny records two main wedge building tectonic phases between the stable European foreland and the African plate. The eo-alpine orogeny in the Cretaceous and the still ongoing alpine orogeny starting in the Eocene. Protoliths of the Eastern Alps are much older and date back into the Palaeocene.

During the Jurassic, intra-continental south directed subduction started inside the Adriatic plate. Uppermost parts like the Gurktaler nappes, the Northern Calcareous Alps and the

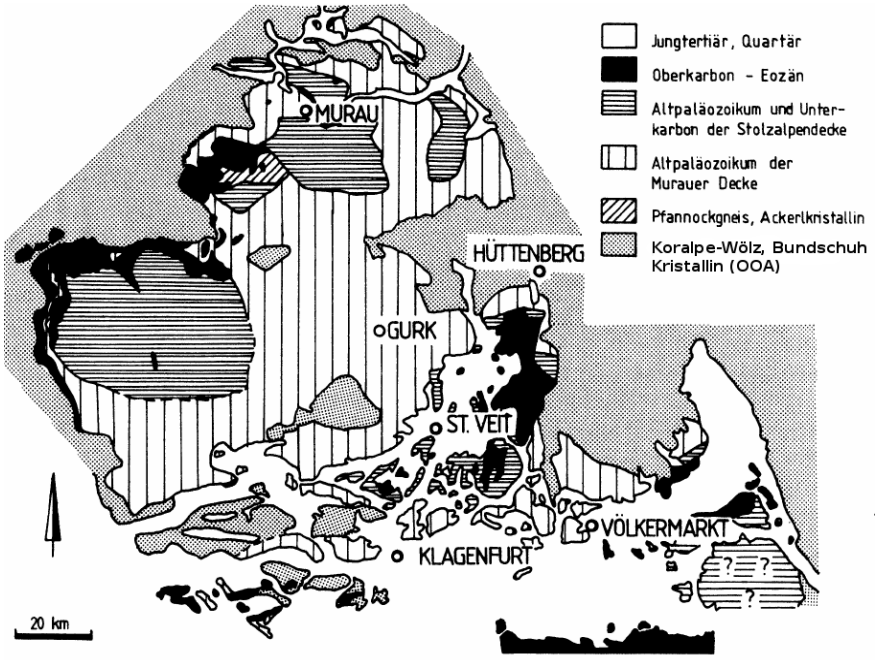

Figure 1.5.: Related Palaeozoic Gurktaler nappes, consisting out of the higher anchi- epi metamorphic Stolzalpen nappe and the lower epi-metamorphic Murauer nappe (Neubauer et al., 1997).

Palaeozoic of Graz were scraped off and transported toward the north where they formed the upper Austroalpine. Lower parts were deeply subducted and formed the high-grade metamorphic rocks from the underlying Bundschuh and Koralpe-Wölz nappe systems. A synopsis of the palaeogeographic evolution of the Eastern Alps is given in the appendix A.1.

The tectonic units of the Gurktaler Alps and its surroundings are shown in Fig. 1.5. All displayed units are accounted to the Upper Austroalpine basement nappes (Schmid et al., 2004). The recumbent nappe of the Gurktaler nappes is built out of polymetamorphic essentially amphibolite-facies crystalline rocks (Neubauer and Pistotnik, 1984). In particular, these are the Radenthein, Bundschuh, Seetaler, Koralpe-Wölz crystalline basements and the rather small Stangalm Mesozoic unit as a transgressive cover at the western margin of the Gurktaler nappes (Pistotnik, 1976).

The Early Palaeozoic Gurktaler nappe complex is divided into two tectonic sub-units, which were over-trusted onto the amphibolite-metamorphic basement described above. The shallow, higher temperate green-schist-metamorphic Murau nappe and the over-trusted Stolzalpen

nappe with varying metamorphic grade from shallow green-schist in the NW corner to anchi-epi zonal at the Saualpe margin (Neubauer and Pistotnik, 1984; Rantitsch and Russegger, 2000).

The stratigraphic classification of the Early Palaeozoic Murauer nappe is still debated and mostly described from data from the northern to western margin. According to e.g. Neubauer and Pistotnik (1984) three rock series are distinguished. Two of them form the fine-clastic series in the recumbent starting with Late Ordovician to Early Silurian dark metavulcanites (green-schists, prasinits), which are overlain by fine-clastic phyllites, phyllite-mica-schists, black shales, lime-phyllites to lime-schist covered by a quartzite horizon. In the upper series, rock types change from Late Silurian to Early Devonian Echinodermata bearing dolomite- and lime-marbles.

The overlapping Stolzalpen nappe starts with Late Ordovician volcanogenic strata - Magdalensbergfolge at the south-western foot of the Saualpe, Eisenhutschiefer at the north-western and shales at the northern margin. In general, the Ordovician and Silurian vulcanites are build out of fine-grained tuffits and ash-tuffits and sparsely distributed diabases, e.g. at the Enge Gurk close to Sirnitz (Neubauer and Pistotnik, 1984). At its NE margin, the volcanogenic strata and metadiabases are transgressively overlain by Upper Carboniferous sediments, which were inverted during the eo-alpine orogeny (Neubauer and Pistotnik, 1984; Von Gosen et al., 1987; Rantitsch and Russegger, 2000).

The Gurktaler nappes show a high correlation of rock type with the Palaeozoic of Graz. Its Silurian rock facies is supposed to be linked to shallow water siliciclastic environment, which later on in the Triassic became the southern margin of the Meliata-Hallstatt Ocean.

East of the Gurk River between Althofen and Weindorf the Upper Cretaceous Krappfeld-Gosau sediments are roofing the Gurktaler nappes (Neumann, 1989). On top of the basal layers consisting of dolomite conglomerates, most of the strata above are interpreted as a turbiditic facies out of lime-arenites to lime-sandstones. The Gosau nappe is underlain by Norian Hauptdolomit in the south - here a transgressive contact is preserved and most likely Early Palaeozoic rocks in the north.

2. Methods and Supporting Data

From July 2016 to September 2017 fieldwork was conducted within the Gurktaler Alps in order to record geology, geological structures and geomorphometric measures, which were derived from digital elevation model (DEM) analysis. This data is described in the following and was used to generate a new more refined outline of the LGM extent in the area of the Gurktaler Alps, which is depicted within the displayed maps in the sequel.

The method of river profile analysis constitutes one of the major tools used in this work and is therefore described in more detail in section 2.2. Numerical aspects and application notes are given in section 2.3.2

2.1. Outcrops of the Area

The river systems of the Gurk, the Wimitz, the Metnitz, the Görschitz and its surrounding drainage areas have been investigated in greater detail, as indicated by outcrop locations in Fig. 2.1. The transparent polygon in depicts the LGM extent according to the findings within this master thesis, which differs from the map in Rocky Austria, Geologische Bundesanstalt (2013) - compare to Fig. 1.4 - and slightly differs from the map given in Van Husen (1987).

The outcrops of all fieldwork are briefly described in the Tab. A.9-A.12. The gathered information contain lithology, structural data, geomorphological data and hydraulic discharges when available. Given discharges are approximated by guessing channel dimensions and averaged stream velocities. As already noticed by Van Husen (2012) it can be confirmed that the lower altitude area of the Gurktaler Alps, in particular within the lower regions inside the

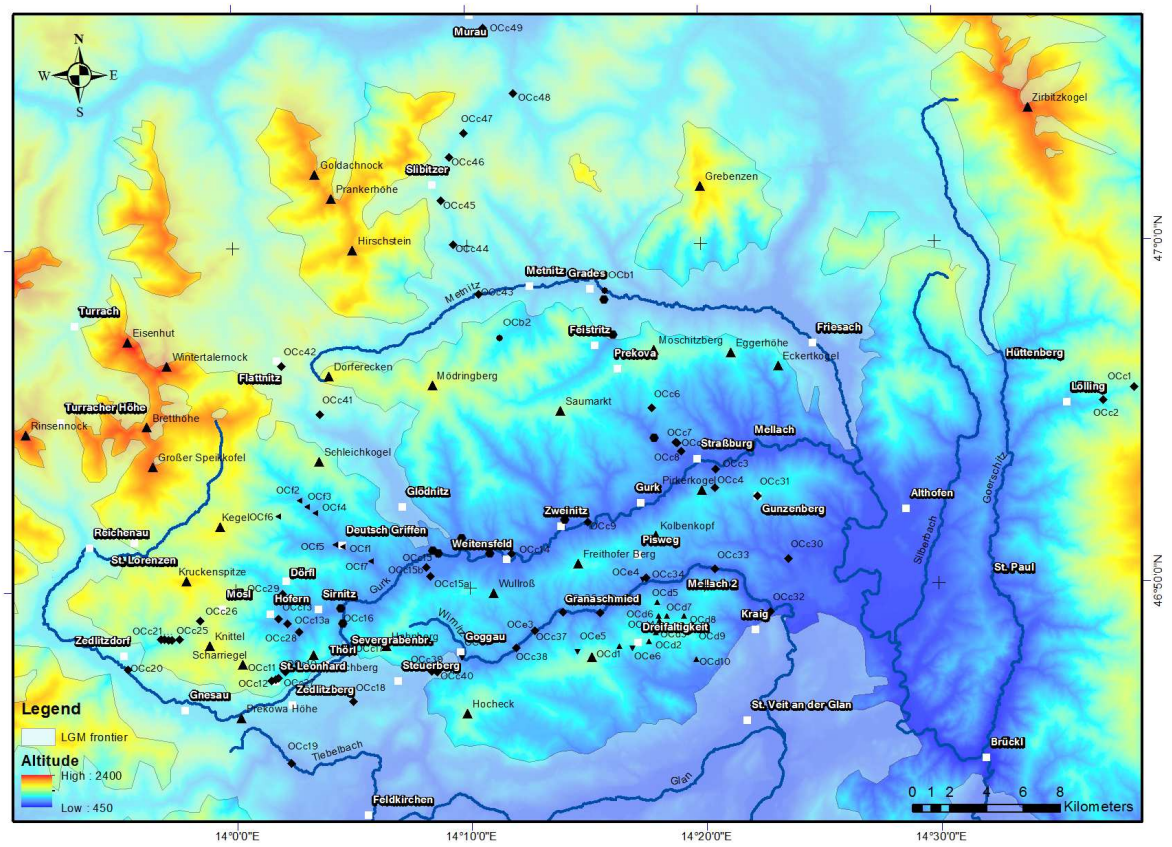

Figure 2.1.: Location of outcrops referenced by tour labels *OCa-f*, which are explained in Tab. A.9-A.12. The beige polygon shows the LGM extent.

Nockberge Senke shows a scarcity of geological outcrops. Most of the landscape is covered by unconsolidated sediments and soils.

2.1.1. Petrology and Geological Map

The availability of geological maps in the investigation area is limited to a few resources. Printed GBA maps (ÖK 1:50.000) are restricted to the 185-Straßburg map (Krenmayr et al., 2014), which covers a small area in the core region. The transition from the higher metamorphic crystalline basement to the Gurktaler nappes is displayed in the 157-Tamsweg map (Exner et al., 2005) in the NW corner and in the northern and southern Saualpe maps and 186-Sankt Veit an der Glan map at the eastern and southern border (Pilger et al., 1978; Thiedig et al., 1999). For Carinthia County, there is no printed GBA map 1:200.000 available, but via the

ATLAS online portal a 1:200.000 geological map is available. A related shapefile was provided by the Amt der Kärnter Landesregierung in Klagenfurt (Schlammberger J., pers. com., 2017). The legend was complemented with information from adjacent geological maps 1:200.000 of the counties of Styria and Salzburg (Flügel and Neubauer, 1984; Pestal et al., 2005). Relevant fault systems were digitalised from WMS Service, Geologische Bundesanstalt (2017).

2.1.1.1. Palaeozoic Rocks

The Gurktaler nappes in the investigated area are dominated by phyllites and quartz-phyllites - see Tab. A.9-A.12 - which is consistent with the geological map in Fig. 2.2. During the fieldwork found occurrences of subordinate rock types are described in the following.

Marble banks of up to 1-3 m thickness with imbrications of phyllites layers and an irregular interlayering of light-grey marbles in centimetre scale are rarely found. A small occurrence *OCc34* is located in the Wimitz valley at the northern roadside below Pisweg.

Compact dark-grey diabase occurs at *OCc26* below the saddle between Görzbachtal and Sirnitz valley, termed Hangschutt in the geological map of GeoServies-KAGIS (2017)). Further uphill green-schist debris and cobbles are found.

The base of the Braunsberg terrace just close to the bridge across the Gurk at *OCc15* exhibits strongly foliated and folded green-schists. In the upper Metnitz valley close to the *Obdach* window (*OCc41*) the phyllites are getting higher metamorphic, but are still considered to be phyllites.

2.1.1.2. Tectonic Windows

Within the Gurktaler nappes crystalline several tectonic windows are exhumed. They are briefly described in the following.

Around Oberhof in the Metnitztal the Oberhof Fenster cuts through the phyllites of the Gurktaler nappes, see Fig. 2.2. Large parts of this rock series termed Übergangsserie consists out of garnet-mica-schists, which constitutes a transition strata between the low-metamorphic

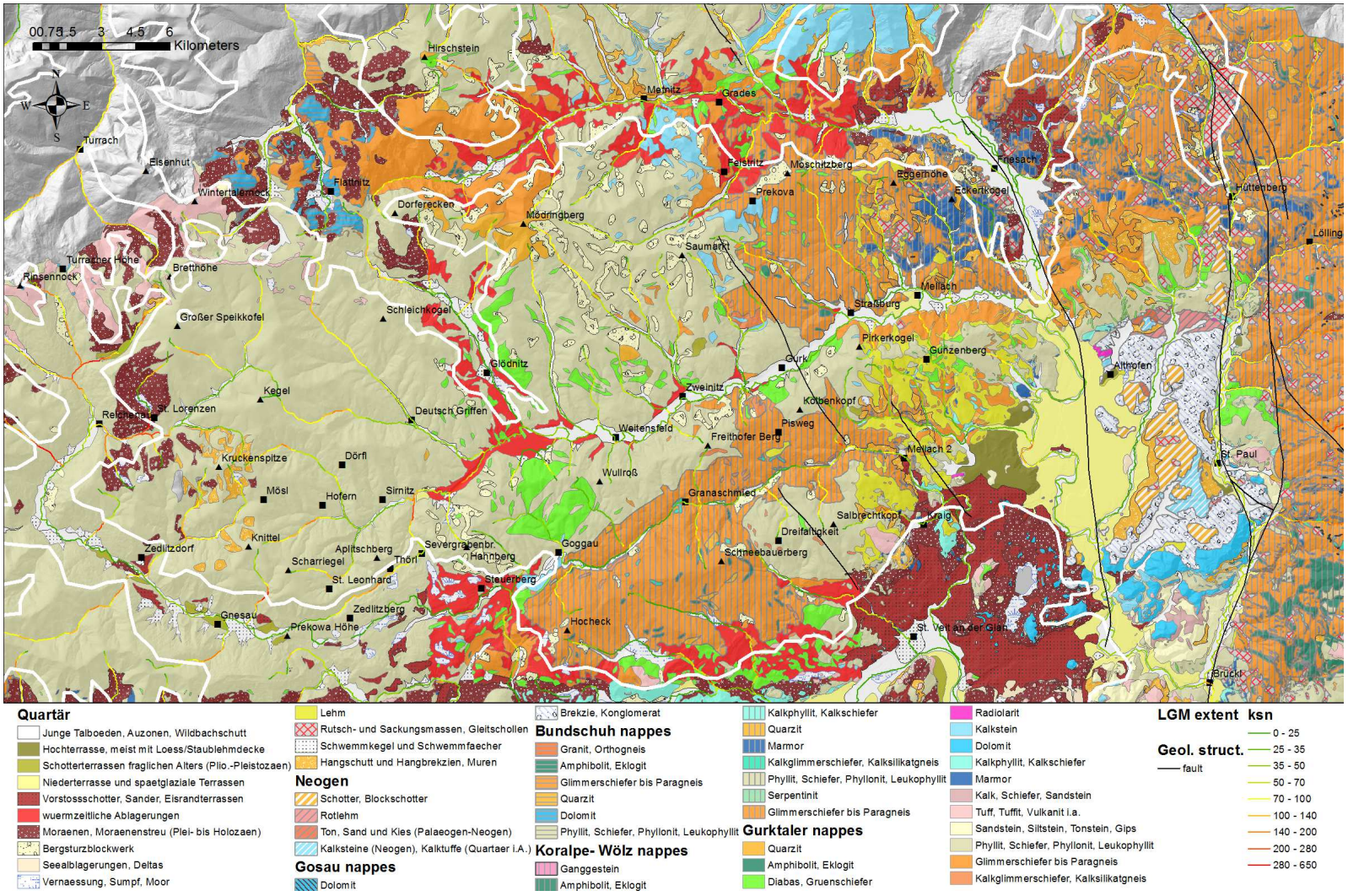

Figure 2.2.: Geological map of the Gurktaler Alps based on digital data provided by GeoServies-KAGIS (2017).

Gurktaler nappes and the medium-metamorphic recumbent Bundschuh crystalline (Von Gosen et al., 1985). According to the geological map in Fig. 2.2 this Übergangsserie is accounted to the Gurktaler nappe system. Within the Übergangsserie an amphibolite metamorphic core appears in small shaped lentil to the north of the Glanzer farm at Oberhof with Bundschuh crystalline parentage (Von Gosen et al., 1985).

Further 15-20 km to the ESE the Friesacher Halbfenster (Appold, 1989) is located. Leucocratic mica-schists are exhumed in the tectonic contact zone - Übergangsserie - between the phyllitic Gurktaler nappes and the recumbent Seetaler- Saualpe crystalline. In the map in Fig. 2.2 this unit is encountered to be part of the Saualpe- Seetaler nappe system. This lithological contrast from low to higher erodibility occurs in the Metnitz River systems between Mellach and Grades and in the middle Gurk valley just two kilometres downstream of the Gurk village.

About ten kilometres to the south the Wimitz Fenster dominantly mica-schists of the Saualpe crystalline are exhuming.

2.1.1.3. Palaeogene to Quaternary Sediments

Sediments related to the Miocene and the glacial history of the study region are mapped in several isolated places throughout the Gurktaler Alps. For example, west of Klein St. Paul the Fig. 2.2 shows Neogene unconsolidated sediments and some isolated Eocene limestones close to the Dobranberg, which are solely mapped in the region between the lower Gurk drainage below Althofen and the Görschitz River at the foot of the Saualpe, constituting a lithological change along the Gurk and Görschitz rivers.

Neogene red loam, which is assumed to relate to typical Mid Miocene Nockfläche palaeo-soil sediments (Exner, 1949), are found at the northern border of the Althofen Basin (Fig. 2.2), but are also observed at its SW margin in the vicinity of Gunzenberg within widespread occurrences of Quaternary loams. In addition, fluvial rounded quartz-rich gravels are reported to occur in the proximity of Pisweg close to the pass in the Wimitzer Berge (Neubauer F., pers. com., 2018).

Pleistocene Higher and Lower Sanders terraces are depositioned to the south of Friesach. Within the Althofen Basin, several Niederterrasse levels with steps in the range of 2-5 m are overlapping. Remnants of a Rißian Hochterrasse are isolated in an area east of Meiselding at a height of 603-370 m only. Connecting to the north and west of the Hochterrasse Quaternary loams are adjoining.

The Würmian Niederterrasse sediments are by far more widespread. They range from altitudes around 830 m at both sides of the Gurk River at Althofen castle close to Sirnitz, further down at the left bank of the Gurk short before Mellach (635-660 m) and within vast areas extending to both sides of the Gurk River bank below the junction with the Metnitz River (640-550 m).

Of high interest is the location of the Schotterterrassen fraglichen Alters within the Gurktaler tributaries. There are tiny remnants located two kilometres east of the Mt. Kolbenkopf in the Wimitz River system (865 m altitude) and also on the northern side of the Gurk River bank between Weitenfeld and Gurk (940 m altitude). These strata are again found in an already pre-glaciated area in the upper Gurk River system upstream of the Prekowa Höhe up to the Saureggenbach starting from a height about 970 m up to 1570 m. These terraces indicate palaeo-water levels and therefore support the hypothesis of later on claimed palaeo-planation surfaces.

In Fig. 2.2 a clear correlation with the deposition of Vorstoßschotter, Sander, Eisrandmoränen, würmzeitliche Ablagerungen and Moränen, Moränenstreu and the margins of the LGM, which is displayed as a thick solid line in the map can be observed. In question is an area NE of Reichenau (upper Andertal valley), were Plio- to Pleistocene Moränen, Moränenstreu is mapped clearly outside the LGM extent.

2.1.2. Structural Analysis

The structural measurements of foliation surfaces within the Nockberge Senke and the two profiles across the rim to Zedlitzdorf and to Murau are analysed. Only the data (Tab. A.9 - A.12) with high confidence for outcropping bed-rock and only data not belonging to apparent folds was used. The measurement quality within the phyllites is problematic due to small scale

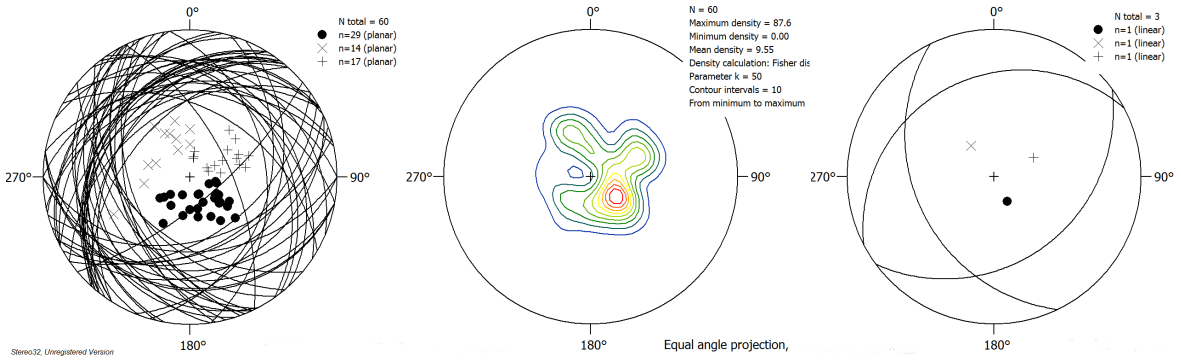

Figure 2.3.: Cluster analysis of foliation planes measured in the Nockberge Senke region. Left-hand side foliation planes, middle figure density plot of surface poles and right-hand side the mean surface poles of the three clusters.

to large scale deformation in addition to jointing and partly strong weathering, which is very common in the area.

The structural data from Tab. A.9-A.12 is shown (Fig. 2.3) within an equal angle lower hemisphere projection. In total there are 60 datasets of foliation planes depicted in the left-hand picture. These data are found to cluster within three regions, which is identified in the density plot in the middle figure. Based on a k-means clustering algorithm, where $k = 3$ was chosen three dominant foliation planes in the right-hand picture were analysed. The direction (332/22) sf with 29 measurements - biggest fraction - is consistent with a general known nappe thrusting direction in NW direction, when the foliation plane is assumed to be parallel to the Upper Cretaceous detachment thrust/normal faults. Most of the data within this cluster are located between the Metnitztal and Murau at the northern part of the rim and also in the Saualpe, which is already outside the Gurktaler nappes. A second set of directions at (143/29) sf with 14 measurements is approximately perpendicular to the first set, while a third set with 17 measurements clusters around (244/33) sf. Apparently, the first and second set could constitute a large scale fold. But on the other hand, the spatial distribution of the directions do not provide a clear picture.

Besides the framing fault systems around the Gurktaler Block (section 1.1.2) smaller faults within the Gurktaler nappes were sampled from the OneGeology project (WMS Service, Geologische Bundesanstalt, 2017) and completed with east-west trending fault data from the

Murtal out of Reinecker (2000).

A nameless NNW directed fault is mapped in the middle Gurk valley crossing east of Gurk. According to later on presented river profile analysis activation proxies are still observable. To the south, two small fault lines of comparable orientation are crossing the Wimitz Berge. Further to the east along the Metnitz and Gurk valley another fault line stretches in a north-south direction through the Althofen Basin and will, therefore, be termed Althofen fault in the sequel. At the western boundary of the map the Görschitz fault system trends in NS direction. The Krappfeld-Gosau basin is bounded by the Görschitz and the Althofen fault indication at least an Upper Cretaceous age of these faults. Due to river profile analysis, the Görschitz fault at the foot of the Saualpe turns out to be a still active fault.

2.2. Introduction to Stream Power Analysis

In fluvial regimes, channel profile analysis turned out to be an important tool for interpreting the geomorphology of landscapes in terms of tectonics. By heuristically analysis channel geometries were found to be related to hydraulic properties when stable fluvial channel profiles and purely erosive transportation processes can be assumed. The expansion to the non-stationary stream power equation makes it possible to link erosion and uplift kinematics to properties of river profiles when equilibrium can be assumed. It is important to have in mind that this link between channel geometry and vertical tectonics is only true for the linear geometry of a river bed. The remainder topography is subject to additional processes, e.g. slope stability, debris flow, landslides, solifluction, pedogenesis and protection by vegetation. In the following important hydraulic channel geometry equations and the non-stationary stream power equations are reviewed.

2.2.1. Hydraulic Channel Geometry

In channel profile analysis typically two distinct view point are applicable for a stable channel geometry (Eaton, 2013). *At-a-station* relations describe fluvial hydraulic river geometry properties like

W channel width in [m]

S slope in [m/m]

D mean hydraulic depth in [m]

V mean velocity in [m/s]

Q discharge in [m^3/s]

at a defined spatial location at a river, which typically also corresponds to a gauging station. In Lacey (1930) a power law assumption $W \propto Q^{1/2}$, $d \propto Q^{1/3}$, $S \propto Q^{1/6}$ was derived for unlined canals, while Leopold and Maddock (1953) related a slightly different set of hydraulic geometry parameters in order to apply for alluvial streams:

$$W = k_a Q^b, \tag{2.1a}$$

$$D = k_c Q^f, \tag{2.1b}$$

$$V = k_k Q^l, \tag{2.1c}$$

for unlined irrigation canals with the parameters $b = 0.26$, $f = 0.4$ and $l = 0.34$. Substituting eq. (2.1a,b,c) into the definition of the discharge results in

$$Q = W \cdot D \cdot V = k_a \cdot k_c \cdot k_k \cdot Q^{b+f+l} \quad \longrightarrow a \cdot c \cdot k = 1,\ b + f + l = 1. \tag{2.2}$$

At-a-station relation require a stable canal geometry and are describing how a discharge is accommodated with respect to canal shape and flow velocity.

On the other hand, the *downstream* relations are relating the hydraulic channel geometry to a *formative* discharge. In this sense, a channel describes natural waterways (open channel flows) and the term *formative* discharge indicates that a channel forming process will be linked with channel geometry. Two concepts of a *formative* discharge (Eaton, 2013) are existent.

Effective flood: means the effective discharge of a flow that is frequent and powerful enough to do most of the geomorphic work.

Bank-full flood: is a morphological definition and describes the elevation of the flood-plain. It is based on the fact that once when the water level reaches the bank-top the flood reaches out into the flood-plain and the water depth will only marginally increase. Therefore the bottom shear stress will also increase marginally.

According to Eaton (2013), the bank-full concepts is limited to self-formed floodplains, which are neither actively aggrading nor degrading.

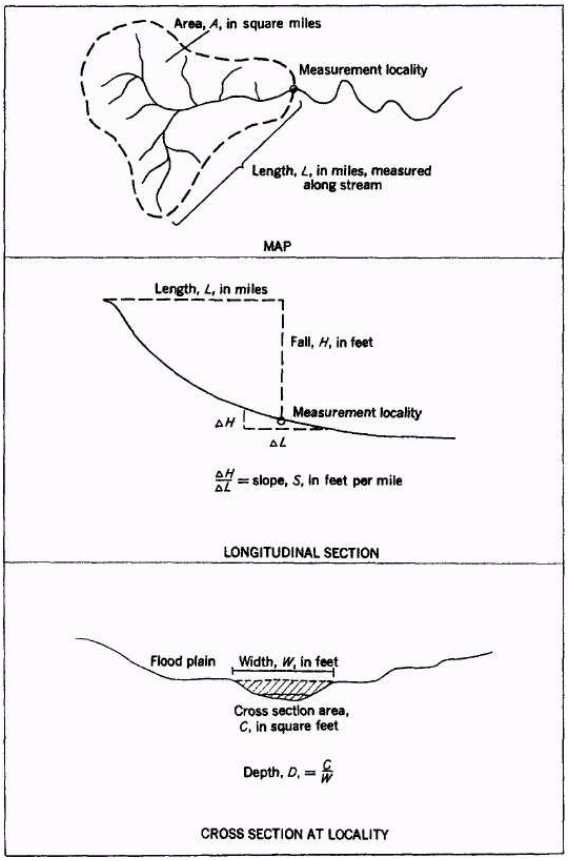

Figure 2.4.: Channel parameters (Hack, 1957).

2.2.2. Fluvial Bedrock Erosion

In Howard and Kerby (1983) morphometric studies of fluvial erosional processes acting over a seven year lasting period within a rather small scale borrow-pit were conducted. They showed that an erosion model based on shear stress was most suitable to describe the genesis of river profiles. Their regression analysis on the model parameters revealed differences between alluvial sand-bed channels and bed-rock channels. The former were distinguished in the field by flat valley slopes and unstable river banks associated with the build-up of winter terraces having its maximum extent in the late winter/early spring and showing low erosional resistance. This terrace aggradation process was associated with mass wasting processes like rain splash and surface run-off erosion, which efficiently decreased the valley slopes, but still an overall small channel incision process was noticeable. On the other hand, bed-rock erosion with no alluvial sediment deposition was observed in river segments with steeper and more stable river bank incisions with steeper valley slopes. The maximum transport load capacity was above the actual loads within this sections leading to degradation and incision processes.

In Whipple and Tucker (1999) the detachment-limited fluvial bed-rock incision model, which was already successfully applied by Howard and Kerby (1983) is given by

$$\epsilon(x) = k(x) \cdot A(x)^m \cdot S(x)^n, \tag{2.3}$$

with the erosion ϵ in [L/T], the erodibility k as a dimensional constant [L^{1-n-2m}/T^{1-n}], the drainage area A in [L^2] and the profile gradient S in [L/T] as displayed in Fig. 2.4. The coordinate x constitutes a linear length variable (projected onto a ground level), which decreases toward the channel heads. For bed-rock channels in bad-lands Howard and Kerby (1983) estimated $m = 4/9$ and $n = 2/3$ as a most fitting estimate.

According to e.g. Howard and Kerby (1983); Whipple and Tucker (1999) eq. (2.3) can be derived from the shear stress erosion model

$$\epsilon = k_b \tau_b^a. \tag{2.4}$$

with the shear stress τ_b in [M/L/T^2] at the river bed and a dimensional total erodibility constant k_b in [$M^{-a}L^{1+a}T^{2a-1}$] and the shear stress exponent a. k_b is sensitive to rock quality in terms of lithology, jointing and weathering, the amount of loaded sediments (depending on Q) and the prevailing erosional process, while a mainly depends on the process and is reported to vary between $1 < a < 3.5$ according to plucking, abrasion or cavitation erosive processes.

With the hydraulic channel geometry equations in eq. (2.1), which are interpreted as at least annual and cross-sectional averages the shear stress can be estimated out of a stationary (no acceleration forces) consideration between the bed-rock shear stress, which is the only counterpart of the tangential momentum of the water load within the volume $W \cdot D \cdot L_{seg}$ due to the slope angle β ($S = \tan(\beta) \approx \sin(\beta)$). The shear stress is then defined as

$$\tau_b = F_t/W/L_{seg} \approx \rho \cdot g \cdot D \cdot S. \tag{2.5}$$

In Whipple and Tucker (1999) a parameter identification shows the equableness of both models in eq. (2.3) and eq. (2.4), but for simplicity this work here stays with the parameters in eq. (2.3).

2.2.3. River Profile Evolution Model

When considering vertical time depended dynamics within the lithosphere, the topographic height $h(x,t)$ of a landscape basically is a result of two processes. On one hand side, tectonic forcing results in vertical uplift/subsidence rates u in [L/T], which are movements of

rock particles relative to a fixed reference level (geoid). On the other hand, exhumation (erosion)/burial rates ϵ in [L/T] are processes relative to the earth surface. The vertical dynamics of the lithosphere surface elevation $h(x,t)$ relative to a fixed reference surface is altered by both processes and need to be described by, e.g. Stüwe (2007)

$$\frac{\partial h(X,Y,t)}{\partial t} = u(X,Y,t) - \epsilon(X,Y,t), \tag{2.6}$$

where the uplift rate $u(X,Y,t)$ is negative for directions toward the earth centre and X,Y are projected surface coordinates. In Kirby and Whipple (2001); Kirby et al. (2003); Wobus et al. (2006); Hergarten et al. (2016) the river profile erosion model of eq. (2.3) is substituted in eq. (2.6). Due to the restriction of the spatial domain of the model eq. (2.3) to linears, the coordiante x needs to be used instead of X,Y.

$$\frac{\partial H(x,t)}{\partial t} = u(x,t) - \epsilon(x,t), \tag{2.7}$$

From eq. (2.6) steady state river profile conditions or equilibrium conditions can be derived by setting $\partial h/\partial t = 0$. When substituting eq. (2.3) this results in

$$S = \left(\frac{u}{k}\right)^{1/n} A^{-m/n} = k_s A^{-\theta}, \tag{2.8}$$

with $k_s = (u/k)^{1/n}$ as the steepness index and $\theta = -m/n$ the concavity index. Eq. (2.8) represents the well-known steady state river profile equation (Whipple and Tucker, 1999; Kirby et al., 2003; Wobus et al., 2006; Hergarten et al., 2016). This law, also referred to as Hack's law was already postulated by Hack (1957) from river profile analysis in the US.

2.2.4. Interpretation of Regression Parameters

From eq. (2.8) it follows that steady state river profile conditions can only occur with an uplift rate $u \neq 0$ and an erodibility $\epsilon \neq 0$, which are constant in time and space.

The given power law in eq. (2.8) can be regressed by a linear model with a constant offset within a $\log(A) - \log(S)$ space, which results in a regression model

$$log(S) = log(k_s) - \theta \cdot \log A. \tag{2.9}$$

Equilibrium segments appear as good linear approximations with small confidence intervals of the parameters k_s, θ. A drawback of this model constitutes the fact, that k_s is no longer a normal distributed parameter due to the logarithmic function. Therefore confidence intervals are large. An alternative is represented in section 2.2.6.

The steepness of the linear log-log model is defined by θ which controls the influence of profile gradient S and discharge, which is proportional to A. High θ values led to an equilibrium with decreasing catchments at a given slope. Therefore, the erosive process is moved toward slope driven processes. Respectively, low θ values correspond to discharge driven erosion.

In general correct values for n, m and θ respectively are still debated. E.g. Whipple and Tucker (1999) (n=2/3, m=4/9); Kirby and Whipple (2001) (m/n=0.46, n=0.66 linear shear, n=1 linear stream power, K=4.3e-4 m^0.2/a) Whipple et al. (2000) (n=0.4+-0.2, K=2.4e-4-9e-4 m^0.2/a)

2.2.5. Transport Equation based on Hack's law

Due to the definition of H in eq. (2.7) the channel gradient can be easily express as $S(x) = dH/dx$. Together with eq. (2.3, 2.7) we get

$$\frac{\partial H}{\partial t} = u(x,t) - k(x,t) \cdot A^m \left(\frac{\partial H}{\partial x} \right)^n . \tag{2.10}$$

But still eq. (2.10) couples the profile elevation with the drainage area. Hack (1957) showed that the drainage area can be expressed in terms of profile length

$$A(x) = k_a x^h \tag{2.11}$$

for channels without tributaries causing the drainage area to become discontinuous along the profile length x.

Substitution into eq. (2.10) results in

$$\frac{\partial H}{\partial t} = u(x,t) - k(x,t) \cdot k_a^m \cdot x^{hm} \left(\frac{\partial H}{\partial x} \right)^n , \tag{2.12}$$

which constitutes a nonlinear transport equation. For $n \approx 1$ this equation is rewritten into

$$\frac{\partial H}{\partial t} = u(x,t) - k(x,t) \cdot k_a^m \cdot x^{hm} \left(\frac{\partial H}{\partial x} \right)^{(1-n)} \cdot \left| \frac{\partial H}{\partial x} \right| . \tag{2.13}$$

For channels with strictly positive slopes along the increasing profile length toward the channel head eqn. (2.13) is interpreted as a non-linear transport equation with a non-constant coefficient $c(x) = -k \cdot k_a^m \cdot x^{hm} \left(\frac{\partial H}{\partial x}\right)^{(1-n)}$, which constitutes the transport speed by which information is transported upstream along the channel profile. For $n = 1$ the eqn. becomes linear. Eqn. (2.13) can be computed using 1D finite element analysis code, e.g. COMSOL Multiphysics in order to predict the temporal behaviour of channel profiles under the restriction that Hack's law is valid.

2.2.6. Transport Equation based on χ Transform

The interpretation of $H(x)$ river elevation profiles according to eq. (2.10) comprises a dependency on drainage area. For equilibrium channels, this forces an abrupt undifferentiable change in slope at each larger tributary junction causing profile slopes to be less interpretable in terms of the existence of a true knick point. In addition, compared to $\log(A) - \log(S)$ plots the $H(\chi)$ representation comprises less signal to noise ratio.

Basically, the χ-transform (Perron and Royden, 2012; Royden and Perron, 2013; Hergarten et al., 2016) is capable to remove the dependency of drainage area out of eq. (2.10). This is achieved by transforming the profile length

$$dx = \left(\frac{A}{A_0}\right)^{m/n} d\chi \quad \longrightarrow \chi = \int_{x_0}^{x} \left(\frac{A(x)}{A_0}\right)^{-m/n} dx \tag{2.14}$$

into a new length scale χ. Substitution into eq. (2.10) yields

$$\frac{\partial H(\chi,t)}{\partial t} = u(\chi,t) - k(\chi,t) \cdot A^m \left(\frac{\partial H(\chi,t)}{\partial \chi}\frac{\partial \chi}{\partial x}\right)^n \tag{2.15a}$$

$$\frac{\partial H}{\partial t} = u - k \cdot A_0^{-m} \left(\frac{\partial H}{\partial \chi}\right)^n \tag{2.15b}$$

For equilibrium conditions it can be concluded

$$\tilde{S}(\chi) = \left(\frac{u}{k}\right)^{1/n} \cdot A_0^{m/n} = k_s A_0^{m/n}. \tag{2.16}$$

After integration along χ

$$H(\chi) = \int_{\chi_0}^{\zeta} k_s A_0^{m/n} d\zeta = H_0 + k_s A_0^{m/n} \cdot \chi. \tag{2.17}$$

Therefore, $H(x)$ constitutes a linear polyline, while slope changes are indicating a change a the uplift/erosion scheme. Knick point can therefore unambiguously be identified by this transform. Furthermore, the regression on the model $H(\chi)$ directly results in an estimate of k_s as a linear parameter and symmetric $\pm\sigma_{ks}$ confidential intervals can be estimated.

2.3. Channel Profile Analysis Settings

The steam-profile analysis is applied to all river systems and its main tributaries from Fig. 2.1. A brief introduction to the theory was given above, numerical aspects and parameter settings are explained in the following.

2.3.1. Pre- and Post-processing on the Digital Elevation Model

The base of the numerical analysis is a digital elevation model (DEM) in MGI coordinates (central meridian 13.33°, std parallels 46° and 49°, false easting and northing 400000 m) with ten metre cell size, which was provided by GeoServies-KAGIS (2015). An also available DEM with fife metre resolution from aero-orthophotometry is not used, because in combination with the rather large extent of the analysis area the memory demands of the GIS software exceeded the available RAM of 6GB on the used computer.

The Militär-Geografisches Institut (MGI) Lambert Conformal Conical (LCC) projection constitutes an angle-preserving (conformal) mapping of the geographical spheroid coordinates (Bessel 1841) onto a cone, which touches the spheroid at the two given standard parallels and with longitude reference at 13.33° instead of Greenwich. The projection is not orthogonal, but the area distortion between the standard parallels and the even much smaller longitude extent $< 1°$ of the area of interest between these parallels was estimated to be small. Therefore, no transformation for area-preserving or orthogonal coordinates is performed. The area preserving property is important for river profile analysis because the catchment size A and profile length coordinate x needs to be properly estimated from cell sizes of the DEM everywhere in the map.

Using ArcGIS 10.4.1 the following pre-processing steps were applied to the DEM:

1. Repair holes (elevation steps, and NaN) within the DEM
2. Filling depressions in the DEM
3. Calculate slopes and D8 flow direction
4. Calculate flow accumulation and constrict for values above $1 \cdot 10^5$ m^2
5. Calculate channel network using *Strahler* algorithms and convert the result to stream poly-lines

Within the post-processing, the extraction of relevant river profile quantities, which were computed in the pre-processing is done. Therefore, the basic post-processing step is the computation of the geographic location of river beds and the extraction of calculated values of elevation H and drainage area A from the pre-processing.

In total two different software toolboxes were used for this process. The Quantitative Geomorphology Toolbox for MatLab (Whipple et al., 2007) is a well-known MatLab (The MathWorks) based software. It is a script- and procedural-based toolbox with strengths in smoothing functions and statistics support, but with the drawback of stability issues and missing error handling (the present DEM processing resulted in errors). In contrast, the MatLab TopoToolbox from (Schwanghart and Kuhn, 2010) is an object orientated code, which appears more stable in the data processing. However, the support for slope smoothing and statistic regression methods is limited. Finally, an approach was chosen, which is based on the TopoToolbox, and which was complemented by regression methods taken from the MatLab Statistics toolbox and from the integration of some functions out of the Quantitative Geomorphology Toolbox. This was necessary in order to compute more stable results for the regression models and to calculate feasible confidence intervals. Furthermore, the ArcGIS tool-bar interface of the Quantitative Geomorphology Toolbox was used for manual picking of channel heads in the DEM and for importing MatLab results into an ArcGIS shape-file.

2.3.2. Signal Processing for Channel Profile Analysis using MatLab

The applicability of river profile analysis is limited to profile sections, which are controlled by fluvial erosion with constant sediment transport and without aggrading conditions. This type of erosion links stream power or bed-rock channel water induced shear stress at any point along the river profile to a local slope, when in equilibrium. In particular, it is assumed that stream power is proportional to discharge, which in consequence is proportional the drainage area when homogeneous precipitation is assumed. For small drainage areas, this is no longer true due to less effective spatial distributed discharges, which alter into slope stability erosive processes, see e.g. Hergarten et al. (2016). Therefore, the small catchment sizes need to be limited below 0.1-5 km^2, before the slope becomes a constant.

Furthermore, glacial erosion also follows different erosion laws, because the erosive capacity also depends on temperature (if the ice is frozen or not at the glacier base), on transported rocks and gravels, which are constituting the main carving tools and on overburden pressure, which makes the erodibility strongly dependent on cross-sectional shapes of the glacier (Egholm et al., 2009). Therefore, in principle regions of know glacial overprint need to excluded from the analysis.

2.3.2.1. Profile Length Elevation and Drainage Area Plots

Based on manually picked channel heads, which corresponds to an upper catchment size of $1 \cdot 10^{-4}$ m^2 within this work the elevation $H(x)$ in [m] and the drainage area $A(x)$ in [m^2] data along the monotonically upstream-wards increasing channel profile length x in [m] are extracted.

The profile origin $x = 0$ m always lies at the Drau river junction. Besides town place-marks for orientation also the LGM extent (Van Husen, 2012, modified) is depicted by brackets above the elevation profile. The elevation profile $H(x)$ shows regions of exponential decay. These segments constitute most likely regions of fluvial erosion in equilibrium. Steps are candidates for knick point and non-differentiable points relate to abrupt changes of the drainage area, which also correlate with steps in the $A(x)$ plot.

2.3.2.2. Stream Profile Regression

From profile elevation and area data $H(x)$ and $A(x)$ the steepness index k_s and concavity index θ of the detachment-limited fluvial bed-rock incision model $k_s = S \cdot A^{\theta}$ in eq. (2.3) can be estimated. After logarithmic transformation the model results in $logS = log(k_s) - \theta \cdot log(A)$ where the parameters $log(k_s)$ and θ can be estimated using a linear regression model $y = a \cdot x + b$ within the transformed data space $log(S(log(A)))$. As detailed in section 2.2 the steepness value $k_s = (u/k)^n$ can be correlated with uplift u in case of homogeneous erodibility k (n is the slope exponent). The concavity index $\theta = m/n$ (m is the stream power exponent) expresses the trade-off between steep valley erosion, which is driven by slope (high θ) and stream power driven erosion, which is driven by catchment size (low θ), which is typically leads to lower slopes and is more close to aggrading conditions.

In general the amount of regression data points $(H(x), A(x))$ along the profile is large and furthermore the slope $S(x)$ implies much quantisation effects and noise due to e.g. resolution and DEM processing effects. Therefore the slope data needs to be smoothed before regressing on it. This is done by classification of slope data within a histogram. The individual histogram slope bin margins are equally spanned in the log(A) axis using 200 bins/decade in this work. All (H, A) tuples are classified and collected within the bins. Many bins remain empty, but for the remaining ones, the mean slope is averaged within each bin. This data constitutes the raw data for the regression. Within the actual investigation typically the log-log plot consists out of different sections:

1. Piecewise linear segments with varying gradient and offset on the log(S) axis: most likely sections where fluvial, equilibrium properties can be assumed. Varying y-offset indicates variation in uplift/erodibility properties

2. Unstructured point clouds: disequilibrium parts or part with glacial overprint

3. Hiatus along log(A) axes: entry of a strong tributary to the river trunk under investigation

4. Transition part between two piecewise linear segments from high slope to low slope in upstream direction: typically a knick point disequilibrium area with the knick point at the top of a knick point zone. The highest gradient is in the mid of the knick point zone.

5. Transition part between two segments with slope flattening at the beginning of a knick point zone in upstream direction: within this work, this is interpreted as glacial overprint at hanging valleys where the main valley glacier flattened out the bottom at the over-steep section.

For good regression results with small confidence intervals, it is crucial to select piecewise linear segments in the log-log data. Therefore the following rules for interval selection were applied:

1. Hiatus intervals should be avoided if possible because stream power parameters often seem to change hardly visible across this junctions.

2. Downstream of a knick point steep (highest slope) a safety margin downstream should be regarded in order to exclude the run-up to the steepest point.

3. The section close to the head at A_{cr} needs to be taken with care. The upper margin should be set without including any negative trend.

The estimate for k_s results in unsatisfactory large and unsymmetrical confidence intervals because $log(k_s)$ is regressed instead of k_s. Therefore the k_s value is regressed in the $H(\chi)$ transformed data, as shown by Perron and Royden (2012), implemented in the Quantitative Geomorphology Toolbox from Whipple et al. (2007) and explained in the next section.

2.3.2.3. χ-transformed Profile Elevation

The so-called $\chi : x \rightarrow \chi$ transform (Perron and Royden, 2012; Royden and Perron, 2013) is used to eliminate the $A(x)$ influence in the elevation plots, as described in section 2.2. When assuming piecewise homogeneity in uplift and erodibility and equilibrium conditions along a profile (sufficient settling time), then each change in the gradient of $H(\chi)$ indicates a change

of equilibrium state caused by a different erodibility or uplift. Therefore, these points are classified as knick points.

As described in section 2.2 the profile length x is transformed into a new length scale χ based on integration along the profile of the catchment size. Consequently the relation $\tilde{S}(\chi) = k_s A_0^\theta$ in eq. (2.16) can be exploited for a now linear regression for the linear parameter k_s. For simplicity A_0 is chosen to one, therefore even no estimate for θ is needed. Using this methods yields into good estimates of k_s with narrow symmetric confidence intervals $\pm 2\sigma$, which is not the case for the log-log regression results.

2.3.2.4. Normalised Profile k_{sn}

The k_s values are found to typically vary strongly due to an apparent strong dependency on θ. A physical interpretation of regression values is therefore difficult. On the other hand, the use of normalised k_{sn} values solves this problem and provides a proxy for uplift/erodibility.

The normalised k_{sn} values are directly computed from eq. (2.8) by $k_{sn} = S/A^{-\theta_{ref}}$. In the diagram, two estimates are provided. In the 'TopoToolbox' the calculation directly uses the gradient $S = dH/dx$ from the profile data. As a consequence, the estimate of k_{sn} is a strong fluctuating function, which needs to be smoothed in order to obtain stable meaningful results. In the present analysis, the averaging is conducted using a 160 m long moving average boxcar window. On the other hand, in the Quantitative Geomorphology Toolbox much more effort is applied on smoothing the gradient estimates before k_{sn} is calculated. The smoothing procedure starts with forcing a strictly monotonous elevation function by modifying the upstream elevation profile, followed by moving average low pass filtering. Finally, the slope is calculated not on the filtered elevation data but between fixed elevation contours, which were set to a 12.192 m difference (default) in this analysis.

Both estimates yield comparable results, but the result from the Quantitative Geomorphology Toolbox show more variability in knick point regions. On the other hand, running offset effects seem, e.g. to occur in the Gurk River trunk middle section.

3. Results

The result of this thesis is a geomorphic map of the Gurktal Alps, that is shown in full extent in the Appendix in Fig. A.2 and of, which a part is shown within this section. In a combination of field mapping, channel profile analysis and DEM interpretation a series of planation surfaces and knick points were discovered that are clearly relics of a potential Miocene landscape evolution in as much as the region of interest was largely ice-free during the glaciation periods. In this part of the thesis, I will first present some results from field observations and then focus on a detailed channel profile analysis

3.1. Geomorphological Analysis based on Field Observation and DEM Analysis

The morphology of the three major valleys of the region, namely the Gurk, the Metnitz and the Wimitz are described.

3.1.1. Upper Gurk Valley

The Gurk valley is the principal drainage of the region of interest and was largely ice-free in its central part (Fig. 3.1). Therefore, the investigation starts with the upper Gurk valley. A coloured slope map (Fig. 3.2) is superimposed on a hill-shaded topography. The courses of the river system network are made visible by means of k_{sn} values, which are referenced by a number code in the legend. River knick points are indicated as star symbols, which typically correlate with high k_{sn} values in the map, indicating a disequilibrium state within

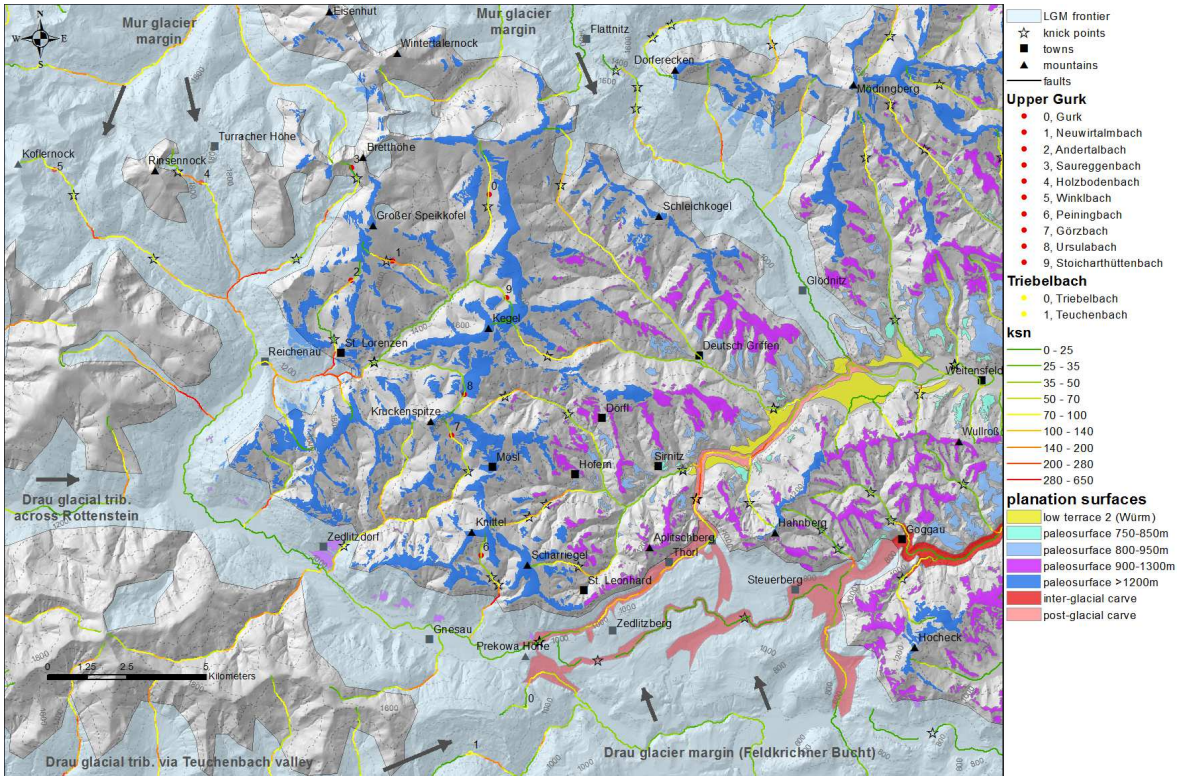

Figure 3.1.: Interpretation of planation surfaces and the LGM extent on top of hill-shaded topography of the Upper Gurk River system. The river network is marked using k_{sn} values.

the river profile. The geomorphological map (Fig. 3.1) display the LGM extent, together with relict or planation surfaces on different levels, which were in detail discovered as a part of this master thesis. These planation surfaces are constituting additional non-glaciated sub-levels at altitudes below the glaciated Nockfläche (Exner, 1949; Reinecker, 2000), which is located to the NW outside the region of the displayed map.

The Gurk springs in the upper Gurk valley east of St. Lorenzen at an altitude above approximately 1900 m in a side valley east from the Turracher Höhe and reaches down along 60 km to the Enge Gurk about fife kilometre NE of Gnesau (knick point location in the map). The highest valley section was never glaciated. From sampled lake sediments Van Husen (2012) claimed this area to be partly filled by two glacial lakes, which were the Andertal lake directly N and a larger one in the Gurk valley to the NE of St. Lorenzen. These lakes are supposed to have built up during the decaying LGM when precipitation rates rose up again in conjunction with the still existent blockade of the connecting Mur glacier. This ice stream swept down

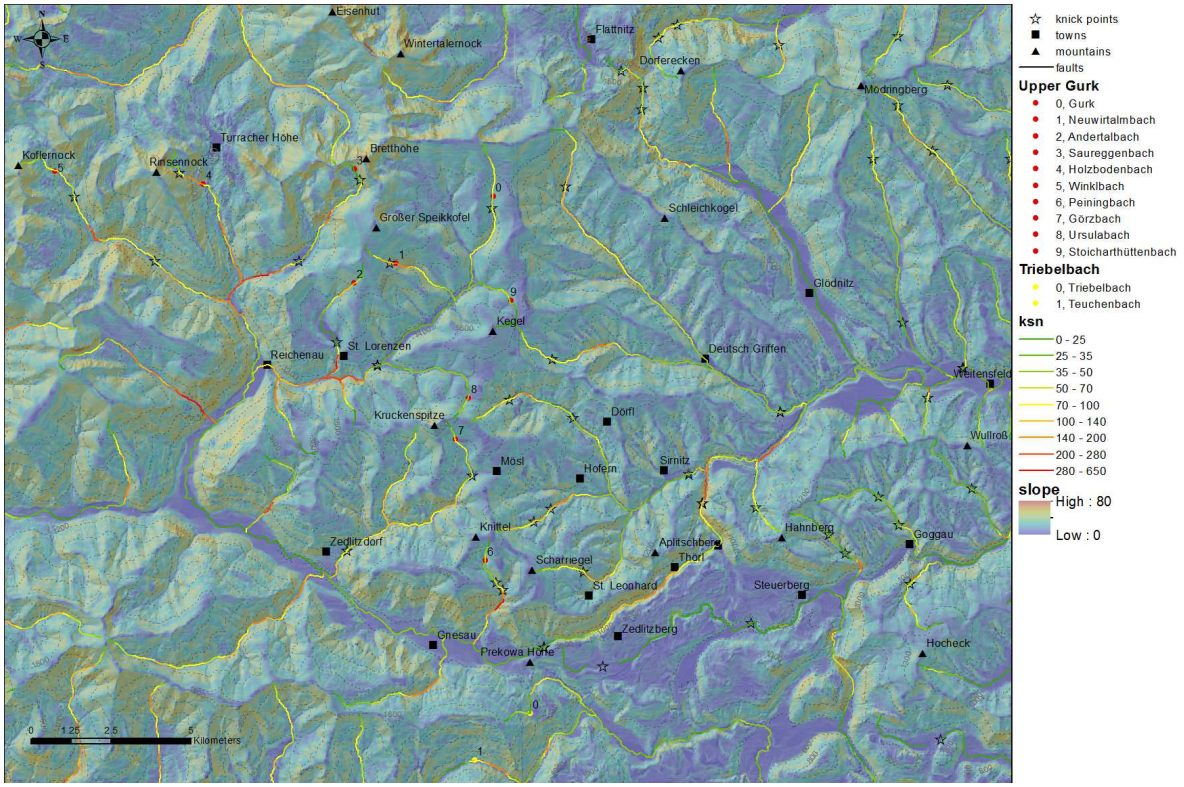

Figure 3.2.: Slope map of the upper Gurk River system. Displayed are topography by hillshading and slope angle by colour. The river network is marked using k_{sn} values.

across the Turracher Höhe down to the Drau glacier in the Feldkirchner Bucht, see Fig. 3.1.

At Ebene Reichenau, the Gurk River joins together with the Saureggenbach, Holzbodenbach and Winkelbach coming down from the Turracher Höhe and adjacent side valleys. Just upstream of Reichenau a steep step of about 200-300 m in the main valley floor can be observed. U-shaped valley floors e.g. to the south of Reichenau and glacial shoulders e.g. around Gnesau indicate the glacial overprint in the Upper Gurk River section.

Downstream of Gnesau the history of the Gurk River drainage gets complex and reflects a varying history of forceful river bed displacement due to the glacial extent of the confluence between Mur and Drau glaciers (Fig. 3.3). To the north of the Feldkirchner Bucht in total, four ice streams joined together in the Pleistocene (Fig. 3.1). These were a side stream from the Mur glacier moving down from Ebene Reichenau, an eastward moving side stream from the Drau glacier through the Rottensteiner valley joined into the upper Gurk valley in Wiedweg, another southern side stream from the Drau glacier flowing eastward through the Teuchenbach valley

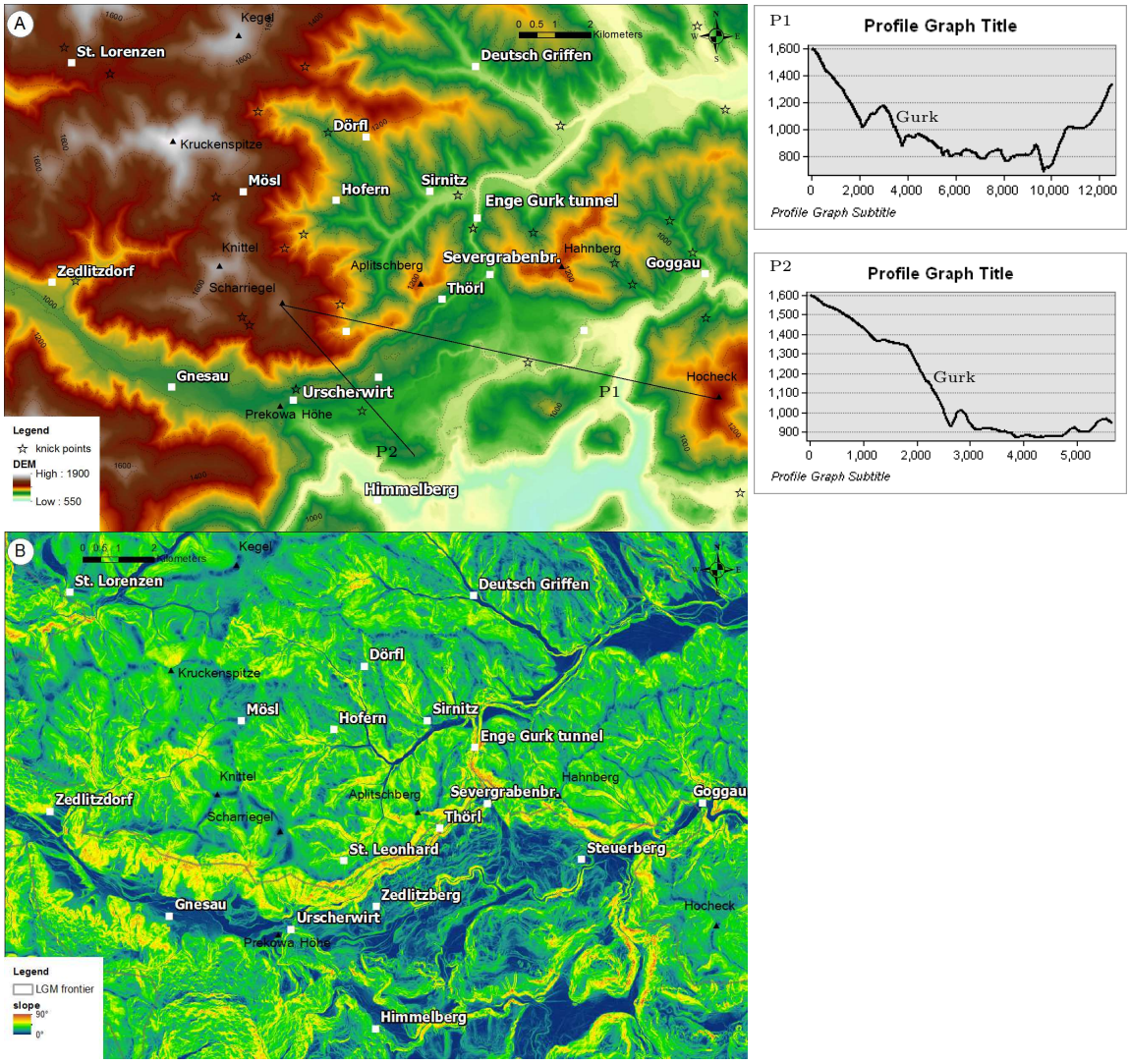

Figure 3.3.: Section of transition between upper and lower Gurk valley around *Prekowa Höhe*. **A**: shows the DEM GeoServies-KAGIS (2015) with tow profiles along the Nockberge Senke rim, **B**: shows the slope map, which emphasises channel slopes and identifies a palaeo-surface to the NE.

and finally the main stream of the Drau glacier itself flowing upward into the Feldkirchner Bucht from the south up to the Prekowa Höhe.

Today the Gurk River turns sharply to the east downstream of Gnesau guided only by a low hilly fluvioglacial sediment covered landscape in the vicinity of the Prekowa Höhe and flows into the gorge section of the Enge Gurk. The Tiebelbach (Fig. 3.2 or 3.1) directly springs in a swampy area only 400 m SE and 50 m below the Gurk channel close to Prekowa Höhe and is supposed to be feed by the Gurk representing the starting of a river piracy event Weiss (1977).

The Tiebelbach is supposed to represent a direct southward drainage of the Pre-Pleistocene palaeo-Gurk River. Weiss (1977) substantiated this by the finding of two SN trending bed-rock gullies beneath the fluvioglacial sediments of the Prekowa Höhe, which are becoming broad channels in the Feldkirchner Bucht.

Besides the above described channel Van Husen (2012) discussed one further possible drainage channel of the palaeo-Gurk with the Prekowa Höhe as a key point, which builds up at the fading LGM. A sedimentary mapping of glacial deposits at the Prekowa Höhe shows a strong influence from the southern Drau glacier and the ice stream from the Teuchenbach, because of the deposition of medium metamorphic material in that area, which bed-rock is only found outside the Gurktaler nappes. Therefore, Van Husen (2012) postulated a varying drainage pattern of the Teuchenbach and the Gurk discharge through the Enge Gurk gorge and the Wimitz across the Goggau watershed during the main glacial phase depending on the glacial advance from the south. During the fading LGM, when the Prekowa Höhe sediments were deposited in a very small time frame the Wimitz valley was probably a drainage for the Teuchenbach and probably even for the Gurk discharge due to partial blockage of the Enge Gurk section (Van Husen, 2012). On the other hand, little is known about the evolution and time constraints of the palaeo-Gurk drainage system, except some models for the LGM time period.

When investigating the river profile section between Gnesau and the junction with the Sirnitz River at Althofen castle two knick points are observed in the field. The upper knick point lies close to Prekowa Höhe. Downstream fluvioglacial sediments are placed along the six kilometres long course of the Gurk between the small village Seebacher (close to Urschlerwirt) and the Severgraben bridge, see Fig. 3.3A. Here the river has carved an up to 50-100 m deep steep-walled valley (see profile P1 and P2) directly leaned to the northern ridge of the Mt. Scharriegel and Mt. Applitschberg. Parallel to this section the deeper rooted waterless palaeo-channel of the Wimitz is only separated by a narrow EW trending ridge build out of ground moraine in the west (Van Husen, 2012) and predominantly phyllites (Fig. 2.2). The slope map (Fig. 3.3B) shows steep homogeneous slopes at the southward orientated flank between the Scharriegel and the Mt. Applitschberg. Above an altitude of 1300-1500 m the topography abruptly gets flat and mountain tops like the Scharriegel and Knittel appear strongly flattened. This contour

Figure 3.4.: **A**: constantly steep ascending Görzbach tributary below Görzwinkel, **B**: Görzbach on top of relict landscape, **C,D** Enge Gurk knick point.

margin is interpreted to be the transition line between the glacial carving (LGM frontier) and a palaeo-surface, which extends to the north. This is also supported by Van Husen (2012) who noted that the Gurk channel bed in this section might be formed sub-glacial. The second knick point cut through solid rock bed-rock at the Enge Gurk just adjacent to a small avalanche protection tunnel about 1.5 km downstream of the Severgraben bridge and pours down 30-40 m abruptly, see Fig. 3.4C, D. The knick point lays within a narrow gorge with a steep rock wall on both sides, which break through the rim of the Nockberge Senke. About 4800 l/s (see *OCc17*) rages down for about 50 m in only 100 m distance.

The abrupt flattening in topography to the east of Reichenau and north of Gnesau can also be observed within the slope maps of Fig. 3.2 and 3.3B. In particular, in broad areas close to summits (e.g. Mt. Kegel, Mt. Kruckenspitze, Mt. Knittel, Mt. Scharriegel) and connecting

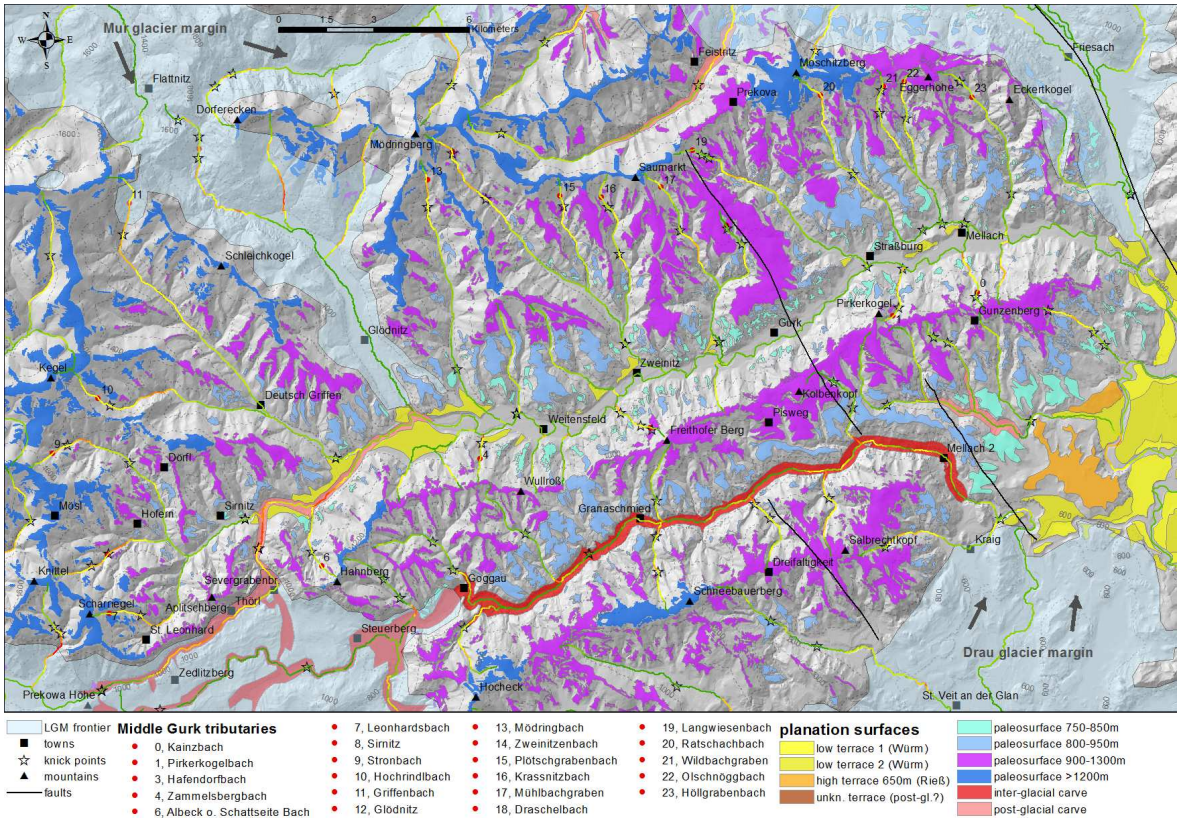

Figure 3.5.: Interpretation of planation surfaces and the LGM extent on top of hill-shaded topography of the Middle Gurk River system. The river network is marked using k_{sn} values.

ridges the surface gradient considerably flattens. This can be observed in the head section of the Görzbach, see Fig. 3.4B. In contrast steep incision along the Gurk River main trunk and moderate incision along tributaries define an incision landscape. In Fig. 3.1 this planation surface was mapped as the highest palaeo-surface with altitudes above 1200 m but with mean altitudes around 1400 m. It can also be seen that planation surfaces are also preserved in adjacent non-glaciated part to the west and north-west of the upper Gurk River.

3.1.2. Middle Gurk Valley

The Middle Gurk River section constitutes the central area of the non-glaciated part within the Gurktaler Alps and comprises three palaeo-surfaces (Fig. 3.5). This is made plausible by low slopes (Fig. 3.6) on top of the northern Mödringberge and also on top the southern Wimitzer

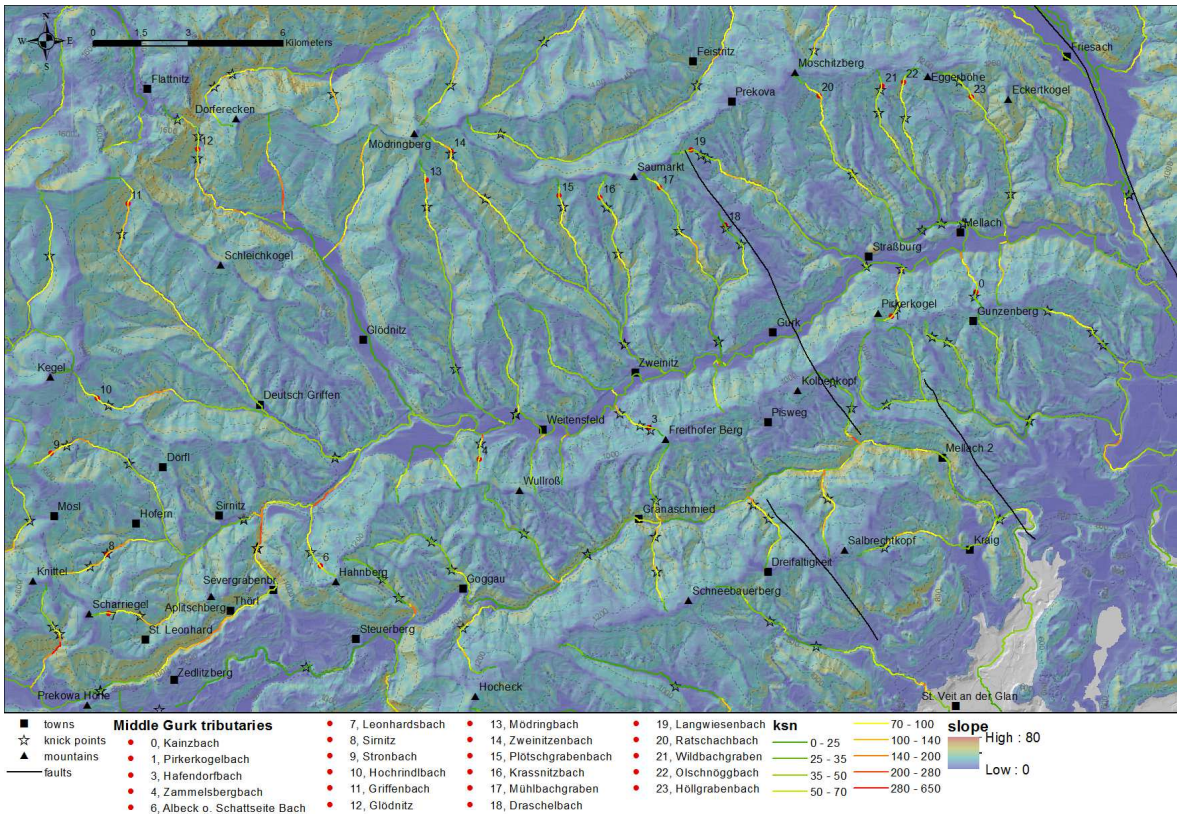

Figure 3.6.: Slope map of the upper Gurk River system. Displayed are topography by hillshading and slope angle by colour. The river network is marked using k_{sn} values.

Berge ridges. Also, the k_{sn} values are quite small within the whole valley, except at the Enge Gurk location and close to knick points in the head section of almost every tributary.

Downward the Enge Gurk the rivers enters the non-glacially overprinted section of the middle Gurk. This region represents the core area of the Nockberge Senke, a circular structure described in section 1.1.2. At Althofen castle the Sirnitz river tributary joins into the middle Gurk from the east, exhibiting the last prominent knick point with a step height of approximately 20-30 m carved into solid bed-rock and a discharge of about 200 l/s, see *OCa7*. The 837 m high terrace, on-top which the Althofen castle is located constitutes the uppermost found occurrence of Niederterrasse sediments in the Gurk valley (Fig. 2.2).

Downstream of the Sirnitz junction the Gurk is about 50-60 m deeply incised into Niederterrasse and Würmian gravels (Fig. 2.2). Past the junction with the Glödnitz, the Gurk valley gets wider and flows between the southern Wimitzer Berge and the northern Mödringberge

within a V-shaped valley. Würmian terraces are getting scarce, but remnants can especially be found on the northern bank between Weitenfeld and Gurk, at Straßburg and Mellach. The hill heights and slopes curb down and the landscape becomes more gentle, see Fig. 3.7A, B, which was taken from the castle in Straßburg in downstream and upstream direction. On the left-hand side of the picture inselberge can be seen, which are completely missing on the right-hand side. On the other hand, the right-hand side shows remnants of terraces. The profile length between the northern and the southern side tributaries are strongly asymmetric as can be seen in Fig. 3.6 or 3.5. To the north about 3-4 km profile length face only about one kilometre length on the southern side.

It is interesting to note that tributaries at the western and eastern side of the Nockberge Senke rim show different slope character. A comparison of e.g. the Leonhardsbach and Sirnitz in Fig. 3.7F, G compared to the Görzbach in Fig. 3.4A, B reveal, that tributaries at the eastern side possess a meandering section at altitudes around 900 m, which is missing on the western side. Fig. 3.3A additionally reveals that even the level of 900 m is missing outside the rim.

It turns out that hardly any discharge accounts to the Gurk from the southern slopes of the Wimitzer Berge (e.g. Pirkerkogelbach 1-1.5 l/s, *OCc3*, Fig. 3.7C), which contrasts to many tributaries with varying discharge from the northern slope of the Mödringberge (e.g. Zweinitzenbach 60 l/s, *OCa10* or Langwiesenbach 50 l/s *OCa1* (Fig. 3.7E), Mödringbach 50 l/s, *OCa9*). Furthermore, the Gurk discharge of approximately 4800l/s at the Gurk bridge west of Weitenfeld (*OCa4, OCa5*) surpasses the total discharge of all tributaries between the Mödringbach and the Metnitz junction of approximate factor ten, without showing emphasised incisions for the Gurk trunk. In summary, the middle Gurk valley shows fluvial incision though Pleistocene unconsolidated sediments in its upper section (e.g. unconsolidated and unsorted coarse sand to pebble two kilometres downstream of Zweinitzen *OCc9*), except at a solid rock blockage at the foot of the Braunsberg terrace (*OCc5*) no bed-rock incisions at all. In contrast, the Wimitz valley shows strong incision characteristics, which is documented by many bed-rock outcrops throughout the valley.

The Glödnitz River is the only river in the Middle Gurk section, which was glacially overprinted in the Pleistocene. According to Van Husen (2012), to surface texture structures from the DEM, the deposition of a huge amount of Würmian sediments along the course and at

Figure 3.7.: A, B) downstream and upstream Gurk view point from Straßburg castle, C) Pirkerkogelbach close to St. Stefan church (close to Gurk junction), D) downstream Glödnitz view, E) upstream view Langwiesenbach, F) Leonhardsbach at transition point from meandering to steep section, G) Sirnitz upper valley.

the Gurk River junction (see Fig. 2.2) and due to the broad cross-section of the valley (see Fig. 3.7D) a strong glacial overprint can be assumed. The Braunsberg terrace, build out of fluvioglacial Würmian phyllitic coarse sand to cobbles at the southern side of the Gurk on-top of a green-schist bed-rock base (*OCc15a,b*) is the largest terrace in the area. The head channel of the Glödnitz steeply accents toward the Flattnitzer Höhe, which is also close to the Metnitzursprung in 500 m distance to the east. This today's watershed between Glödnitz, Metnitz and the Flattnitzbach was overridden by the Mur glacier sidearm through the Flattnitz Furche from the north during the Pleistocene.

East of the Glödnitz valley the Mödringberge massif stretches until the NS course of the Metnitz down-to Althofen. The Mödringberge with the Mt. Dorferecken as its highest mountains with 1720 m lay completely within the Nockberge Senke structure. In this area, between the Mödringberge and the opposite Wimitzer Berge several terraces can be identified, which are depicted in the map in Fig. 3.5. As already mentioned the Niederterrasse can be found on the lowest level about 30-50 m above river bed level at the terrace close to the junction with the Metnitz (645 m altitude) and at the Braunsberg terrace (765 m altitude). In addition, strath terraces (fluvial formed in bed-rock covered by a thin unconsolidated alluvial mantel only) can be found 200-300 m above the river bed on both sides of the channel. In particular, the terrace stretches on the northern side. In total, four different planation surfaces are distinguished by hypsometric analysis and by field observation, but it is not clear if this granularity is existing in a larger extent.

In Fig. 3.7A, B the strath terrace is depicted on both sides close to the village of Straßburg. The left-hand side of the picture relates to the northern relict landscape and shows already strongly eroded remnants of a plateau. Here the lateral rise forms long parallel NS trending ridges, which tops are supposed to represent the remainder of an old relict landscape. In contrast, the southern terraces are very small and unimposing. Due to the advanced state of erosion within bed-rock and the amount of incision of approximately 200-300 m a Pre-Pleistocene age can be assumed for the relict landscape when it was in a low altitude erosion protected long-term stable position.

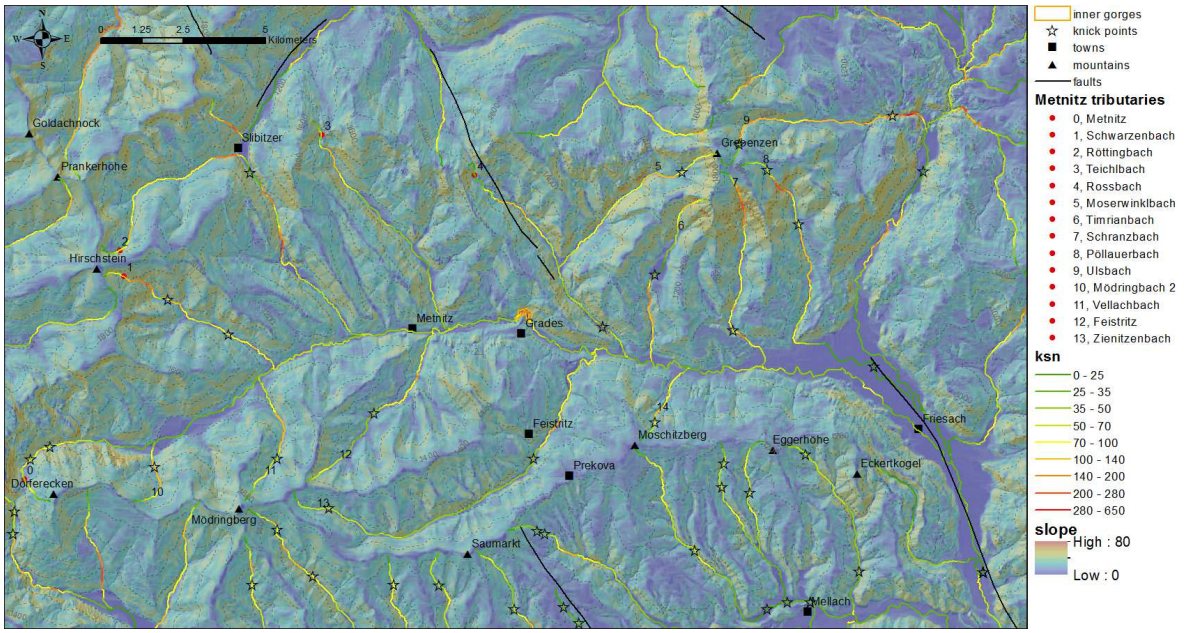

Figure 3.8.: Slope map of the upper Metnitz River system. Displayed are topography by hillshading and slope angle by colour. The river network is marked using k_{sn} values.

3.1.3. Metnitz Valley

The Metnitz is the most northern river system of this study and already comprises non-glaciated areas, especially at low levels. It springs in a swampy area in the upper Metnitz valley at about 1200 m to the north of the 1726 m high Mt. Dorferecken, close to the triple junction with the Glödnitz and the Flattnitzbach, see Fig. 3.8. As can be seen in the map in Fig. 3.9 the whole main trunk of the Metnitz up-to one kilometre before the confluence with the Gurk was glacially overprinted during the LGM up to an altitude of 1000-1200 m. Surpassing massifs were pointing out as Nunataks during the glaciation events, which is true for e.g. the Mt. Grebenzen, Mt. Prankerhöhe and Mt. Hirschstein.

At lower levels, remnants of the glacial overprint can be seen along many places along the river course. In Fig. 3.10C a ground moraine about one kilometre downstream of Metnitz gives further evidence.

Below the castle of Grades the Metnitz is deeply incised into a curved inner gorge (Montgomery and Korup, 2010), see *OCb1*, representing a glacially protected gully with fluvial genesis, see Fig. 3.10D and *OCb1*.

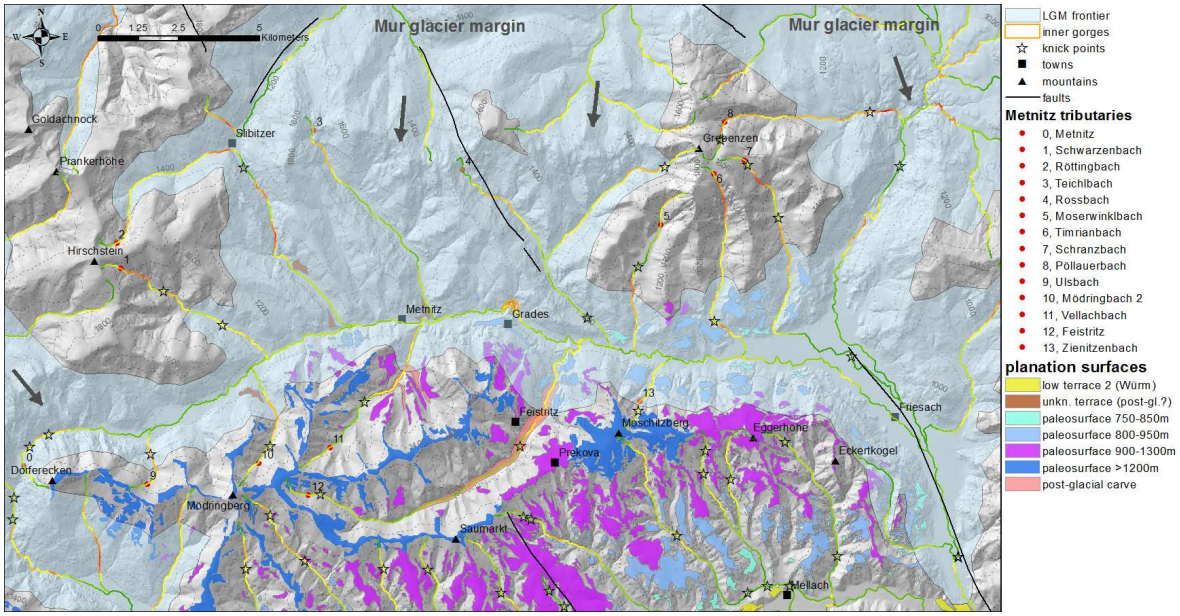

Figure 3.9.: Interpretation of planation surfaces and the LGM extent on top of hill-shaded topography of the Metnitz River system. The river network is marked using k_{sn} values.

In Fig. 3.10B the view to the north of the pass between Metnitztal and the Murtal at Stiblitzer farm is depicted. Apparently, rounded summits and a very broad valley floor is present. They are likely to be formed sub-glacial by a side arm of the Mur glacier, which entered the Metnitztal from the north.

A comparison of sediments between the Metnitz valley and the Gurk valley in Fig. 2.2 reveals by fare more Würmian sediments. These are represented e.g. as side- and ground moraines in the Metnitz valley. In terms of bed-rock the phyllites are receding into the background and mica-schists, para-gneisses and carbonate become more dominant. The discharge of the Metnitz is approximately 5000 l/s. This is about 30-40% less in comparison to the Gurk River.

At Grades a relatively broad side moraine (Fig. 3.9) stretches along the southern valley side. The photo in Fig. 3.10A shows the view from this moraine to the east. Apparently, several stages of a landscape evolution cycles can be identified within this NS orientated profile of the middle section of the Metnitz valley between Mt. Grebenzen and Mt. Eggerhöhe. In the centre, a V-shaped valley structure with about 100-150 m depth is depicted, which is overlay

Figure 3.10.: **A**: Eastern Metnitz valley from Grades terrace, **B**: Röttingbach with Stiblitzer farm, **C**: ground moraines before Metnitz, **D**: Metnitz River in inner gorge at Grades, **E**: Vellach valley with Mt. Grebenzen view, **F**: Lower Feistritz valley.

by two more stages above. The lower stage clearly shows a U-shape morphology indicating glaciation, while the top stage on the right-hand side of Mt. Grebenzen is more flattened and even might consist itself out of several sub-stages.

The Feistritz valley is the largest unglaciated tributary on the southern side and is identified as a V-shaped valley in Fig. 3.10F. The Zienitzenbach is a very small mostly glaciated tributary coming down from the Mosinzberg, which constitutes the easternmost tributary from the Mödringberge. The Vellach River is the next unglaciated tributary upstream, see Fig. 3.10E. It represents a smoothly descending rather broad V-shaped valley. An outcrop of cross-bedded sediments was found at an altitude of 1100 m close to Pollinger farm (*OCb2*) about 100 m above the valley ground and document fluvial dynamics.

Despite the glacial character of the Metnitz valley planation surfaces are also found here (Fig. 3.9). Basically, two levels at 900-1300 m and above 1200 m are existent. In particular, the slope analysis (Fig. 3.8) shows flattened top-hill landscapes in the vicinity of the Feistritz and Vellach valley and even at low levels between 750-850 m downstream of Grades in glaciated areas. It is not clear if this level was created by glacier buzz-saw or if it is a preserved planation surface.

A comparison of slopes of the northern and southern valley side in the vicinity of Metnitz reveals a difference in the distribution of slope angle due to glacial overprint. The relict landscape on the southern side shows widespread flattened topography at top heights, while in the glacially overprinted areas on the northern side on very narrow low slope stripes are existent at the top ridges and more widespread flattened areas are only found at valley floors.

Low slopes (Fig. 3.8) and smooth surface textures (Fig. 3.9) indicate the existence of further planation surfaces at higher altitudes on top of the Nunataks toward the north, e.g. on top of Mt. Grebenzen. Interestingly a huge planation surface is also visible on the southern slopes of the Metnitzberge toward Murau, between Stiblitzer farm and the Mt. Grebenzen. This zone is clearly within the LGM zone. Therefore, it might be an extension to the Nockfläche to the west of the Flattnitzer Furche. All these areas were not investigated closer to this work.

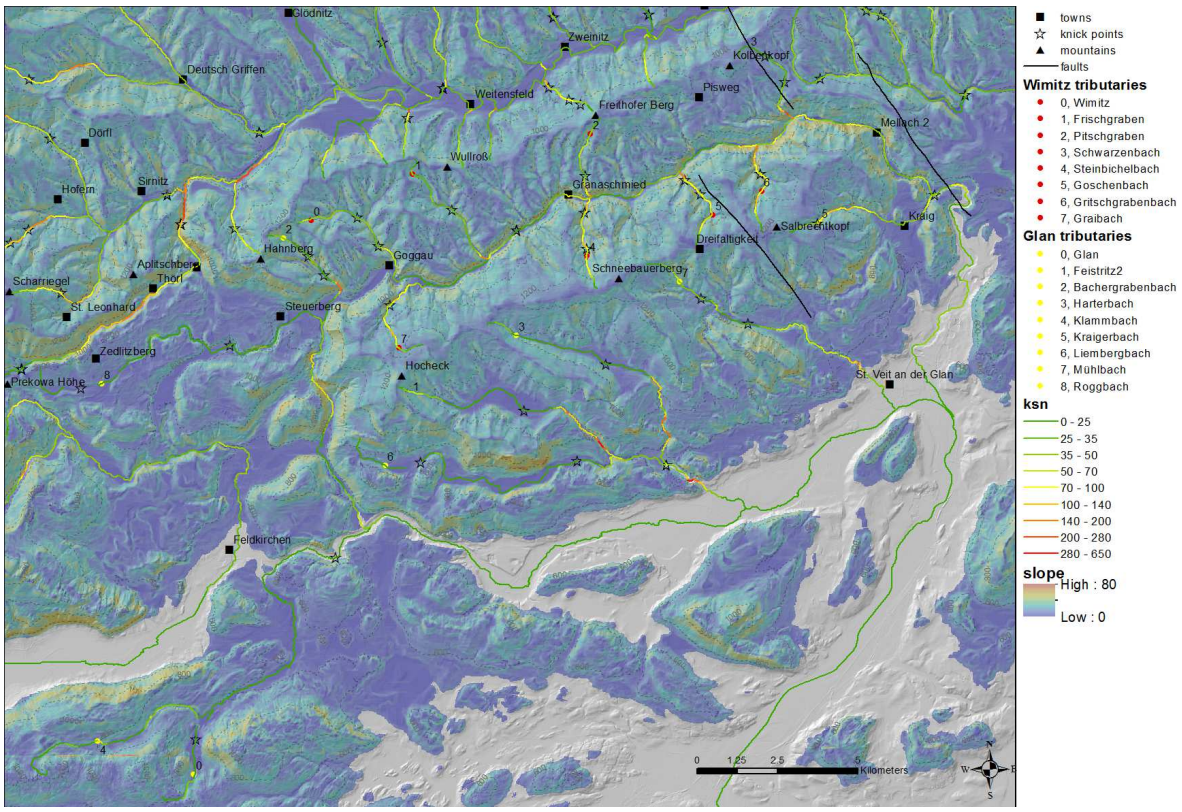

Figure 3.11.: Slope map of the Wimitz and Glan River system. Displayed are topography by hill-shading and slope angle by colour. The river network is marked using k_{sn} values.

3.1.4. Wimitz Valley

The strongly V-shaped Wimitz valley comprises the southernmost river system, within the fluvial regime of the Gurktaler Alps. Further to the south the palaeo-Drau glacier already strongly overprinted the basin toward Klagenfurt.

The Wimitz River springs within the NW end of the Wimitzer Berge (Fig. 3.11 and 3.12). It flows in parallel to the east-west trending middle Gurk River and sharply turns to the south toward the Klagenfurt Basin past Mellach village. Compared to the Middle Gurk River the length of tributary profiles show NS symmetry and have a mean length of about 2.5 km, which is an intermediate value compared to the length distribution in the Middle Gurk valley.

The Wimitzer Berge are consisting of two parallel ridges. The northern Zammelsberger Rücken is confined by the Middle Gurk and Wimitz rivers and shows its highest topography at the

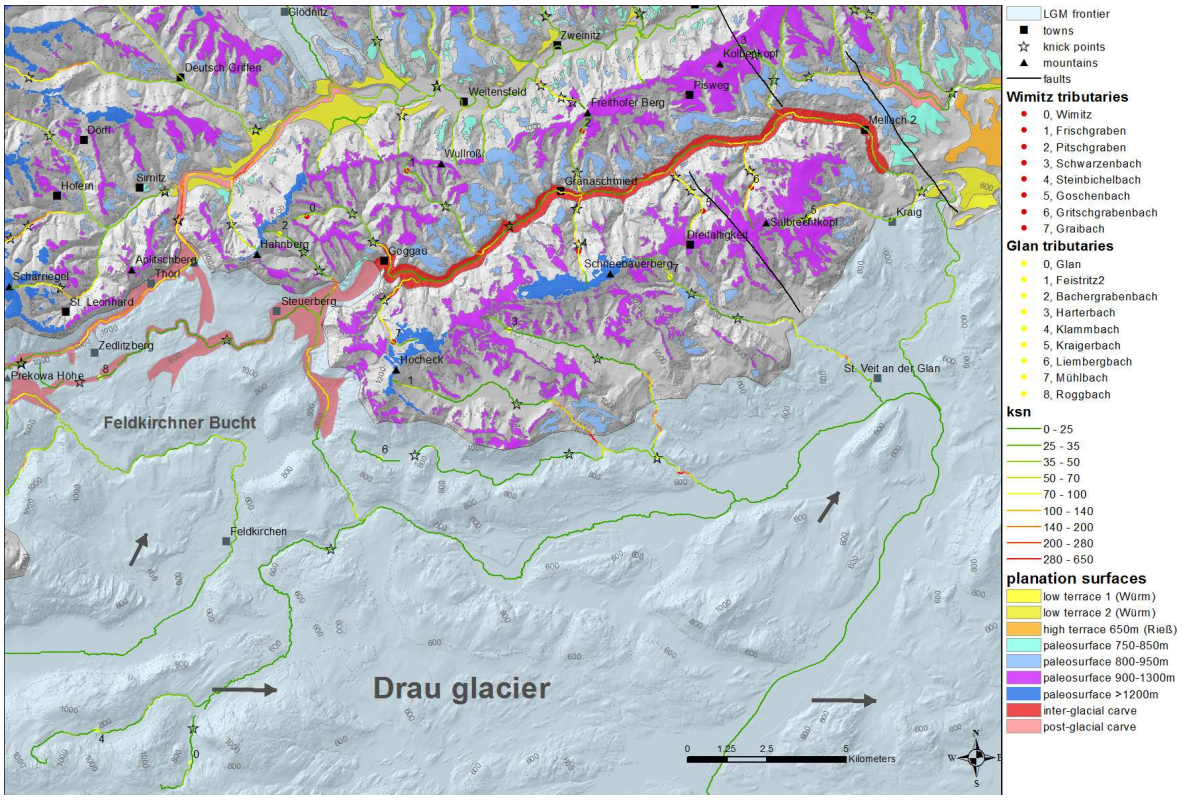

Figure 3.12.: Interpretation of planation surfaces and the LGM extent on top of hill-shaded topography of the Wimitz and Glan River system. The river network is marked using k_{sn} values.

Mt. Hahnberg with about 1260 m altitude. The slightly more elevated Schneebauer Rücken is the southern ridge with the 1335 m Mt. Schneebauerberg as the highest summit. It is bordered by the Wimitz and the Glan River.

In the vicinity of Goggau (few houses at Goggauwirt) a strong disturbance of the valley can be observed. Before Goggau in the upstream direction, the river changes its east-west trending direction, turns north and steeply climbs before it reaches around Oberort the channel head where the topography leans back again. The northward turn of the Wimitz is marked by a very unpronounced and flat watershed (Fig. 3.13B, C). In the vicinity of the watershed, the valley is very broad. It is soon getting a V-shaped steep valley about 500 m downstream of the watershed (Fig. 3.13B). At the Granaschmied further fife kilometre downstream the Wimitz valley reaches a knick point (60 l/s, *OCc36*) within a steep small V-valley. Hardly the single lane road and the river beds fit into the valley floor (Fig. 3.13E), which is in apparent

contrast to the broad valley entrance at Goggau. To the east of the flat watershed downstream the Roggbach, which drains into the Glan the valley gets even broader (Fig. 3.13C). This morphology and the rather small discharge at the upper Wimitz River makes it plausible, that the valley close to Goggau was formed by glacial processes - see LGM extent in map 3.12 - in conjunction with additional high water discharges from the palaeo-Gurk as already described in section 3.2.1 within the Pleistocene.

Slope analysis (Fig. 3.11) reveals very strong incisions downstream of Goggau up to Mellach but also in the western extension of the valley. A palaeo-river-bed can be observed on the way to Steuerberg and the Prekowa Höhe, see also section 3.1.1. In map in Fig. 3.12 these channels were interpreted as inter-glacial cave areas.

Downstream of Granaschmied the valley remains a typical steep V-valley (Fig. 3.13D). A variety of phyllitic outcrops (*OCc32,... OCc38*) are indicating a beck-rock incision within hard-rock. Apparently, the V-valley is incised between 170-200 m into a planation surface between Goggau and the Schwarzenbach junction. Further downstream the reliefs increases to about 300 m. The upstream incision between 170-200 m is comparable to the situation in the Metnitz valley downstream of Grades. Therefore, this correlation indicates the relevance of Pleistocene inter-glacial fluvial incision also for the Metnitz valley.

Close to Mellach the discharge already increased up to approximately 320 l/s, which is still a rather small run-up compared to the Gurk and Metnitz River discharge. But on the other hand, the Wimitz run-off is supposed to have been much larger in the Pleistocene due to bypasses of the Gurk and Teuchenbach into the Wimitz river-bed.

Between Mellach and Kraig the Wimitz leaves its V-shaped valley section at a Würmian terrace toward the north of Kraig and enters the Klagenfurter Basin where it joins the Glan River.

In Fig. 3.13A the planation surface above the Wimitz apparently fills the background of the picture, while the strong valley incision is only hinted. By hypsometric analysis in total two planation level are mapped within the Wimitzer Berge (Fig. 3.12).

In comparison to the parallel flowing and also non-glaciated middle Gurk River the Wimitz River appears by fare more steeply incised (Fig. 3.6). The Gurk valley is approximately twice

as broad as the Wimitz but discharges about ten times more water. But on the other hand, the Wimitz River shows a more rugged (hard-rock incision) and more narrow incised valley.

Figure 3.13.: **A**: Planation surface at the horizon above V-shaped incision of Wimitz valley, **B,C**: Wimitz valley at Goggau to the east and west, **D**: V-shaped Wimitz valley (east-ward view from Pisweg side road), **E**: Wimitz valley at Granaschmied knick point.

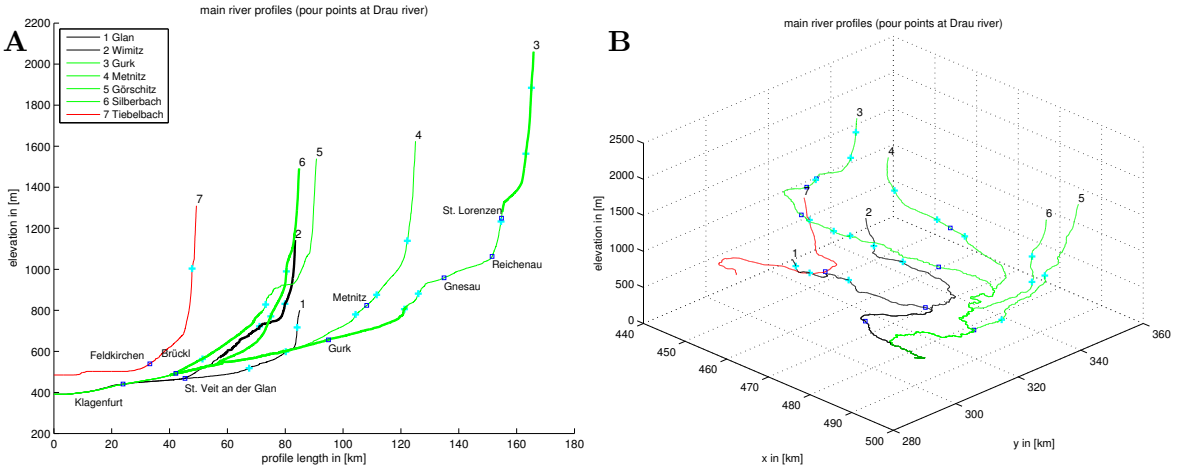

Figure 3.14.: **A**: Shows the river profile elevation of the main streams. Thick solid lines indicate non-glaciated parts. Knick points are marked with '+'. **B**: Visualises the steep channel slopes to the eastern Saualpe/Seetaler Alps and the western Nockberge, which surround the Nockberge Senke.

3.2. Stream Profile Analysis of the River Network based on DEM

Stream power analysis is applied to the Gurk and the Tiebelbach river systems. Both are tributaries to the Drau River. Besides a division of the Gurk River main trunk into an upper, middle and lower section also some of its major tributaries, namely in downstream direction the Metnitz, the Silberbach, the Görschitz, the Wimitz and Glan system are separately treated for a better spatial imagination. For the Gurk, Metnitz, Wimitz and Görschitz a detailed analysis is given. On the other hand, the appendix A.2 collated regression result tables of all investigated streams. The knick points of all river system are depicted within all the slope and geomorphological maps.

The elevation-profile overview of all main river trunks is given in Fig 3.14A. There are two pour points for all rivers at a junction to the Drau River. The lower pour point east of Klagenfurt is located at 405 m altitude, while the Tiebelbach pour point is located west of the Wörthersee at all altitude of 485 m. Fluvial main trunk segments (thick lines) are existent for the Gurk, the Wimitz, the Silberbach and the Görschitz. Except for the Tiebelbach also the remainder main river trunks of the Metnitz and the Glan possess sections of tributaries, which were never glaciated.

The Tiebelbach up to Feldkirchen shows very low slopes. Within the Gurk trunk above Klagenfurt, the Glan tributary departs from the main trunk of the Gurk. The Glan heads eastward against the flow direction of the palaeo-Drau glacier, while the Gurk sharply turns northward. The low slopes of the Tiebelbach and the Glan (Fig. 3.14B) are correlating with a flow direction in parallel to the palaeo-Drau glacier, while they are larger perpendicular to this direction.

At profile length upstream of Brückl the fluvial regime of the Gurk starts and the Görschitz and Silberbach depart from the main trunk. Both tributaries roughly show comparable slope values. At profile length of approximately 90 km, the Metnitz tributary departs and enters a glaciated region again.

The imagination of a bowl-shaped depression (Fig. 3.14B) was termed Nockberge Senke in section 1.1.2. This structure of unknown origin is penetrated by the Gurk River in EW direction and the Olsa River, a northern tributary of the Metnitz River in NS direction. The Olsa river system is not further regarded in this work. But for simplicity this notation was replaced by the Pöllauerbach, which floats down from the Mt. Grebenzen into the Olsa and after a few kilometres into the Metnitz, see Fig. 3.9.

Inside the depression to the west of the NS trending Althofen fault a dominant EW trending subsequent river network of Trellis type is observed (Fig 3.5, 3.9 and 3.12). This drainage type with parallel main trunks (Wimitz, Middle Gurk and Metnitz) and much shorter perpendicular tributaries is linked to tectonic root causes. This pattern is likely to develop within dipping or folded mountains out of low-grade meta-sedimentary rocks. The three parallel approximately EW trending ridges of the Wimitzer Berge (Zammelsberger and Schneebauerberg Rücken) and Mödringberge are showing an imbrication pattern with flat southern and steep northern slopes, which might represent the controlling factor. To the east, this pattern is broken by the NS trending Althofen and Görschitz faults. In this region of the Krappfeld-Gosau, the EW parallel imbrication is no longer apparent and consequently an insequent or dendritic river network developed in the vicinity of the Silberbach. Further to the east the Görschitz River and its eastern tributaries again become a Trellis type river network. Here active uplift can be observed, see section 3.2.5.

3.2.1. Upper Gurk River Network

The upper Gurk River profile (Fig. 3.15) is related to a river part with the highest topography and highest Pleistocene glacial incision dynamics compared to all other investigation areas in this work. Displayed are the elevation profile, the k_{sn} values, the log(slope)-log(catchment) plots and the χ-transformed elevation plot of the Gurk River main trunk.

Within the upper Gurk River down to approximately 130 km profile position three equilibrium river segments H_2, H_3, H_4 are found. The transition between glacial and fluvial regimes separates segment H_2 from the upper two fluvial segments H_3, H_4 (all profile segments in the figures within brackets were glaciated during the LGM).

In addition, the tributaries of the upper Gurk separate into fully glaciated regimes, which are joining in from the north (e.g. Saureggenbach, Holzbodenbach, Winkelbach) and many fluvial regimes, which flow down from a relict landscape from the east. As examples for the fluvial regimes, the uppermost two segments of the Gurk channel and the Görzbach channel are discussed in greater detail due to its relation to a planation surface and to highlight morphometric aspects of the Nockberge Senke rim.

3.2.1.1. Glacial Regimes

The segment H_2 downhill of a big elevation step within the glaciated area of the upper Gurk (Fig. 3.15) exhibits extreme low regression estimates for k_s and θ, with very high uncertainty for the θ values. This parameter finding is interpreted as one proxy for a glacial regime.

The glacial transition zone is probably reflected by a kick point just below St. Lorenzen (Fig. 3.15) situated on top of a steep slope above Ebene Reichenau where the glaciated zone is entered. This about 220 m high step might represent a hanging valley, which probably formed by the extensive carving of the glacier coming from the Turracher Höhe during the Pleistocene. On the other hand, the geological map (Fig. 2.2) shows moraine sediments also in the head section of the Andertalbach. Therefore, it is not clear whether this step is already retreated for approximately 2.5 km upstream from Reichenau, which suggests older formation ages than the LGM, or if the LGM map together with the Andertal lake hypothesis needs to be revised.

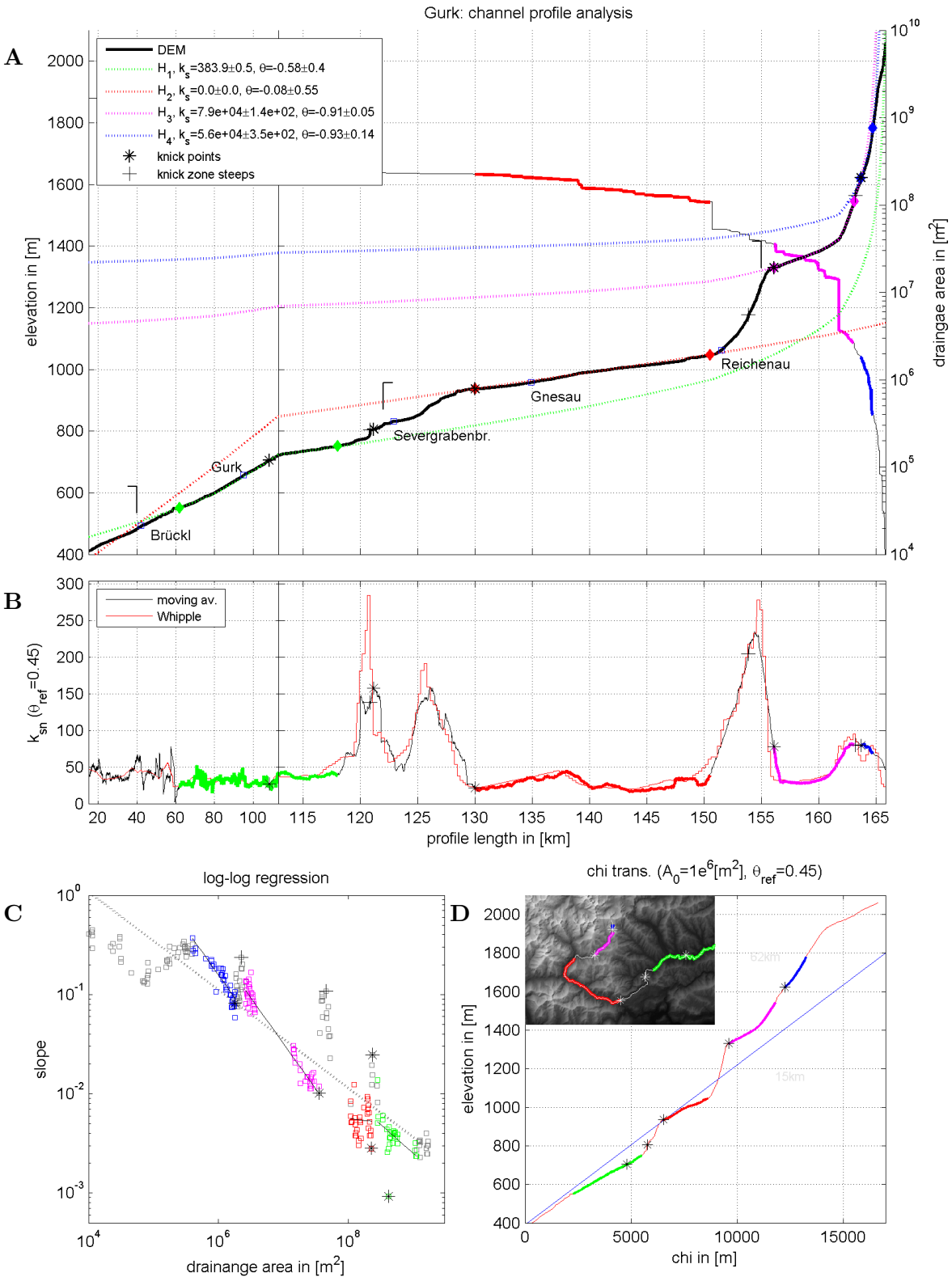

Figure 3.15.: The Gurk River main trunk with glacial overprint in its middle section (red) reveals two planation surfaces for H_3, H_4. H_2 alings with a planation level of the middle Gurk. **A**: Elevation and drainage profile, brackets indicate LGM extent, **B**: k_{sn} plot, **C**: log(S)-log(A) plot and **D**: χ-transformed elevation plot. Colours relate to k_s, θ regression sections.

A hanging valley can also be interpreted in the river profile analysis of the Peiningbach more downstream but is hardly visible in the Görzbach profile (Fig. 3.16).

3.2.1.2. Fluvial Regimes

The upper two segments H_3, H_4 above the big elevation step in the upper Gurk River profile belong to the non-glaciated area (Fig. 3.15). Both segments reveal with $0.91 < \theta < 0.93$ relatively high θ values, which indicates that the bed-rock shear stress is driven by velocity, which correlates with slope driven river-bed erosion. On the other hand, the k_{sn} value for the lower segment is by factor two smaller compared to the upper segment. In consensus with the findings of Van Husen (2012) this could be explained by the erosive protection of the river bed by lake sediments, see also section 3.1.1. A comparable k_{sn} pattern but with much smaller extent of the lake section is observed for the Andertalbach (not shown).

The Görzbach was investigated closer as it accents on top of the rim structure of the Nockberge Senke and due to its non-glacial overprint above the village of Zedlitzdorf. The profile shows no pronounced hanging valley despite its proximity to the palaeo-glacier in the Gurk River main valley. Two equilibrium segments H_2, H_3 are separated by a knick point in its upper reaches (Fig. 3.16). Both θ values are identical at 0.76 suggesting a rather slope driven regime. The river bed shows steady steep accent without any meandering sections (Fig. 3.4A) and a flattened topography in the head area (Fig. 3.4B), which belongs to the relict landscape.

The mean k_{sn} values of H_2, H_3 with approximately $60 - 100$ of the Görzbach are comparable with the upper reach H_4 of the Gurk and also with the two uppermost segments H_3, H_4 of most rivers at the eastern side of the rim, see next section. Therefore, a moderate uplift/erodibility signals can be observed for the western Nockberge Senke rim. For the Görzbach the k_{sn} is decreasing toward the channel head, which can also be observed for the Peiningbach in the downstream direction.

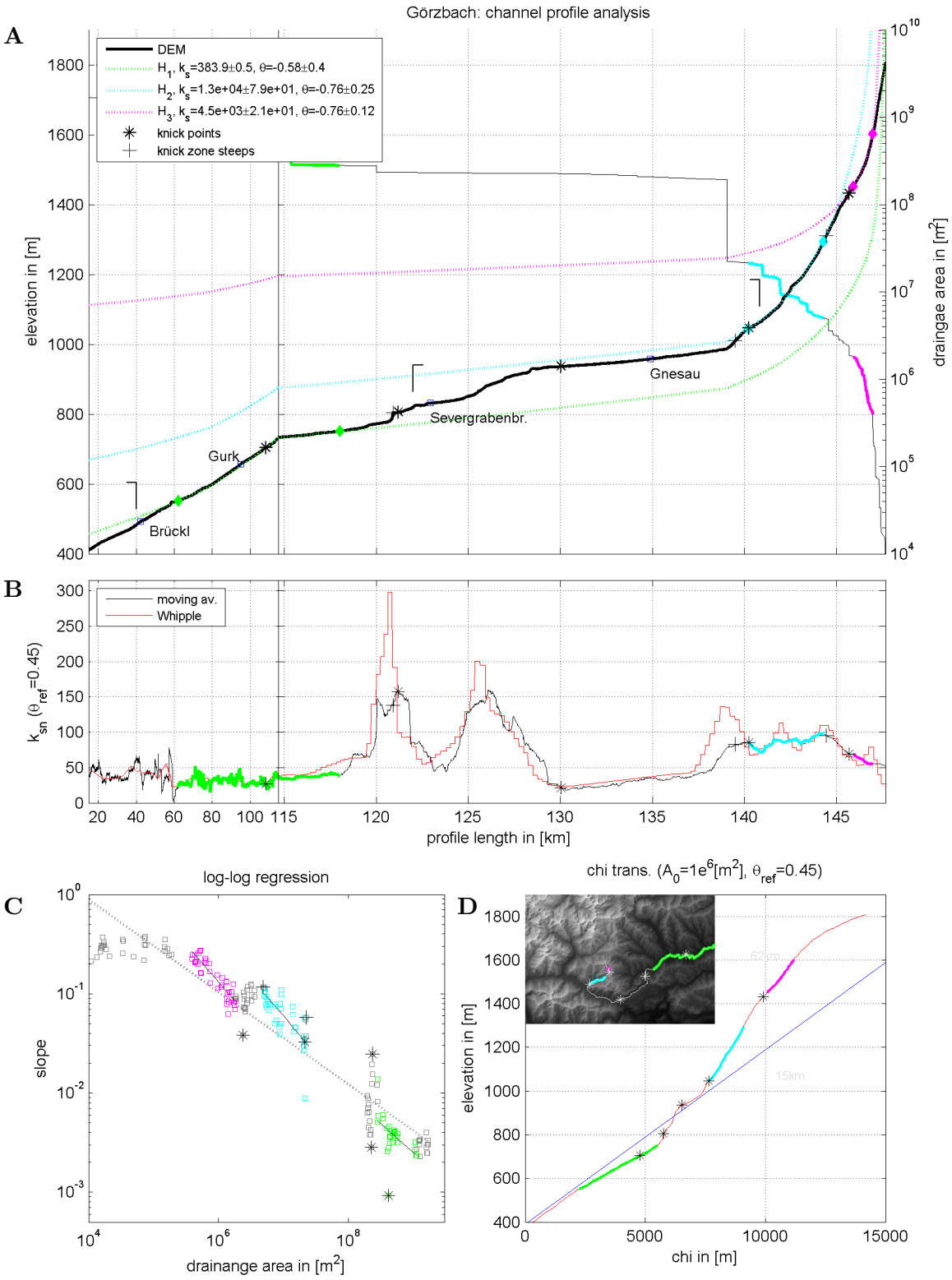

Figure 3.16.: The Görzbach (fluvial channel head) flows down to the western side of the Nockberge Senke rim. A planation level is identified for H_3. **A**: Elevation and drainage profile, brackets indicate LGM extent, **B**: k_{sn} plot, **C**: log(S)-log(A) plot and **D**: χ-transformed elevation plot. Colours relate to k_s, θ regression sections.

3.2.1.3. Nockberge Senke Rim Breakthrough

Back within the Gurk River trunk a comparison of H_1, H_2 (Fig. 3.15) shows equal low k_{sn} values on the eastern (H_1) and western side (H_2) of the rim, but high values are gained within the cutting zone through the rim, indicating high uplift/erodibility (see also the k_{sn} mapping in Fig. 3.1). Within this high k_{sn} region a second big step of about 120 m height along approximately ten kilometres distance is located. The Enge Gurk is part of this section but shows no glacial imprints at its side walls, which is interpreted to be the LGM transition margin (Van Husen, 2012). Therefore, the whole step can't be explained by glacial processes but is supposed to refer to uplift/erodibility at the Nockberge Senke rim.

In addition, the profiles P1 and P2 above Thörl (Fig. 3.3) are sampling the reliefs at two cross-sections within the glacially overprinted section, estimating a maximum incision depth through the Nockberge Senke eastern rim between 1600-900 m = 700 m and 1600-950 m = 650 m. Therefore, it is likely that the incision from top heights down to the glaciated segment H_2, which results in an incision of 650-700 m is supposed to be eroded by glacial buzz-saw.

3.2.1.4. Summary of Planation Surfaces and Erosion/Uplift Regimes

The prolongation of all three segments H_2, H_3, H_4 of the upper Gurk main trunk (Fig. 3.15) are interpreted as proxies for planation surfaces at 900 m, 1200 m and about 1400 m measured at the Enge Gurk location (121 km profile length). Interestingly the glaciated segment H_2 aligns quite well with a dominant planation surface within the downstream middle Gurk valley.

The regression segments within all upper Gurk tributaries are classified with respect to altitude levels at profile length position 130 km (Fig. 3.17A). It turns out that clustering is apparent and relict surfaces at about 900 m (cyan), 1200 m (magenta) and at 1400 m (blue) are existent. The steep step represents the potential hanging valley. It is even more enlarged for the Holzbodenbach, the Saureggenbach and the Winkelbach, which come down from the Turracher Höhe. All rivers down from the Turracher Höhe do not show equilibrium segments above the step and are therefore not presented. Due to the absence of faulting systems and lithological

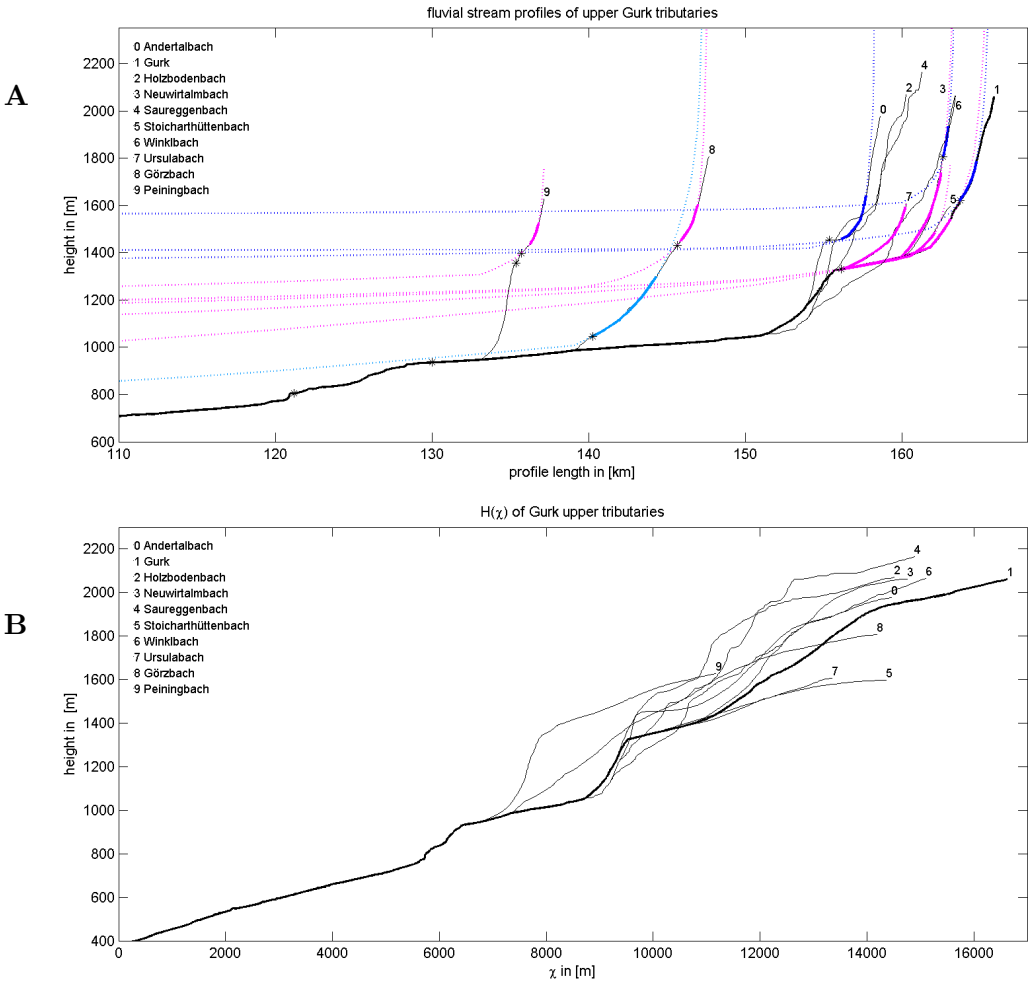

Figure 3.17.: **A**: Overview of prolonged (colour, dashed) upper Gurk River tributaries regression segments of 960 m, 1220 m and >1460 m height above Enge Gurk location (121 km profile length). **B**: Shows the elevation model $H(\chi)$ with strong deviations from linear trends.

unconformity in this area, it seems likely that the erosive power of the palaeo-glacier may have changed at this altitude, e.g. by ground temperatures high enough to allow for groundwater.

In the χ-transformed elevation model $H(\chi)$ overview of all tributaries (Fig. 3.17B) linear segments are indicating stable equilibrium channel segments. It turns out that the downstream tributaries of Peiningbach and Görzbach considerably vary at $\chi \approx 8000$ from the history of all remainder rivers. This might be explained by a transition from the glacially overprinted upper Gurk, to the hanging valley section of the Peiningbach and the possibly fluvial developed

Görzbach. But within its head section, both curves appear to have an equal linear trend, which gives further evidence to the existence of the planation surface above 1400 m. For $\chi > 9000$ most profiles show close neighbouring $H(\chi)$ curves. In particular, all tributaries turning east from Ebene Reichenau show parallel lines up to $\chi < 11000$, which might be explained by their common history as being part of glacial lakes. But for higher χ values and for the remainder glacially overprinted reaches more distortion in the trends can be observed, indicating a variable setting of uplift/erosive processes.

3.2.2. Middle Gurk River Network

Inside the Nockberge Senke, the middle Gurk River section is located. The main water course with the highest discharge in the study region is fed by tributaries with mostly negligible water supply except for the Griffenbach and the Glödnitz. In addition, both tributaries are the only glaciated river courses of the middle Gurk section. To the west of these tributaries the Leonhardsbach, Sirnitz, Stronbach and Hochrindlbach flow down the Nockberge Senke rim and to the east many tributaries from the Mödringberge and Wimitzer Berge are characterising the topographic low of the Nockberge Senke area.

3.2.2.1. Fluvial Regimes from the Nockberge Senke Rim

Above the Sirnitz River knick point at 120.8 km profile length all tributaries (Figs. 3.18, 3.19 and 3.20) show a regression segment H_2, which identifies a planation surface at about 800-820 m height. With $0.84 < \theta < 1.76$ all H_2 segments show slope dominated regimes, which is already outside a plausible range for the Leonhardsbach. In contradiction, field observation proved for the Sirnitz and the Leonhardsbach (Stronbach not visited) meandering river-beds (Fig. 3.7F,G) at altitudes below 900 m. Those segment regression should result in low θ values, which is not the case.

The $H(\chi)$ analysis shows for all rivers clearly a knick point between the H_2 and H_3 segments, which is difficult to find in the log-log data and also in the field (upper Sirnitz private land not visited). For all above given tributaries also a short segment H_3 is found, which identifies a planation surface around 880-1000 m.

The k_{sn} values for all three river shows highest values around 100 within the H_2 segment but plunges for about 30% within the H_3 segment. This decay indicates a decrease of erodibility/uplift in the summit region, which is interpreted as the transition between incision and relict surface. The already mentioned knick point within this zone is supposed to mark the border of the planation surface.

It is interesting to note that the Görzbach tributary at the western side of the rim starts above that altitude of 900 m, missing out the low k_{sn} segments of H_2 on the eastern side (Fig. 3.3A). The k_{sn} values of the Görzbach to the west and all eastern tributaries Leonhardsbach, Sirnitz and Stronbach identify an uplift/erodibility impulse for the western Nockberge Senke rim of comparable strength.

The Hochrindlbach (not displayed here) also shows increased k_{sn} values in the upper reach at the rim area and a decrease again for the top region. This decrease is much more pronounced for the Hochrindlbach compared to Leonhardsbach, Sirnitz and Stronbach, which gives evidence that this decrease in the head section is real and relates to an older relict landscape.

3.2.2.2. Glacial Regimes inside the Nockberge Senke

The next tributary further four kilometres downstream of the Hochrindlbach - Gurk River junction is the Griffenbach. It contributes to about 1000-2000 l/s discharge a large fraction into the Gurk. The river profile analysis (not displayed) reveals a steadily growing k_{sn} value from 50 up to 100. This k_{sn} ramp is also discovered more downstream of the Gurk at tributaries within the Mödringberge. The top-most equilibrium segment H_3 of the Griffenbach profile plunges in its downstream prolongation below the given channel profile, indicating a serve disequilibrium. On the other hand, a cirque-glacier is revealed in the upper Griffenbach valley (Fig. 3.5). Therefore, the upper valley is regarded to be glacially overprinted.

The Glödnitz river tributary is located further two kilometres downstream. Its discharge is comparable to the Griffenbach. According to Van Husen (2012), to DEM surface textures, the deposition of a huge amount of Würmian sediments along the course and at the Gurk River junction (see Fig. 2.2) and due to the broad cross-section of the valley (see Fig. 3.7D) a strong glacial overprint can be assumed. The Braunsberg terrace, build out of fluvioglacial Würmian

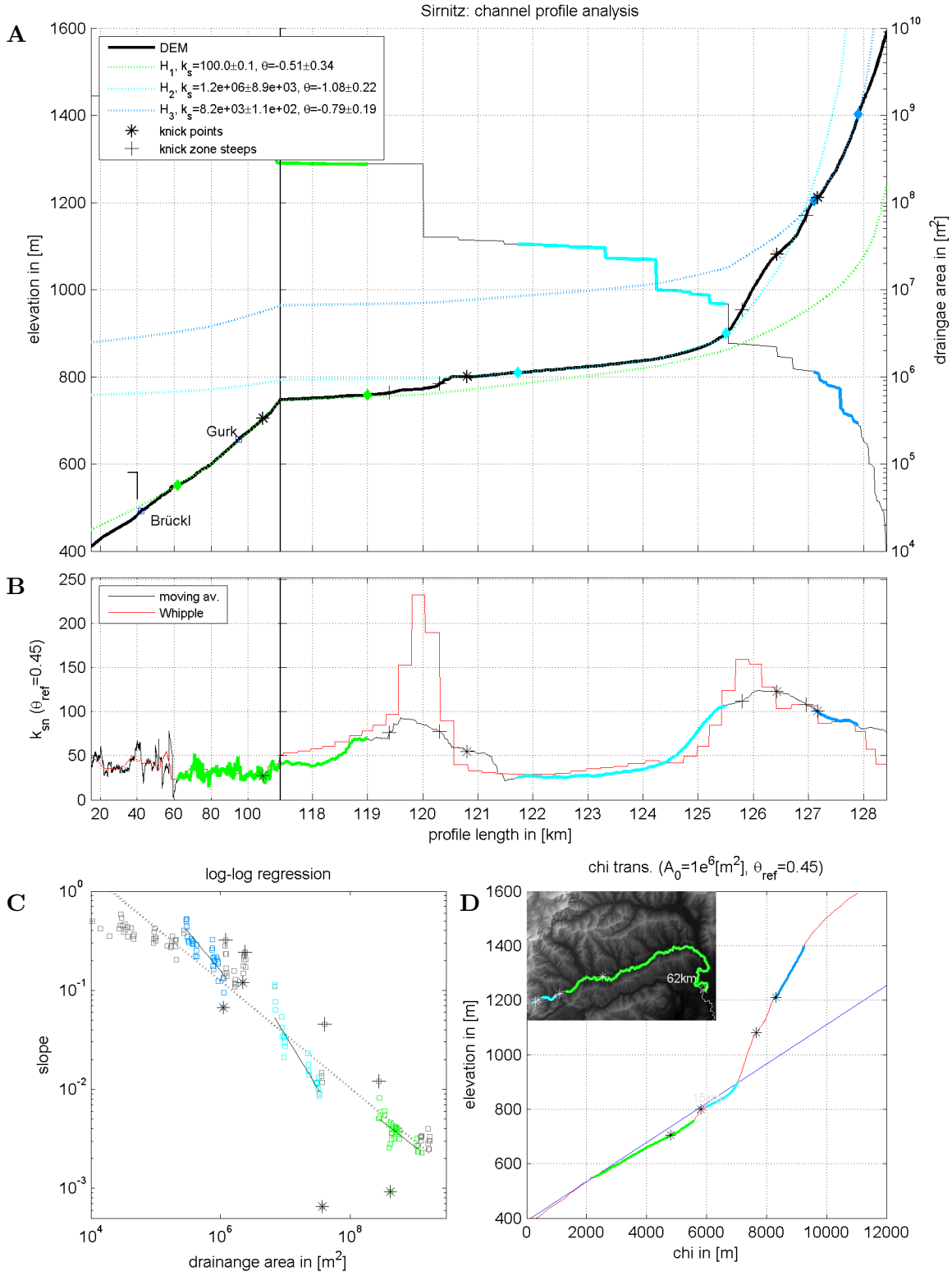

Figure 3.18.: The Sirnitz (fluvial channel) flows down to the eastern side of the Nockberge Senke rim. Two planation levels for H_2, H_3 are observed. **A**: Elevation and drainage profile, brackets indicate LGM extent, **B**: k_{sn} plot, **C**: log(S)-log(A) plot and **D**: χ-transformed elevation plot. Colours relate to k_s, θ regression sections.

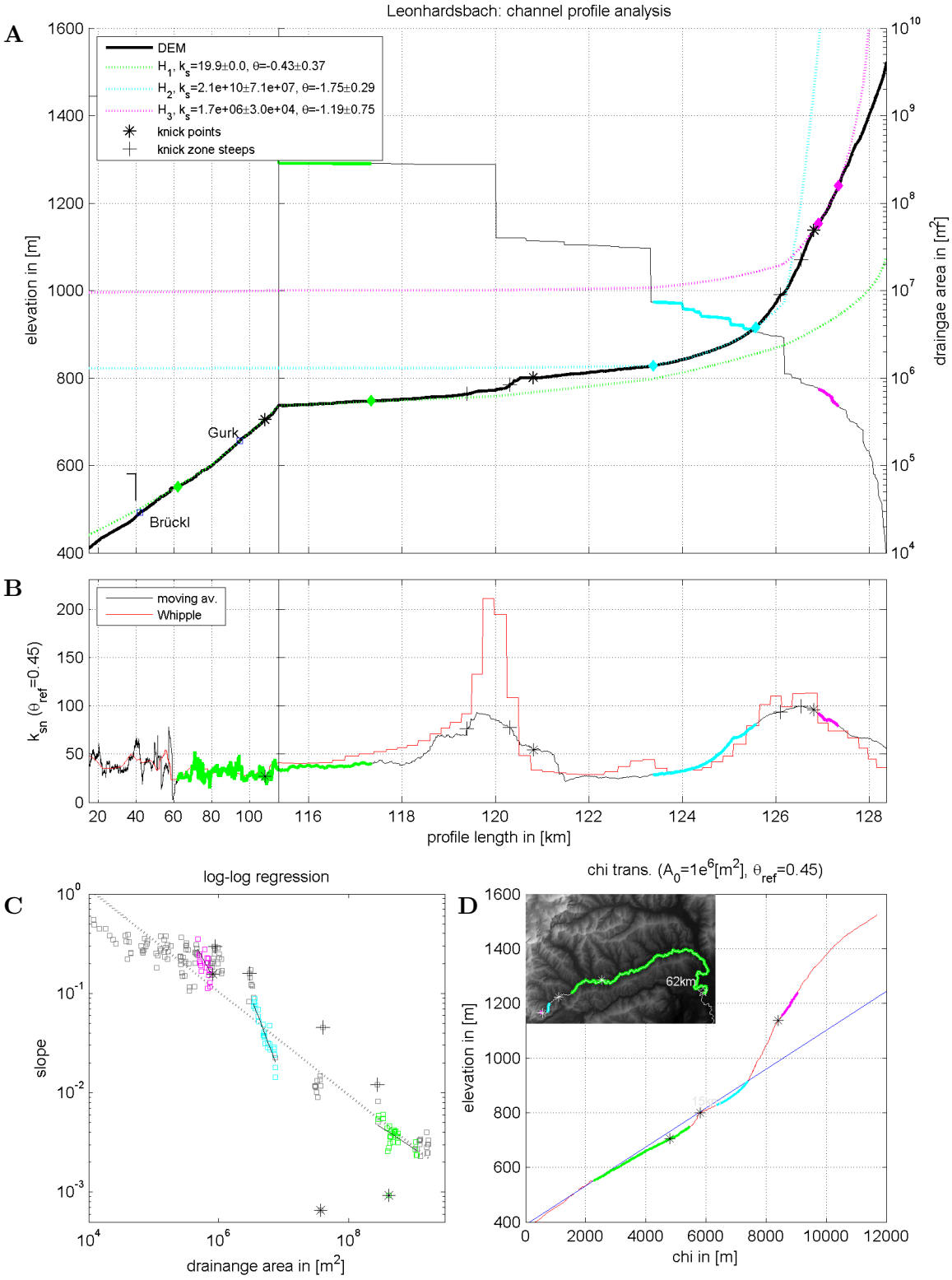

Figure 3.19.: The Leonhardsbach (fluvial channel) flows down to the eastern side of the Nockberge Senke rim. In analogy to the Sirnitz two planation levels for H_2, H_3 are observed. **A**: Elevation and drainage profile, brackets indicate LGM extent, **B**: k_{sn} plot, **C**: log(S)-log(A) plot and **D**: χ-transformed elevation plot. Colours relate to k_s, θ regression sections.

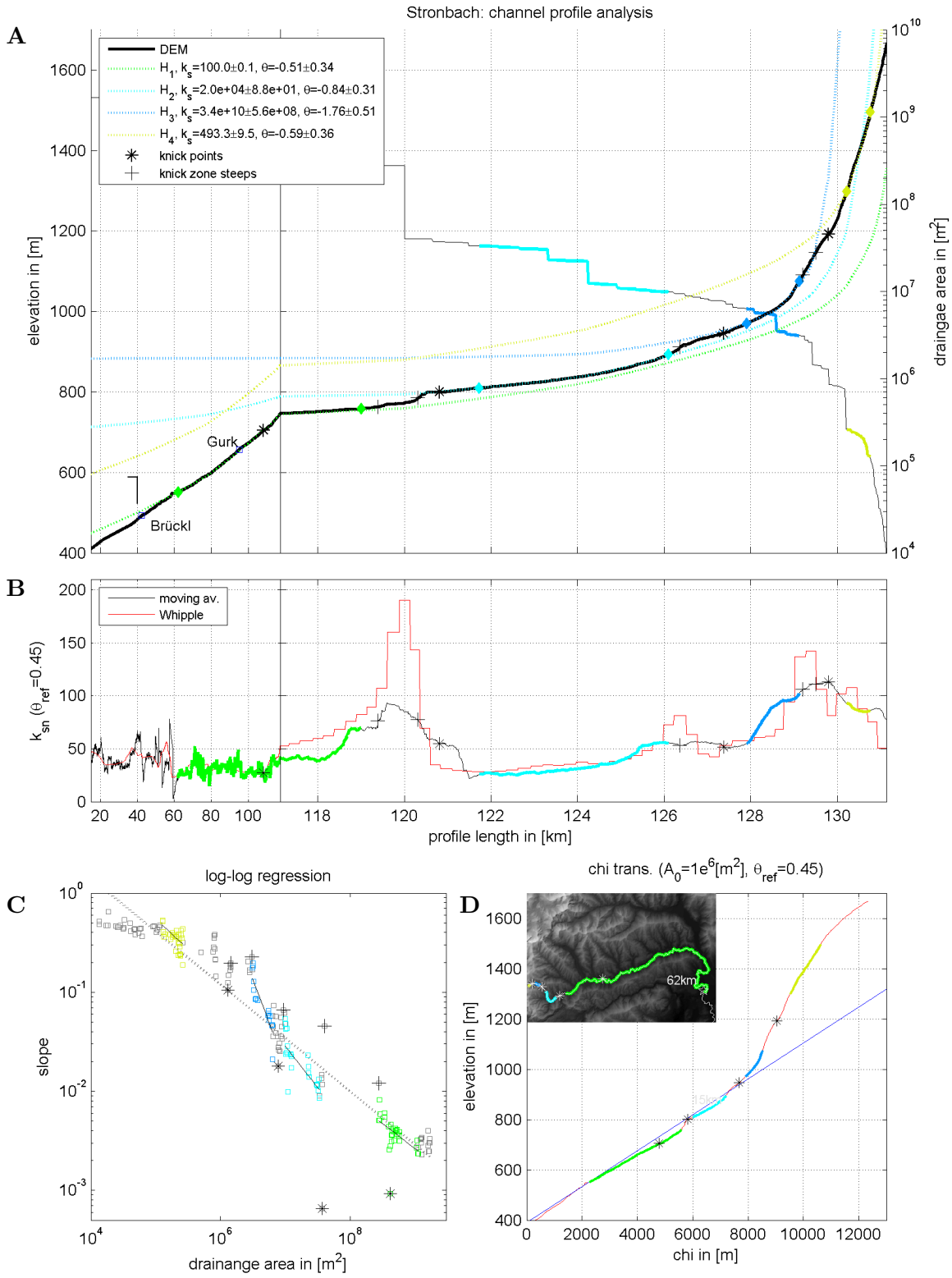

Figure 3.20.: The Stronbach (fluvial channel) flows down to the eastern side of the Nockberge Senke rim. Two planation levels for H_2, H_3 are observed. The highest level for H_4 is not taken into account. **A**: Elevation and drainage profile, brackets indicate LGM extent, **B**: k_{sn} plot, **C**: log(S)-log(A) plot and **D**: χ-transformed elevation plot. Colours relate to k_s, θ regression sections.

phyllitic coarse sand to cobbles at the southern side of the Gurk on-top of a green-schist bedrock base (*OCc15a,b*) is the largest gravel terrace in the area. The river profile analysis of the Glödnitz (not shown here) shows two regression segments upstream of the junction. The lower H_2 regression ($\theta = 0.8$) shows no sign of glacial overprint and seems to be equilibrated but on the other hand, it is hardly possible to find an equilibrium channel above 850 m altitude upstream of a steep valley step of 50 m height. In addition, the k_{sn} values remain small below 30 and do not show the ramp signature of adjacent tributaries. Because of this inconsistencies, the Glödnitz river knick point was not used for geomorphological interpretations.

3.2.2.3. Fluvial Regimes and Gurk Valley Fault Activity inside the Nockberge Senke

The Mödringberge massif stretches eastward to the Glödnitz. Along with its southern ridge in total eleven tributaries were investigated. Within the Wimitzer Berge in total fife tributaries joining in from the south were studied.

Exemplary for the Mödringberge the river profile analysis of the Mödringbach, the Draschelbach and the Langwiesenbach (Fig. 3.7E) and the Olschnöggbach are displayed (Figs. 3.21-3.24). The Draschelbach and the Langwiesenbach represent two tributaries before and after a fault system just 500 m downstream of the village Gurk (Fig.3.5).

The Mödringbach profile shows an abrupt slope angle change at the junction to the main stream, which correlates with the strong change of drainage area at that point. Only 500 m downstream within the Gurk trunk a knick point is observed, which is attributed to a dam construction in Weitenfeld. The Draschelbach is the next river downstream but the first tributary upstream of the fault. It exhibits a small step of ≈20 m height at the junction of the Gurk and a pronounced knick point zone above 900 m, which is located close to the fault region. After crossing the fault (95 km profile length) downstream no sign of a disequilibrium is observed (Fig. 3.22). Only the k_{sn} values based on Whipple et al. (2007) show a ramp up signature, which needs to be questioned as it occurs for each Gurk River junction. Downstream of the fault the Langwiesenbach and the Olschnöggbach no longer show a pronounced transition point at the Gurk River junction. In analogy to the Draschelbach also the Langwiesenbach shows a pronounced knick point in its upper reach above 1000 m.

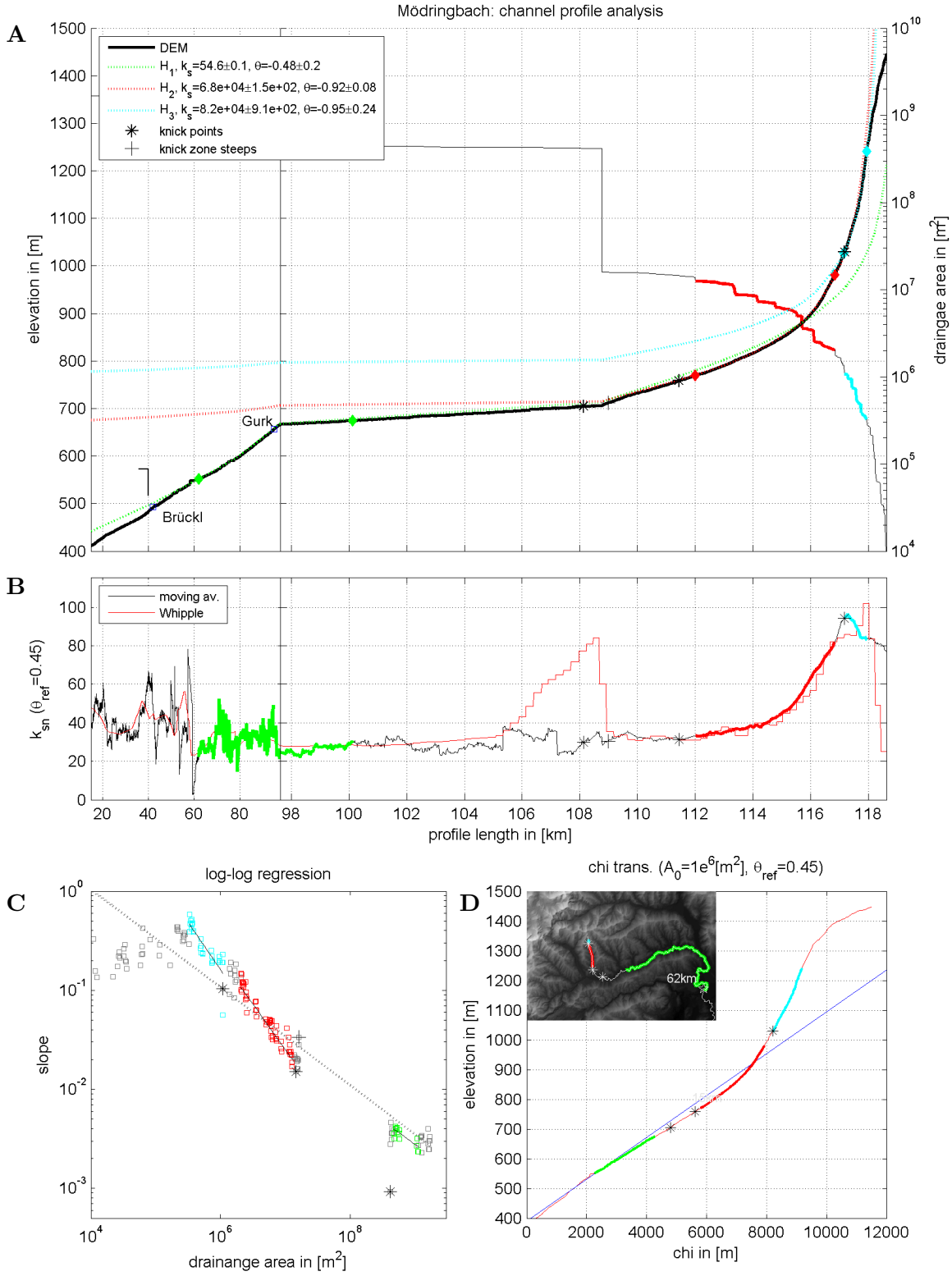

Figure 3.21.: The Mödringbach (fluvial channel) is a Mödringberge tributary and reveals a common planation surface for H_3. **A**: Elevation and drainage profile, brackets indicate LGM extent, **B**: k_{sn} plot, **C**: log(S)-log(A) plot and **D**: χ-transformed elevation plot. Colours relate to k_s, θ regression sections.

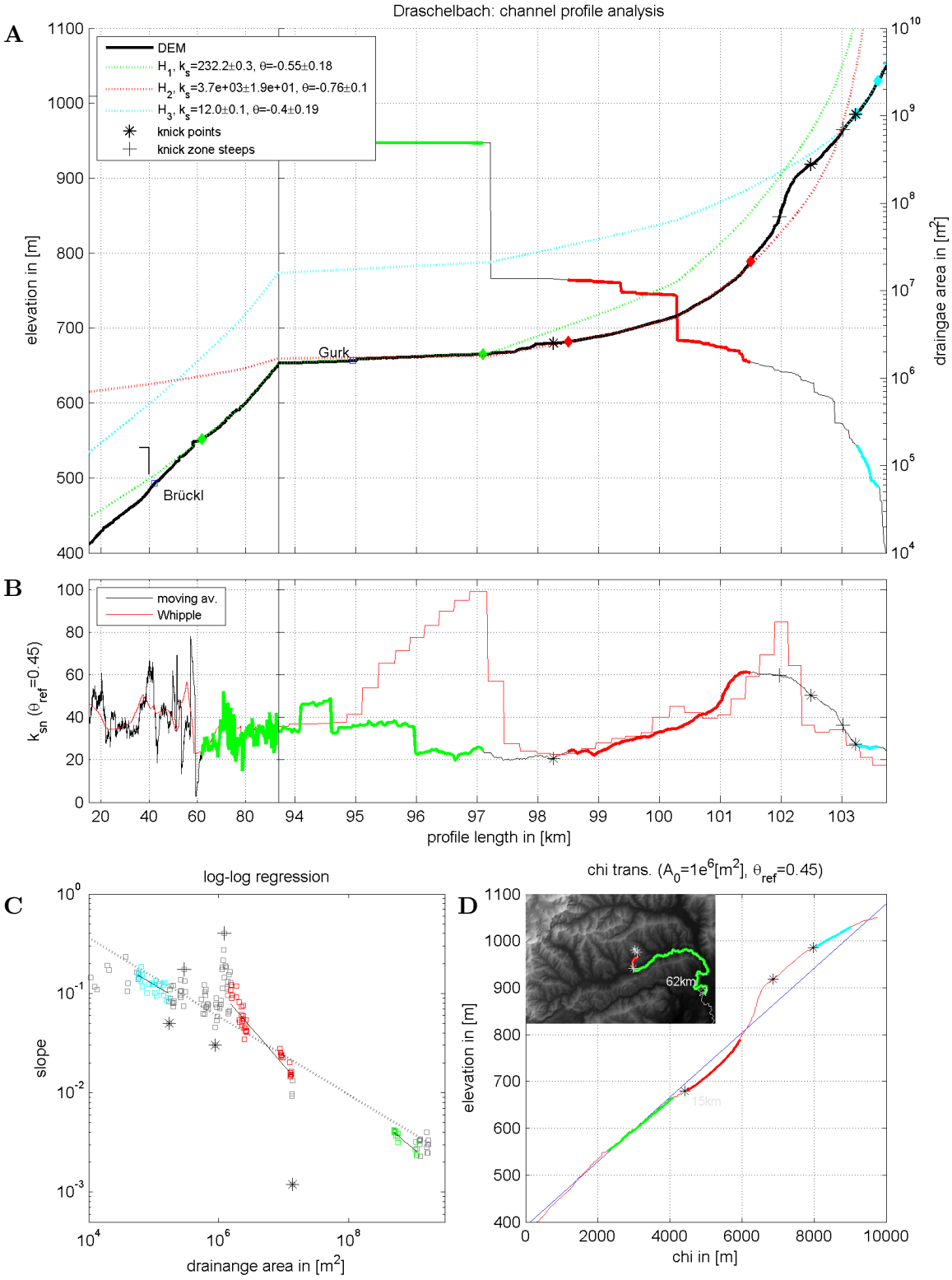

Figure 3.22.: The Draschelbach (fluvial channel) is a Mödringberge tributary just upstream of a NW trending fault at Gurk village. A planation level is identified for H_3 and a pronounced knick point is supposed to relate to the fault. **A**: Elevation and drainage profile, brackets indicate LGM extent, **B**: k_{sn} plot, **C**: log(S)-log(A) plot and **D**: χ-transformed elevation plot. Colours relate to k_s, θ regression sections.

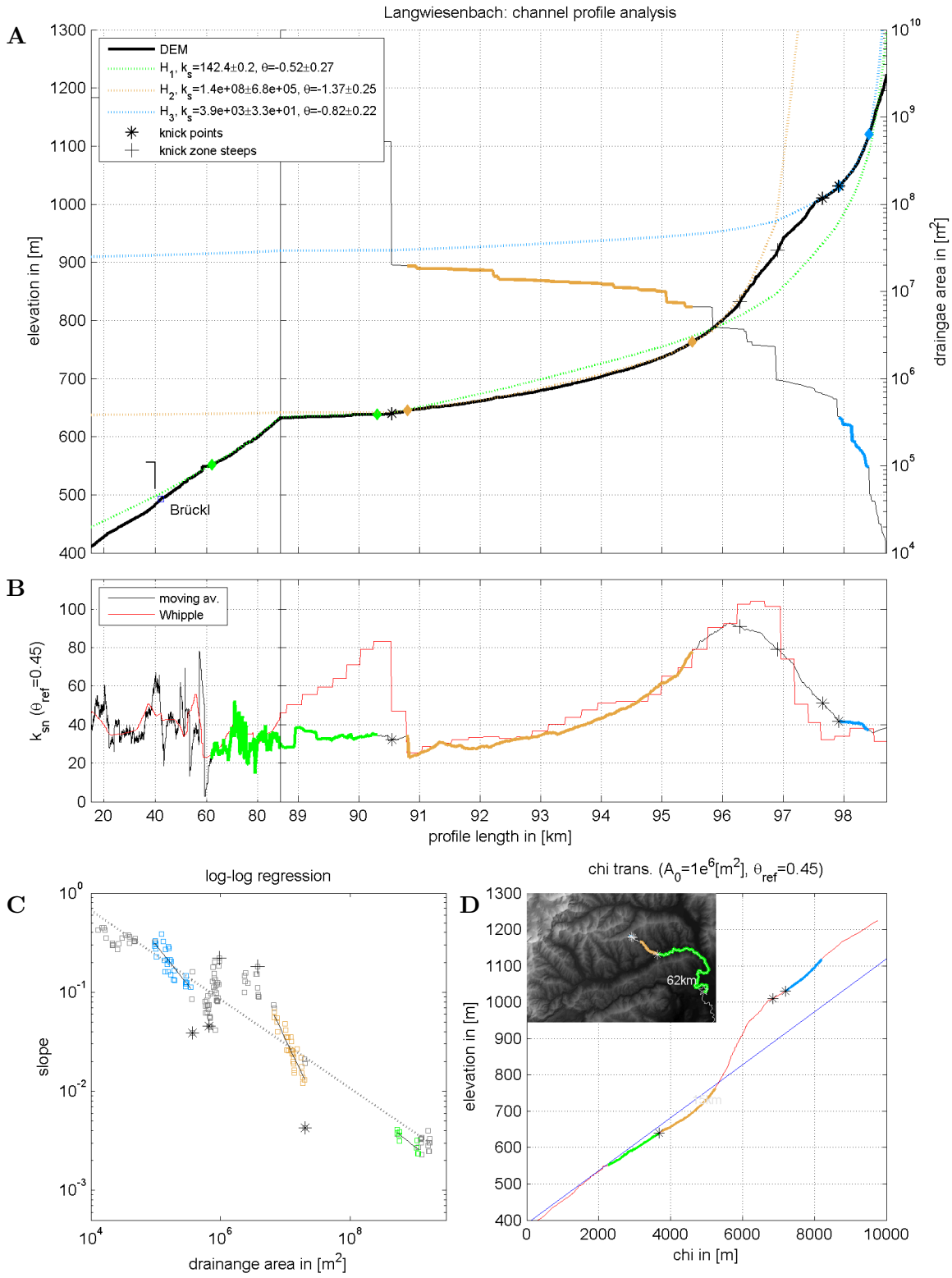

Figure 3.23.: The Langwiesenbach (fluvial channel) is a Mödringberge tributary just downstream of a NW trending fault at Gurk village. A planation level is identified for H_3 and a pronounced knick point is supposed to relate to the fault. **A**: Elevation and drainage profile, brackets indicate LGM extent, **B**: k_{sn} plot, **C**: log(S)-log(A) plot and **D**: χ-transformed elevation plot. Colours relate to k_s, θ regression sections.

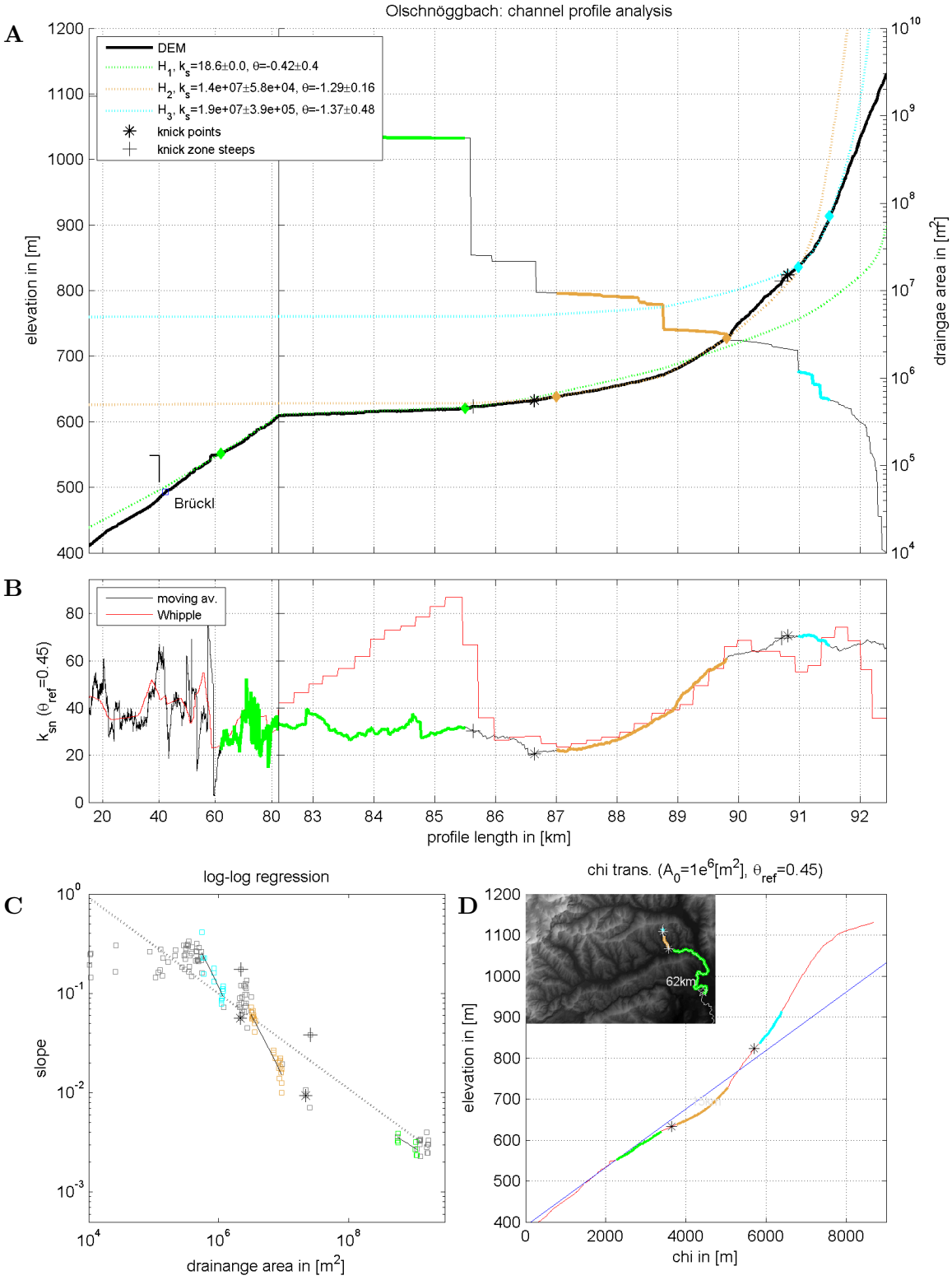

Figure 3.24.: The Olschnöggbach (fluvial channel) is a typical fluvial Mödringberge tributary. A planation level is identified for H_3. **A**: Elevation and drainage profile, brackets indicate LGM extent, **B**: k_{sn} plot, **C**: log(S)-log(A) plot and **D**: χ-transformed elevation plot. Colours relate to k_s, θ regression sections.

All tributaries also exhibit a short head segment H_3 with high regression uncertainty, often already within very small catchments. In particular, the log-log regression and the $H(\chi)$ plots are identifying a knick point between segment H_2 and H_3, which is not easily recognised in the field. A hypsometric investigation of the knick points reveals a jump from 820 m at the Olschnöggbach to above 920 m for all remainder rivers. This results in an abrupt change of level of approximately 100 m at the Mödringberge between eastern and western Langwiesenbach riverside. This can also be observed in the field (*OCc4, OCc6, OCc7*) and in the geomorphological map (Fig. 3.5).

In summary, the fault downstream of Gurk village can be considered as a now inactive fault. In the past it decoupled the up- and downstream tributary properties slightly (still preserved due to a lack of stream power), but since its inactivity, the strong stream power of the Gurk already transported this probably small tectonic uplift step far upstream, e.g. up to the rapid beside the Braunsberg terrace.

Interestingly, the investigation of the H_2 segments exhibits steadily increasing k_{sn} values along the slope toward the channel head (see also Griffenbach). In general, the values remain below 100. This is interpreted as an uplift/erodibility event, which gently increases upslope. In addition, the parallel shift in the log-log plot between H_2 and H_3 and the smooth transition zone in the $H(\chi)$ plots - termed stretch zone in Royden and Perron (2013) - are backing up this finding. Both, k_{sn} values and the parallel shift are indicating a higher pulse for the H_2 compared to the H_3 section. But without existing fault systems on a local scale, high uplift at ridge slopes appears unlikely. Therefore, when assuming equilibrium conditions this phenomenon is interpreted to be controlled by erodibility. Because of this, high k_{sn} values correspond to landscapes with low erodibility, e.g. bed-rock. For the main trunk of the middle Gurk $k_{sn} \approx 35$ is found, indicating very low uplift/erodibility for H_1 along the valley. On the other hand, when assuming disequilibrium, a knick point steep zone is expected to travel upstream. This characteristic can only be weakly observed in the field.

The opposite side of the middle Gurk valley down from the Wimitzer Berge is even more difficult to investigate due to mostly missing watercourses. Fife channels were investigated, namely the Albeck Schattseite river, the Hafendorfbach, the Pirkerkogelbach, the Kainzbach and the

Zammelsbergbach. The Pirkerkogelbach with about 1-1.5 l/s discharge close to Straßburg was visited in the field, see Fig.3.7C.

In total two equilibrium segments were identified above the main trunk (Fig. 3.25). In the log-log plot a clear knick point between H_1, H_2 and H_2, H_3 can be identified. The lower one shows a strong reduction in slope at the foot of the knick point steep, which is characteristic for glacial induced hanging valleys. But in this case, the reason might be an anastomosing Gurk River bed - maybe short term - of the downstream main trunk, which could have flattened the foot of the knick point zone. At the highest knick point at about 880 m a clear parallel shift of the two segments H_2, H_3 indicates an uplift/erodibility pulse within the lower section H_2, which is also confirmed by k_{sn} values. Again here this phenomenon is interpreted by low erodibility in the H_2 section (bed-rock) but a slightly higher erodibility in the H_3 part (unconsolidated terrace sediments).

The $H(\chi)$ plot is interpreted likewise. Between H_1, H_2 a stretch zone is identified, which means as a consequence, that the vertical profile movement of H_2 supersedes H_1. Together with the interpretation that erosion is the key, this means that the Gurk trunk is eroded more strong that its slope leading to deeper valley incisions. Between H_2, H_3 an abrupt gradient change can be observed, which is interpreted as a consuming knick point (Royden and Perron, 2013). It follows that H_2 is elevating more rapidly than H_3, which is in consensus with a higher erodibility in the H_3 section. Furthermore, out of the existence of the mentioned zone types, it can be followed that the slope exponent needs to be $n > 1$. Only then steeper slopes travel faster upward compared to flatter ones.

Finally, the downstream prolongation of the highest H_3 segment reveals a planation surface also on the southern side of the Gurk valley of about 785 m height above the Gurk main trunk. This fits quite well with the finding at the Olschnöggbach from the opposite northern side. Therefore, additional evidence of the existence of a relict landscape within the middle Gurk valley section is given. In Fig. 3.7A this terraces at the mid to right-hand side of the picture can be seen.

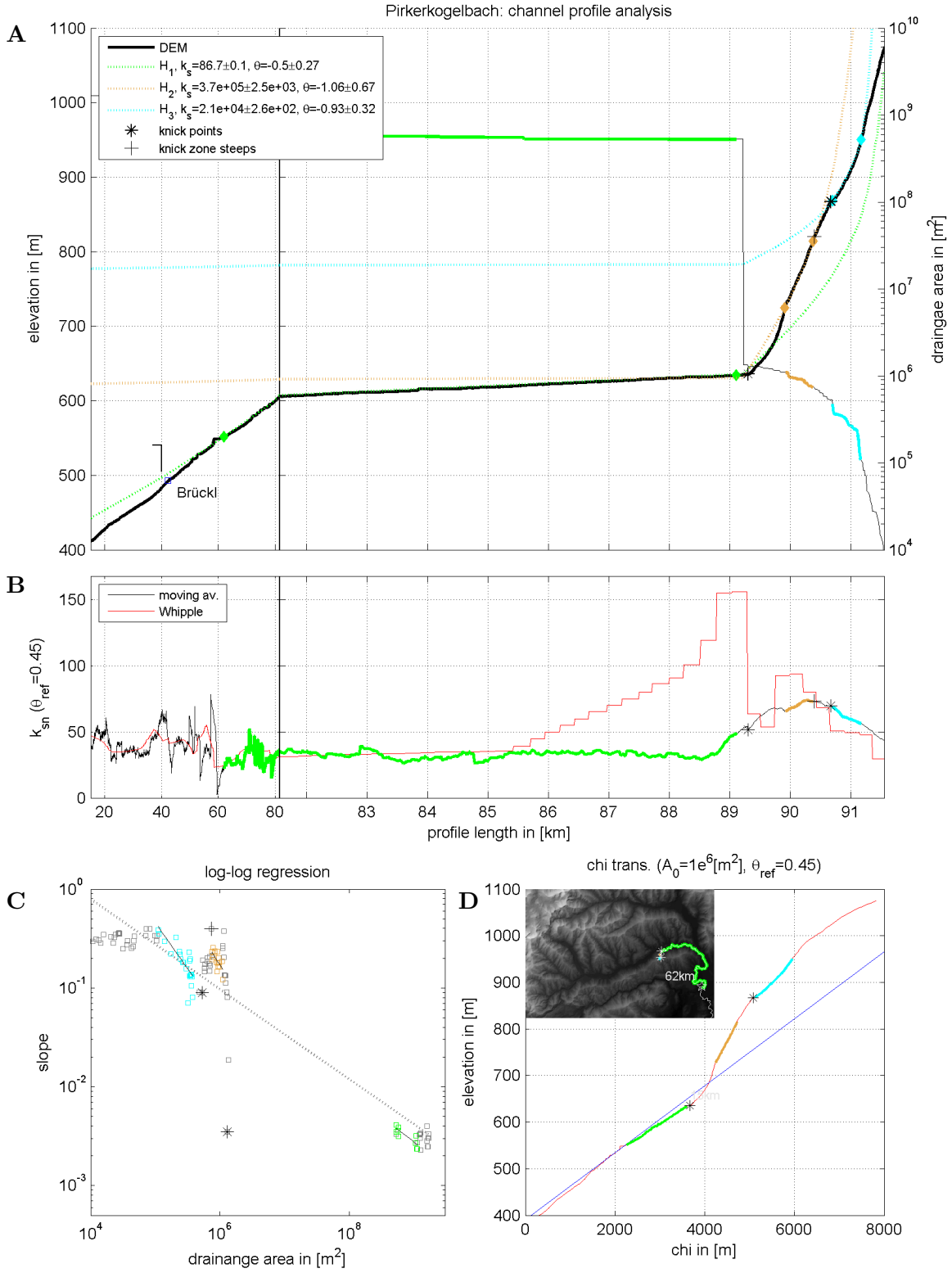

Figure 3.25.: The Pirkerkogelbach (fluvial channel) is a typical Wimitzer Berge tributary and reveals a planation level for H_3. **A**: Elevation and drainage profile, brackets indicate LGM extent, **B**: k_{sn} plot, **C**: log(S)-log(A) plot and **D**: χ-transformed elevation plot. Colours relate to k_s, θ regression sections.

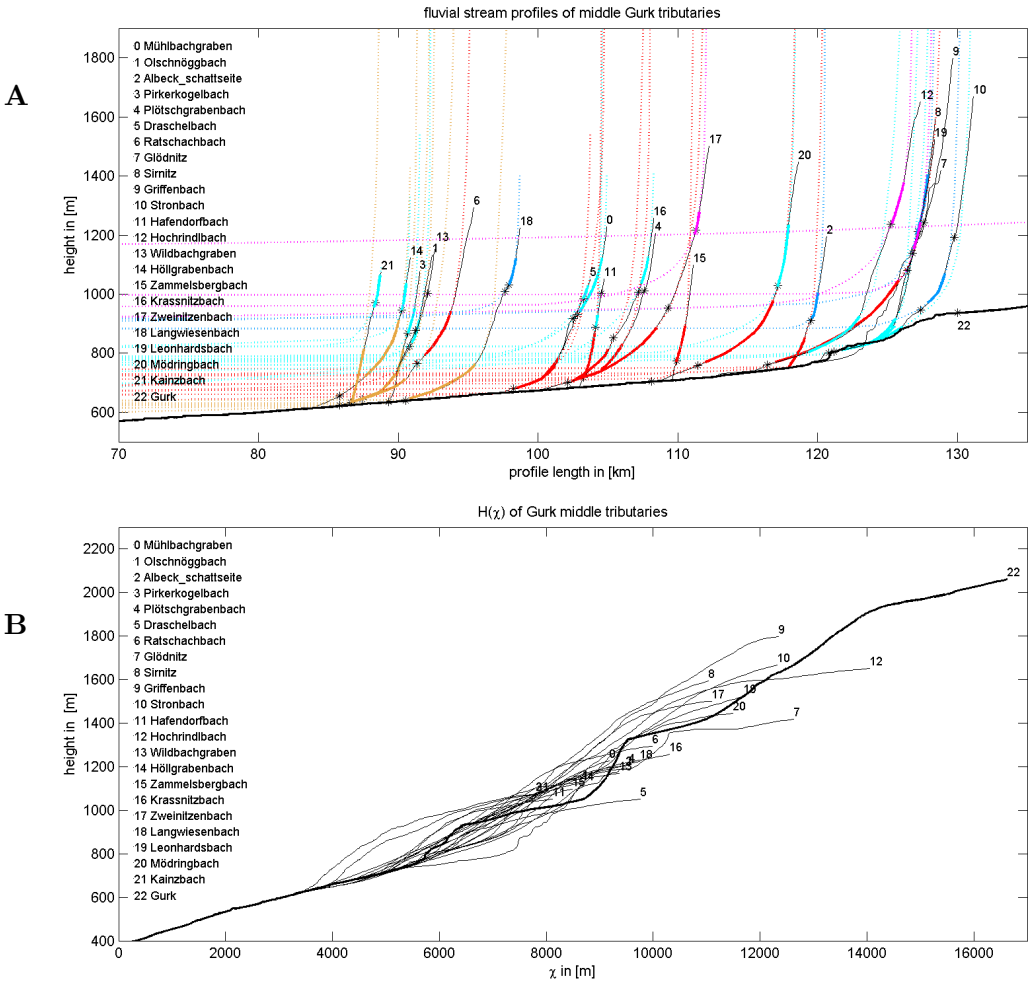

Figure 3.26.: **A**: Overview of prolonged middle Gurk River tributaries regression segments showing planation surfaces around 780 m, 930 m and 1012 m. **B**: Shows the elevation model $H(\chi)$. All channel are clustering close thogether.

3.2.2.4. Summary of Planation Surfaces and Erosion/Uplift Regimes

The regression segment altitude classification (Fig. 3.26A) of all middle Gurk tributaries at profile length 82 km identifies three planation surfaces but the lowest one (red) is omitted due to an unobvious accumulation point. In particular, three planation surfaces around 800 m, 900 m and a higher one around 1015 m become apparent. The separation of the upper two levels is unobvious.

From analysis comparison between the middle Gurk planation surfaces (Fig. 3.26A) and the

Görzbach H_2 segment (3.16) a good alignment with lower 800 m high middle Gurk relict landscape is observed. In addition, the actual height of 832 m of the Severgraben bridge aligns approximately with the top end of this level. Therefore, it seems likely that the palaeo-surface with altitudes between 750-850 m in the middle Gurk valley might have extended up to Severgraben bridge or even beyond to Thörl. As a consequence, it might be concluded that the high altitude palaeo-surface to the north of Severgraben bridge on-top to the eastern Nockberge Senke rim with height above 1200 m is a separated older level.

In Fig. 3.26B the $H(\chi)$ plots of all middle Gurk tributaries are shown. All curve remain narrow grouped around the main trunk curve. This indicates homogeneous tectonic/erosive processes acting within this river section.

3.2.3. Metnitz River Network

Despite the glacial overprint of the main trunk of the Metnitz River (Fig. 3.27) some of the tributaries comprise fluvial sections within its upper channel heads. Tributaries coming down from the north belong to the Nockberge Senke rim and are mostly glaciated. An exception are rivers from Nunataks, e.g. Mt. Grebenzen and Mt. Hirschstein. All southern tributaries from inside the Nockberge Senke reveal a fluvial head section.

3.2.3.1. Glacial Regimes

In total the Metnitz main trunk shows three equilibrium segments. The lowest one H_1 results in regression results $\theta = 0.67$, which could also be found in fluvial regimes of the Gurk River area.

The steep transition zone between the segment H_1, H_2 is represented by the inner gorge section. The slope changes between both segment and the $\theta = 0.26$ value for H_2 becomes considerably smaller indicating the dominance of discharge based processes. The log-log plot reveals a steep zone inside the inner gorge and a slope flattening in the upstream direction. Therefore, no knick point was selected. This is also confirmed by the $H(\chi)$ analysis, which shows no gradient change but a small parallel shift. On the other hand, k_{sn} and also the elevation profile itself

are identifying an uplift/erodibility impulse. A dam construction at the entrance of the gorge needs to be considered.

In the head section of the Metnitz a segment H_3 is identified. Again the regression results $k_s = 455, \theta = 0.61$ are pointing to a fluvial regime instead of a postulated glacial one. Between H_2, H_3 two knick points at above 122 km profile length are identified. As they are difficult to distinguish in the log-log plot and also in the $H(\chi)$ plot they also might represent a single spot. In the field, they were not recognised.

The head section shows an increase of k_{sn}, which is in accordance with the middle Gurk River tributaries - Stronbach, Hochrindlbach, Sirnitz and Leonhardsbach - at the western Nockberge Senke rim side.

3.2.3.2. Fluvial Regimes inside the Nockberge Senke

In the following the tributaries coming down from the Mödringberge at the southern side are investigated (Fig. 3.28 to 3.30) namely the Zienitzenbach, the Feistritz and the Vellachbach. All of these rivers possess a non-glaciated upper segment H_3. In accordance with the findings in the middle Gurk valley again planation surfaces cluster between 900-950 m altitude at profile location 81 km. In comparison, they are about 50-100 m higher compared to the middle Gurk section. Accordingly, also the base level between these two valleys differ by this amount of elevation.

The investigation of k_{sn} values for these tributaries results in a more complex situation. For the Zienitzenbach the fluvial segment H_3 reaches values of approximately 80, which are comparable to the middle Gurk side of e.g. the Olschnöggbach. Interestingly, the increase in k_{sn} is completely missing for the Feistritz and shifted toward the foot slopes H_2 for the Vellachbach. These findings can be confirmed by the investigation of parallel shifts between the H_2, H_3 segments within the log-log plots. The Zienitzenbach shows clear parallel shift, the Feistritz only small shift and the Vellachbach no shift but a change of θ. The reason for this prolonged high altitude k_{sn} depression zone is most likely related to the fact that the head sections of the Feistritz and the Vellachbach are trending in a parallel to the EW stretching Mödringberge. When assuming, that the k_{sn} drop in the head region is dominated by erodibility, than the

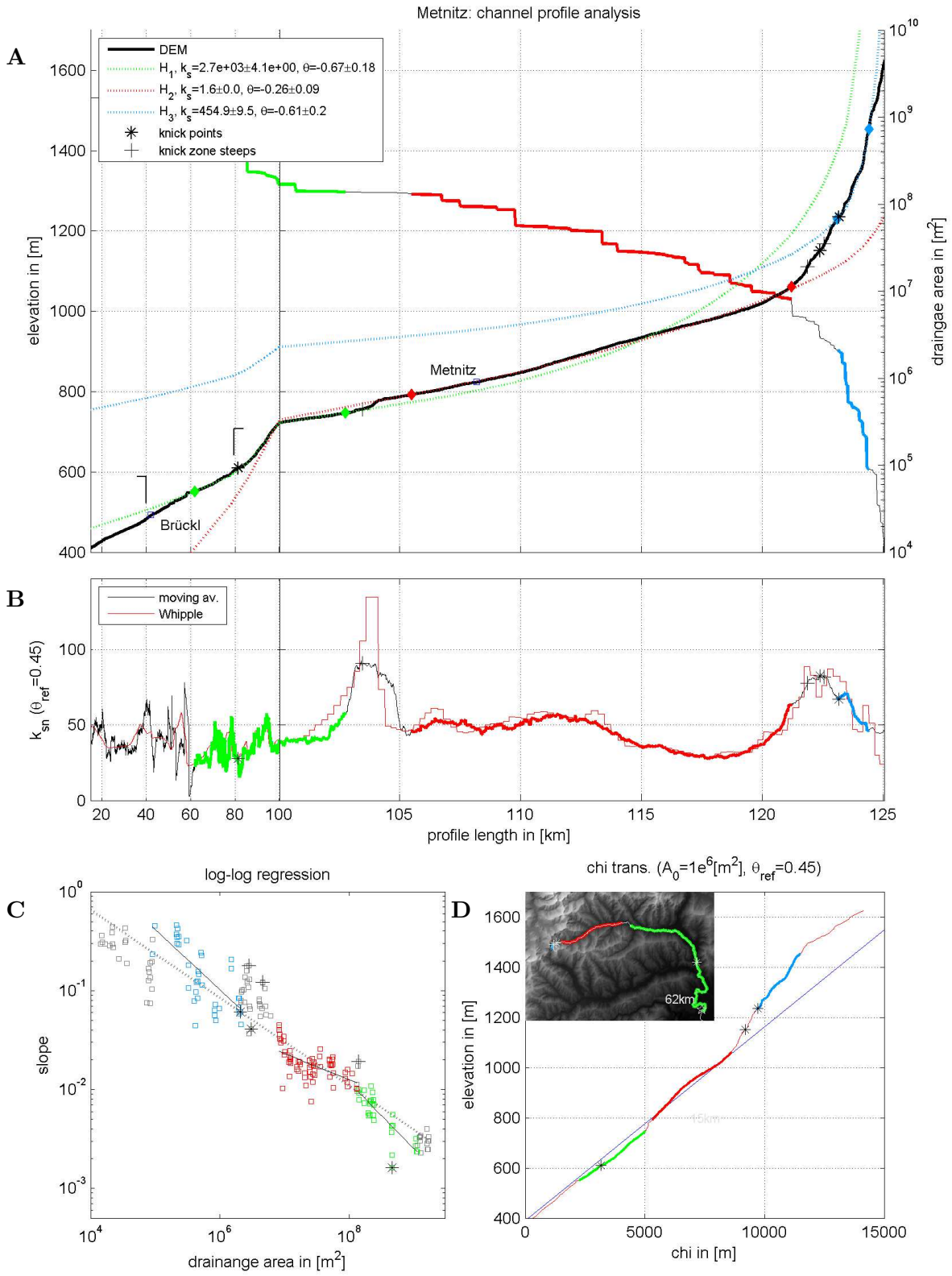

Figure 3.27.: The fully glacially overprinted Metnitz channel is located within the Nockberge Senke. At the channel head a planation surface is found for H_3. **A**: Elevation and drainage profile, brackets indicate LGM extent, **B**: k_{sn} plot, **C**: log(S)-log(A) plot and **D**: χ-transformed elevation plot. Colours relate to k_s, θ regression sections.

erodibility in elevated sections is higher (e.g. due to unconsolidated sediments) compared to the lower slopes (bed-rock channel).

3.2.3.3. Summary of Planation Surfaces and Erosion/Uplift Regimes

The Metnitz tributary regression segment classification (Fig. 3.31A) results in three main levels around 900 m 1200 m and 1400 m elevation.

The comparison of $H(\chi)$ of all tributaries (Fig. 3.31B) reveals a divergence of mostly all tributaries toward higher slopes compared to the main trunk. All fluvial tributaries from the Mödringberge gather close together toward the Metnitz River main trunk graph.

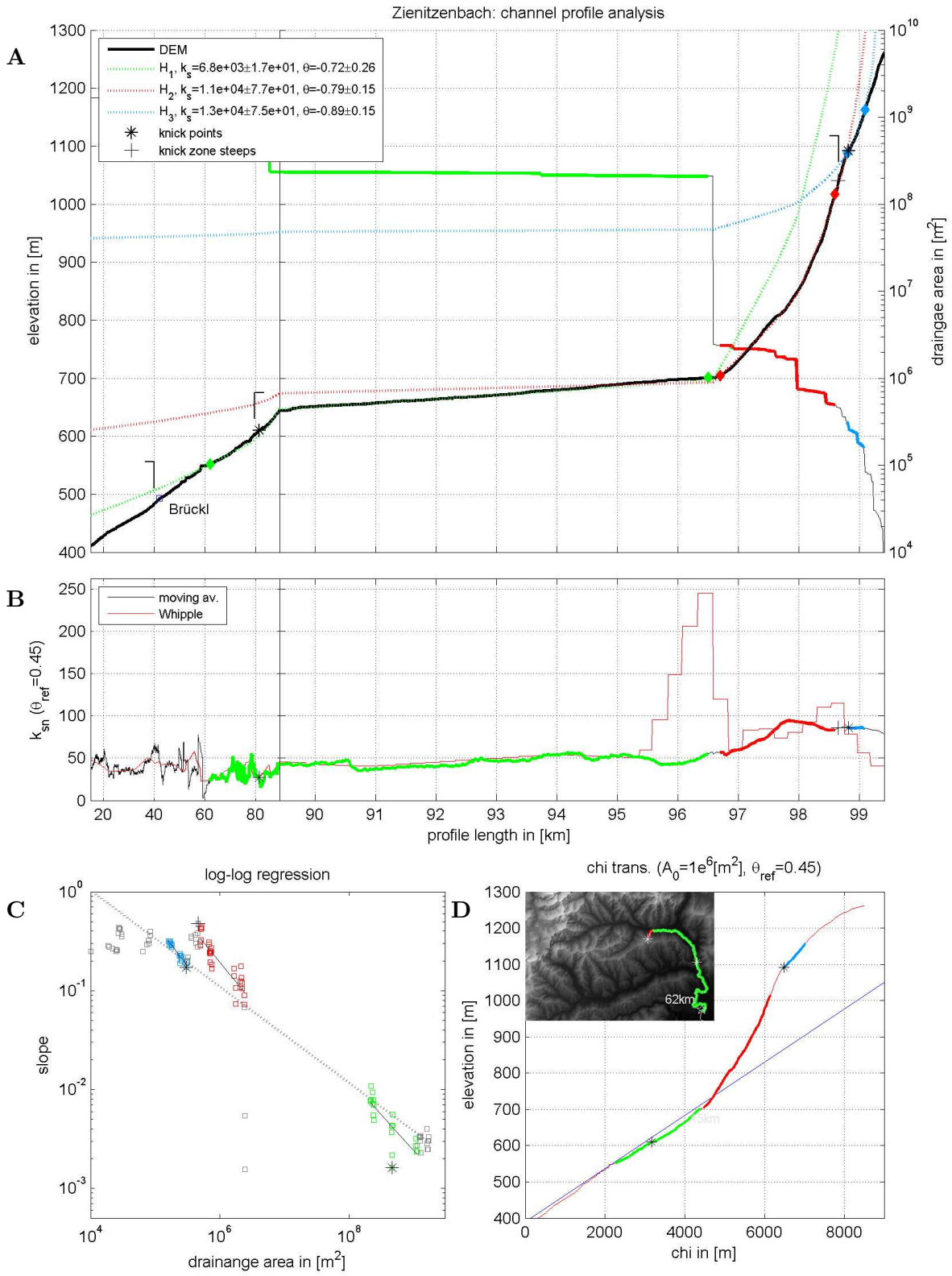

Figure 3.28.: The Zienitzenbach (fluvial channel) is located within the Mödringberge. A planation surface for H_3 is identified. **A**: Elevation and drainage profile, brackets indicate LGM extent, **B**: k_{sn} plot, **C**: log(S)-log(A) plot and **D**: χ-transformed elevation plot. Colours relate to k_s, θ regression sections.

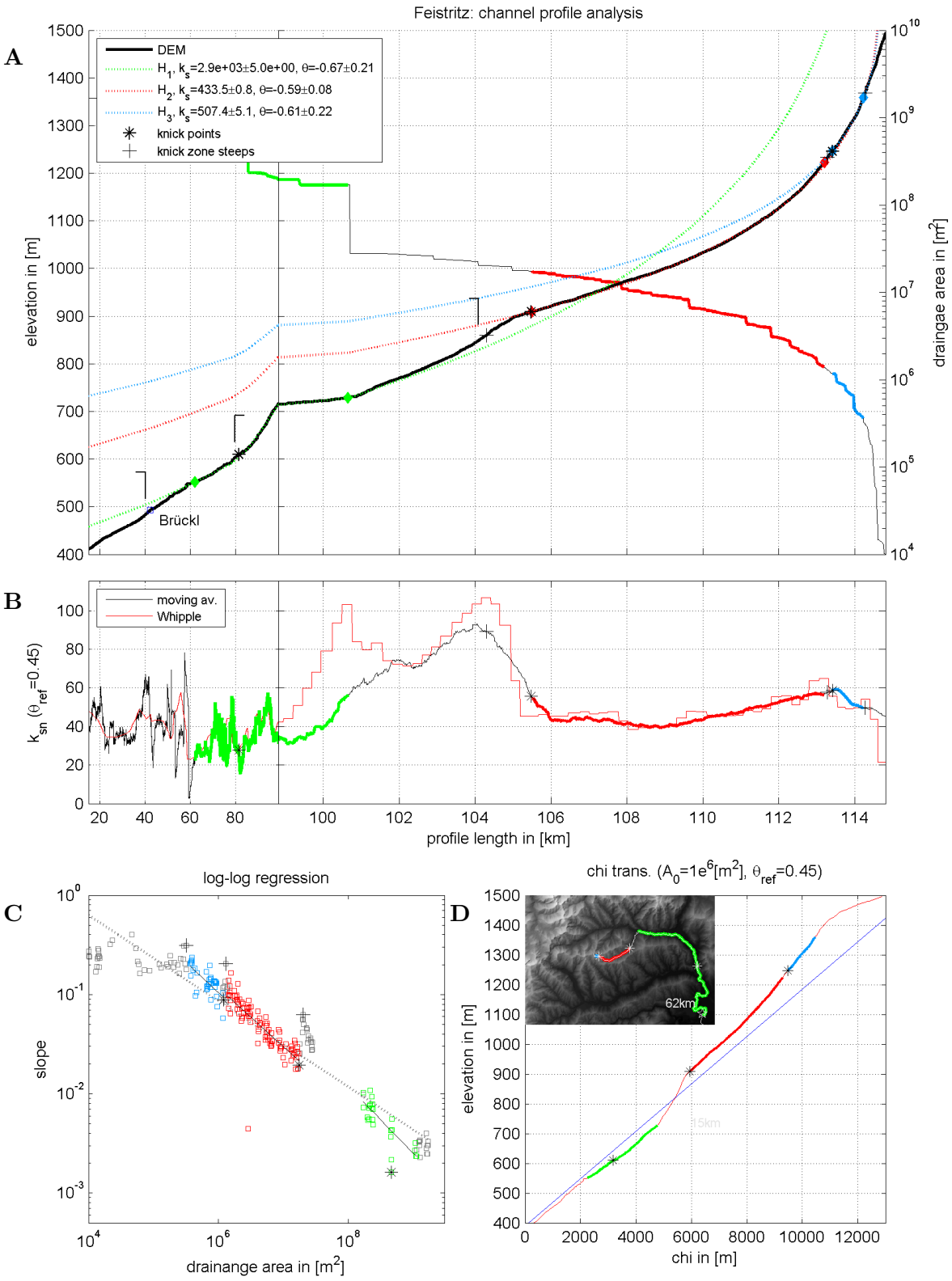

Figure 3.29.: The Feistriz is the largest fluvial channel located in parallel orientation along the Mödringberge ridge. A planation level is identified for H_3. In contrast to other channels no strong k_{sn} peak in the head section is found. **A**: Elevation and drainage profile, brackets indicate LGM extent, **B**: k_{sn} plot, **C**: log(S)-log(A) plot and **D**: χ-transformed elevation plot. Colours relate to k_s, θ regression sections.

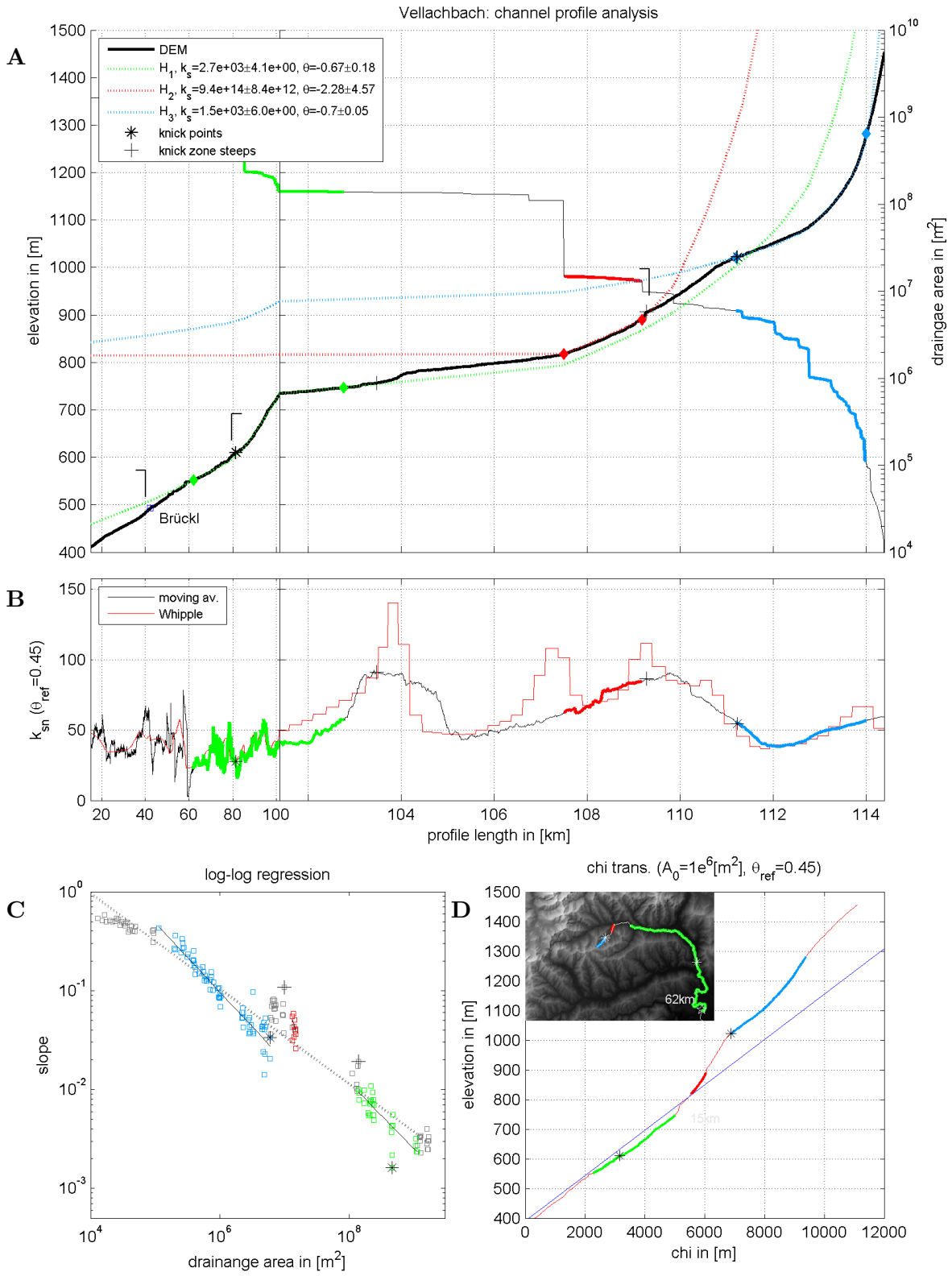

Figure 3.30.: The Vellach is the second largest fluvial channel from the Mödringberge. A planation level is identified for H_3. In contrast to other channels no strong k_{sn} peak in the head section is found. **A**: Elevation and drainage profile, brackets indicate LGM extent, **B**: k_{sn} plot, **C**: log(S)-log(A) plot and **D**: χ-transformed elevation plot. Colours relate to k_s, θ regression sections.

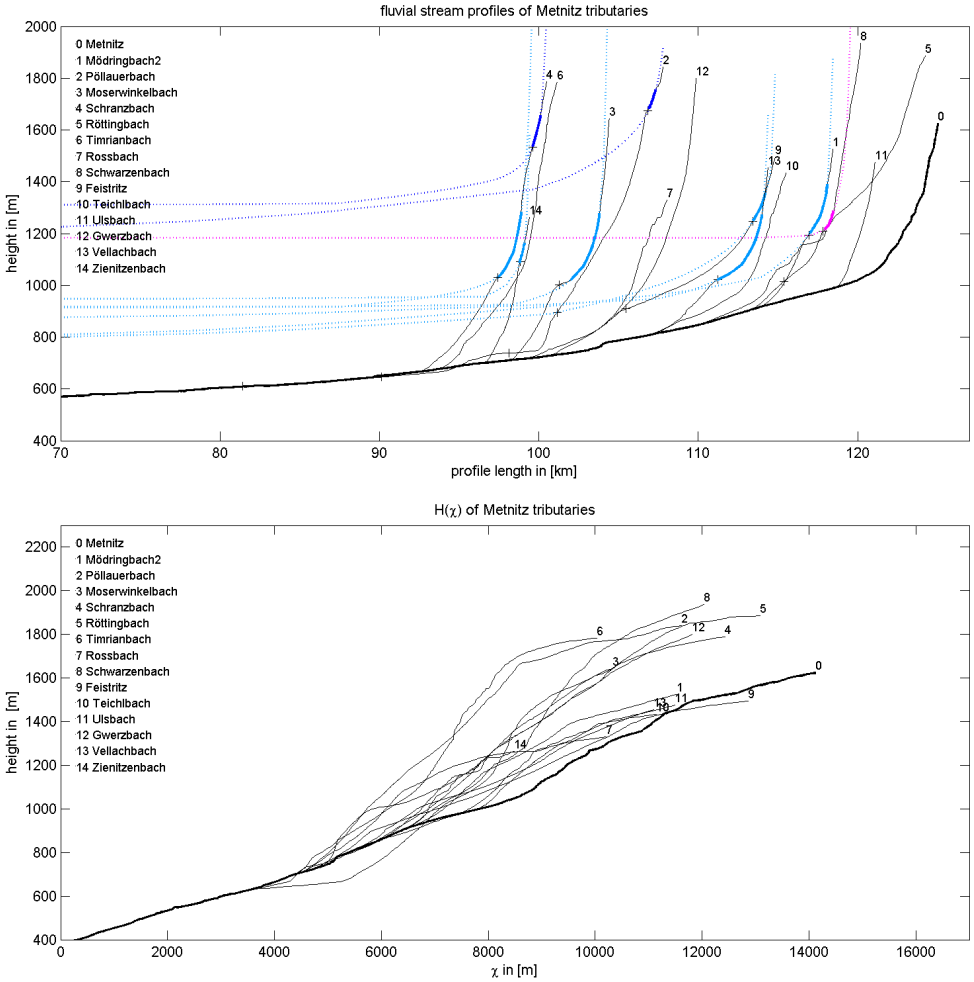

Figure 3.31.: **A**: Overview of prolonged Metnitz River tributaries regression segments showing planation surfaces at 890 m, 1180 m and >1290 m. **B**: Shows the elevation model $H(\chi)$. All Mödringberge tributaries cluster close to the main trunk.

3.2.4. Wimitz River Network

In comparison to the gentler Gurk valley, the Wimitz valley to the south shows strong and steep V-valley incision, implying a diverse genesis. Within the Wimitz main trunk (Fig. 3.32) four regression segments were found.

H_1 is still within the glaciated part and therefore not regarded.

3.2.4.1. Fluvial Regimes inside the Nockberge Senke

The Segment H_2 starts from the fluvioglacial terrace near Kraig up-to Granaschmied just below the knick point in the main valley. The elevation profile of this segment appears pure linear and accordingly the catchment size is almost a constant. The regression estimates $\theta = 0.01$ shows quite untypical values for fluvial incision with high uncertainty. Also, the appearance of the profile segment is very rugged and unstable. This section of the Wimitz valley constitutes the deeply incised V-valley. It seems possible that this observed profile instability is caused by mass movements from the side-walls during already postulated heavy intra-glacial incision periods, which are still not equilibrated (moved upward) now.

Above the Granaschmied knick point the valley slope abruptly gets flattened up to Goggau. The regression estimate of H_3 is already out of the plausible range for fluvial erosion. Therefore, a glacial overprint seems likely, but due to missing surface textures in the DEM, this finding was disregarded.

Between H_3, H_4 a knick point is investigated on-top of a steep step. Here the Wimitz leaves the broad main valley and the step is interpreted as a hanging valley, formed by the main glacier coming from the west. The k_{sn} between H_3, H_4 again show an increase followed by a drop in the top section but on values below 60, which is 40% smaller compared to the Gurk region. A non-equilibrated uplift/erodibility impulse can be assumed.

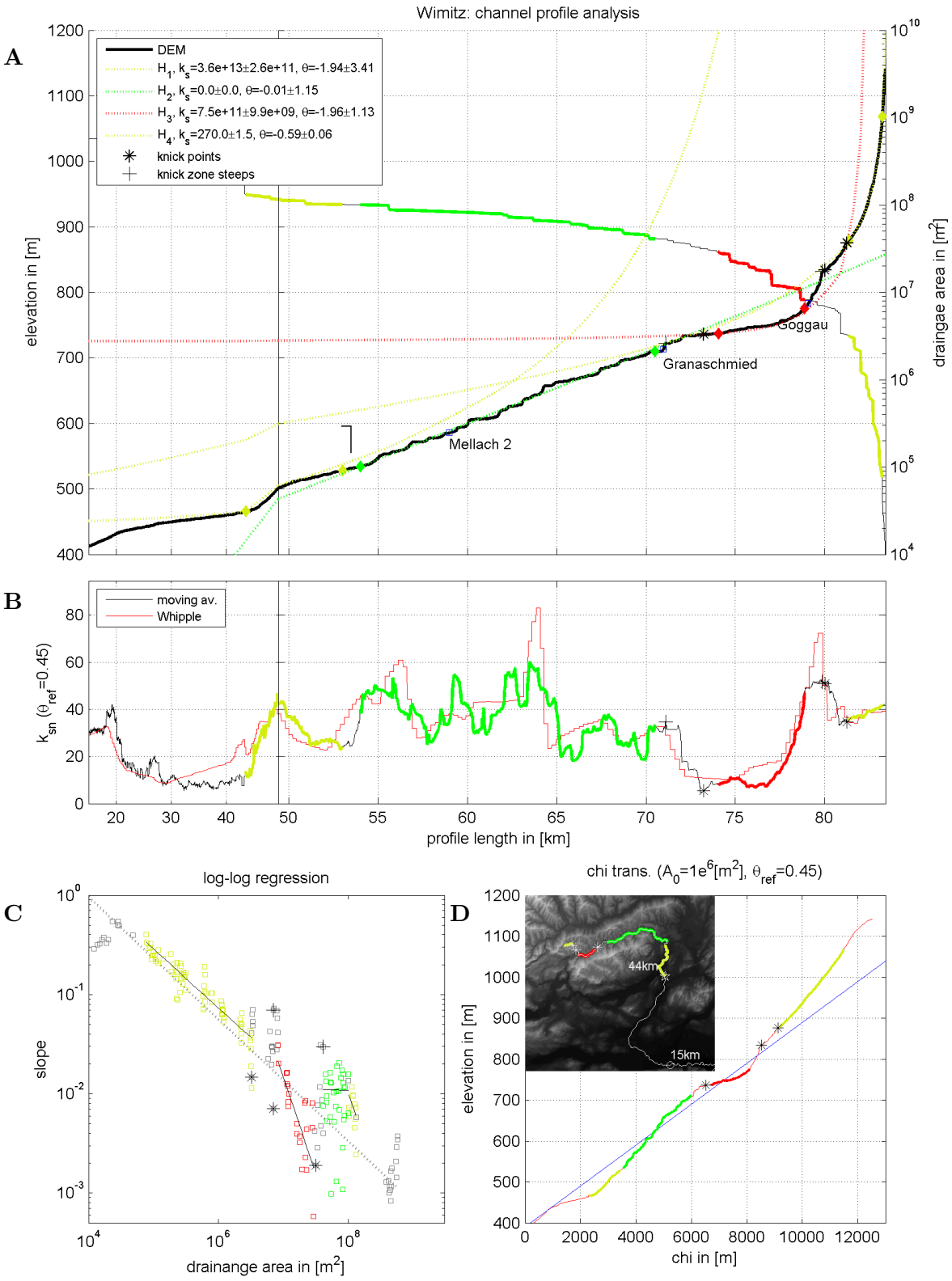

Figure 3.32.: The Wimitz channel is located inside the Nockberge Senke. Around Goggau the channel was glacially overprinted and in downstream direction it appears unstable. A planation surface for H_3 is observed, which might align the the Hochterrasse. **A**: Elevation and drainage profile, brackets indicate LGM extent, **B**: k_{sn} plot, **C**: log(S)-log(A) plot and **D**: χ-transformed elevation plot. Colours relate to k_s, θ regression sections.

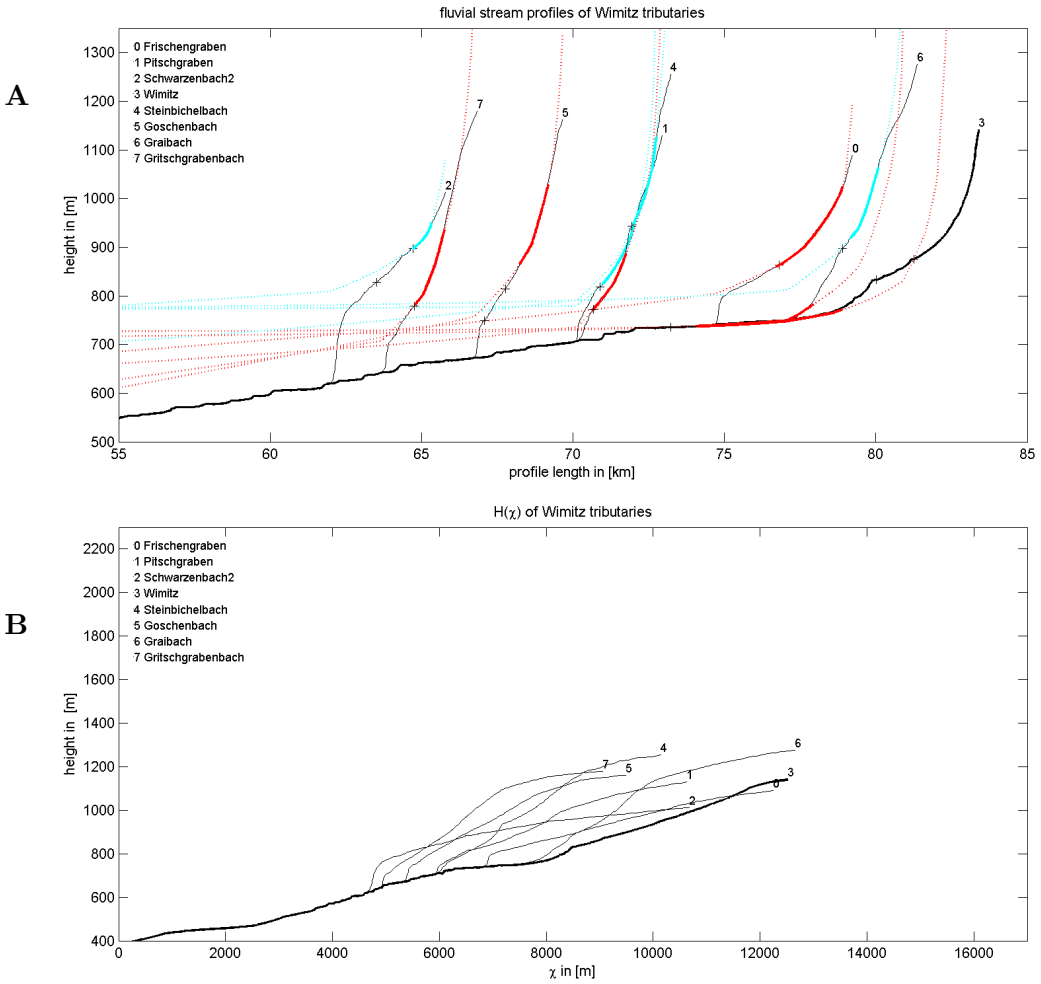

Figure 3.33.: **A**: Overview of prolonged Wimitz River tributaries regression segments, which identifies one planation surface at 770 m. The lower surface around 650 m was not taken as a new surface as it correlates with the Hochterrasse level. **B**: Shows the elevation model $H(\chi)$. The tributaries appear parallel shifted from the main trunk.

3.2.4.2. Summary of Planation Surfaces and Erosion/Uplift Regimes

The regression segment classification (Fig. 3.33A) for all Wimitz tributaries at profile length 60 km reveals two planation surfaces around 650 m and around 770 m. The lower one correlates in altitude with the Hochterrasse level. Due to the strong V-valley incision, all tributary profiles show a steep step departing from the main trunk. This incision event can be interpreted as young uplift because only minor knick point retreat took place until now. On the other hand,

it needs to be taken into account, that the catchment sizes of the Wimitz tributaries are quite small. Therefore, erosive processes might be considerably slowed down.

Apparently, the Wimitz main trunk above approximately Granaschmied underwent a different uplift/erosive history due to $H(\chi)$ plots (Fig. 3.33B) compared to the downstream tributaries. No strong gradient turns are visible. On the other hand, all tributaries show a positive curvature between two parallel shifted line segments. Due to Royden and Perron (2013), this might indicate consuming knick points, which indicates a recent increase in uplift rate assuming a slope exponent $n < 1$. Based on this explanation the slope exponent seems to vary. Within the middle Gurk valley, a proxy indicated $n > 1$ while we have $n < 1$ in the Wimitz valley.

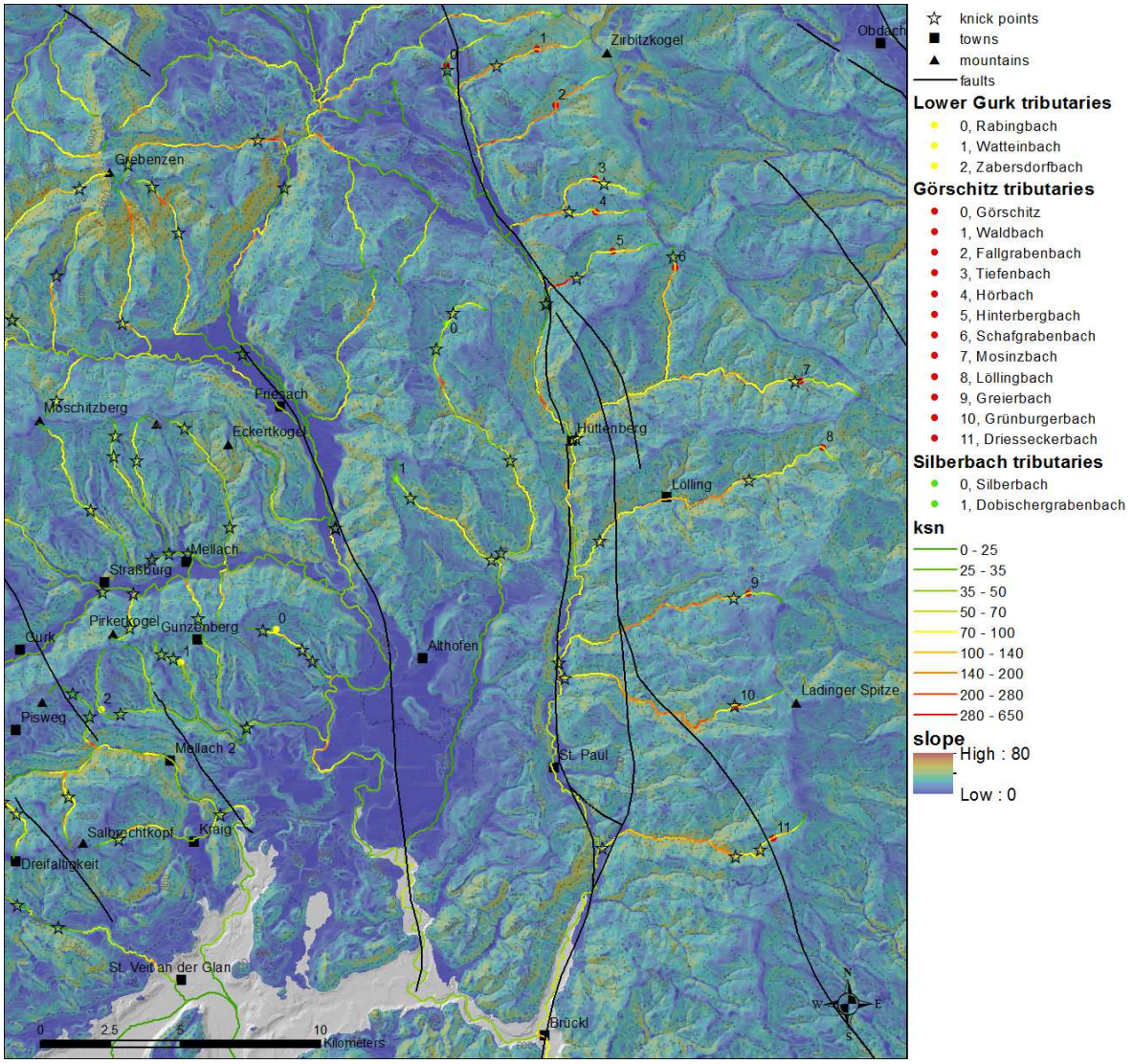

Figure 3.34.: Slope map of the Görschitz, Silberbach and lower Gurk River system. Displayed are topography by hill-shading and slope angle by colour. The river network is marked using k_{sn} values.

3.2.5. Görschitz and Lower Gurk River Network

For the Görschitz, the Silberbach and the lower Gurk River no extensive geomorphological field observation was performed.

The slope map (Fig. 3.34) reveals planation surfaces within the lower Gurk valley, which are mapped at 750-850 m altitude (Fig. 3.35). The lower knick points of the Rabingbach, the Watteinbach and the Zabersdorfbach are reflecting this level quite reasonable. According

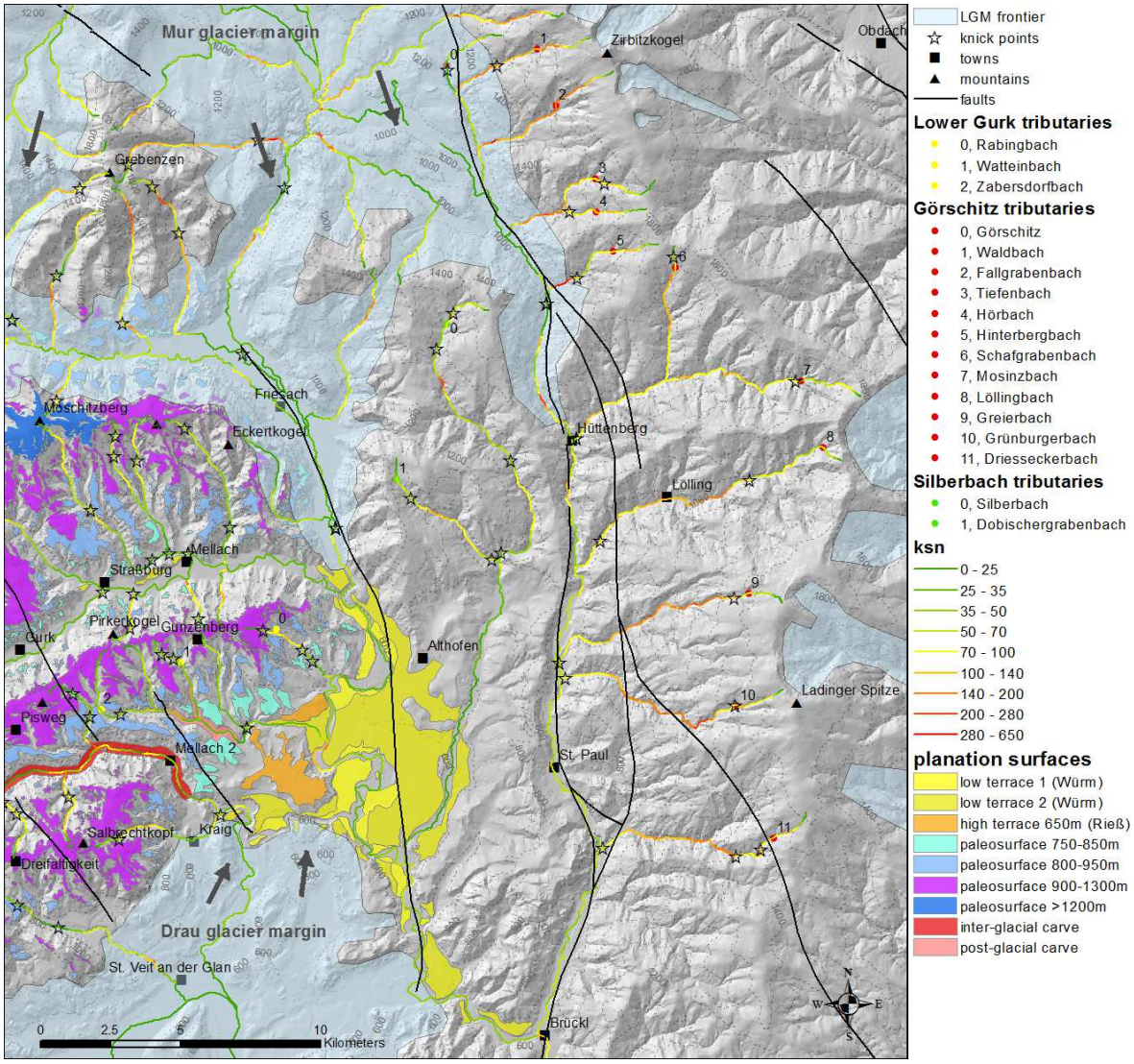

Figure 3.35.: Interpretation of planation surfaces and the LGM extent on top of hill-shaded topography of the Görschitz, Silberbach and lower Gurk River system. The river network is marked using k_{sn} values.

to Fig. 2.2 the lithology within this area changes into loam soils. In the Zabersdorfbach this was approved by soil fractions in the channel sediments (*OCc30*). According to Franz Neubauer (pers. com. 2018), there are also red palaeo-soils (red loam) in this region, which are interpreted to document the Miocene peneplane of the Nockfläche. In the geological map red palaeo-soils only occur at the NE margin of the Althofener Basin.

Two further planation surfaces at 800-950 m and 900-1300 m are separated due to knick point analysis in the Watteinbach and Zabersdorfbach channel.

On top of the Seetaler Alps and at the Saualpe between Mt. Zirbenkogel and the Mt. Landinger Spitze also textures of planation surfaces can be observed in the maps in Fig. 3.34 and 3.35. On the other hand, they were not mapped within this work.

The Görschitz and exemplary for a tributary the Grünburgerbach is investigated. Both river reveal a segment H_1 within the non-glaciated part upstream of Brückl with low θ values between 0.44-0.49, indicating discharge dominated processes (Fig. 3.36 and Fig. 3.37).

Upstream of the Löllingbach junction the Görschitz River again is within glacially overprinted regions. In this segment, a 100 m high step about two kilometres upstream of Hüttenberg can be observed. Above the knick point the slopes are becoming very low indicating glacial overprint. Still within the glacially overprinted part, in the channel head, a segment H_2 was found. It indicates a planation surface at 1000 m, which is also found within the Görschitz tributaries and the Silberbach and Dobritschergrabenbach (not shown here).

The Grünburgerbach profile analysis (Fig.3.37) constitutes a typical Görschitz River tributary coming down from the Saualpe. On the upstream slope toward the channel head, two equilibrium segments are found. In contrast to the Görschitz, these segments belong to a fluvial regime with θ between 0.96-0.97 indicating slope dominated erosive processes. Between both segments, a strong parallel shift in the log-log plots is observed. In addition, the H_2 segments shows highest k_{sn} values in the whole region. Both findings indicate a strong uplift/erodibility impulse in this location at the western slopes of the Saualpe.

In analogy to previous investigated river systems, a k_{sn} decrease in the head section is found, thus being interpreted as a channel profile disequilibrium state. When excluding the LGM transition zone in contrast, the k_{sn} values remain small for the whole Görschitz course, compared to its tributaries. This is explained by the parallel path of the Görschitz with the Görschitztal fault.

3.2.5.1. Summary of Planation Surfaces and Erosion/Uplift Regimes

The classification of regression segment altitudes of the Görschitz River tributaries at profile length 50 km reveals planation surfaces at 760 m, 1000 m and 1460 m (Fig. 3.38A), which fit

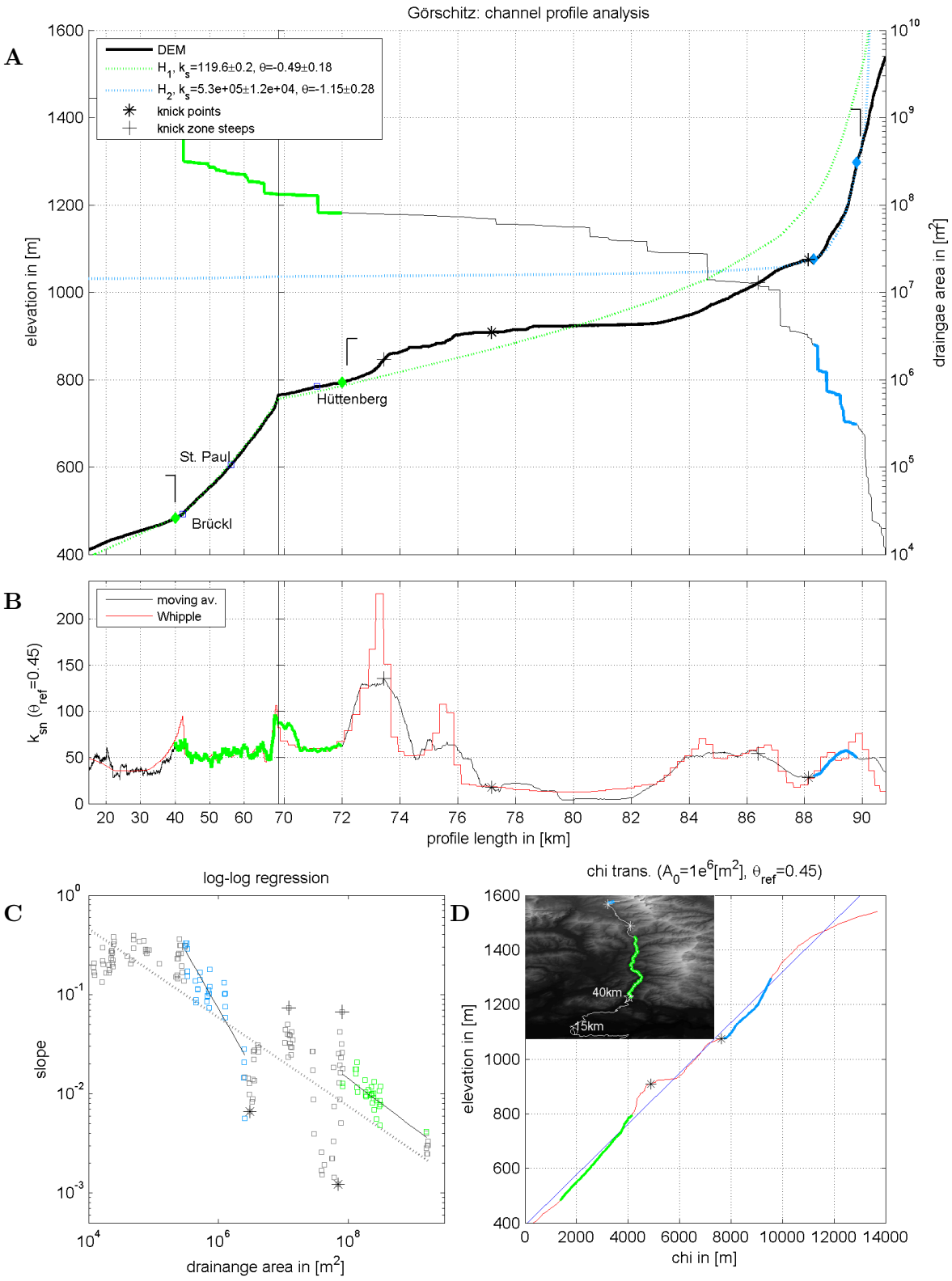

Figure 3.36.: The Görschitz channel is glacially overprinted above Hüttenberg. A planation surface is identified for the H_2 segment. **A**: Elevation and drainage profile, brackets indicate LGM extent, **B**: k_{sn} plot, **C**: log(S)-log(A) plot and **D**: χ-transformed elevation plot. Colours relate to k_s, θ regression sections.

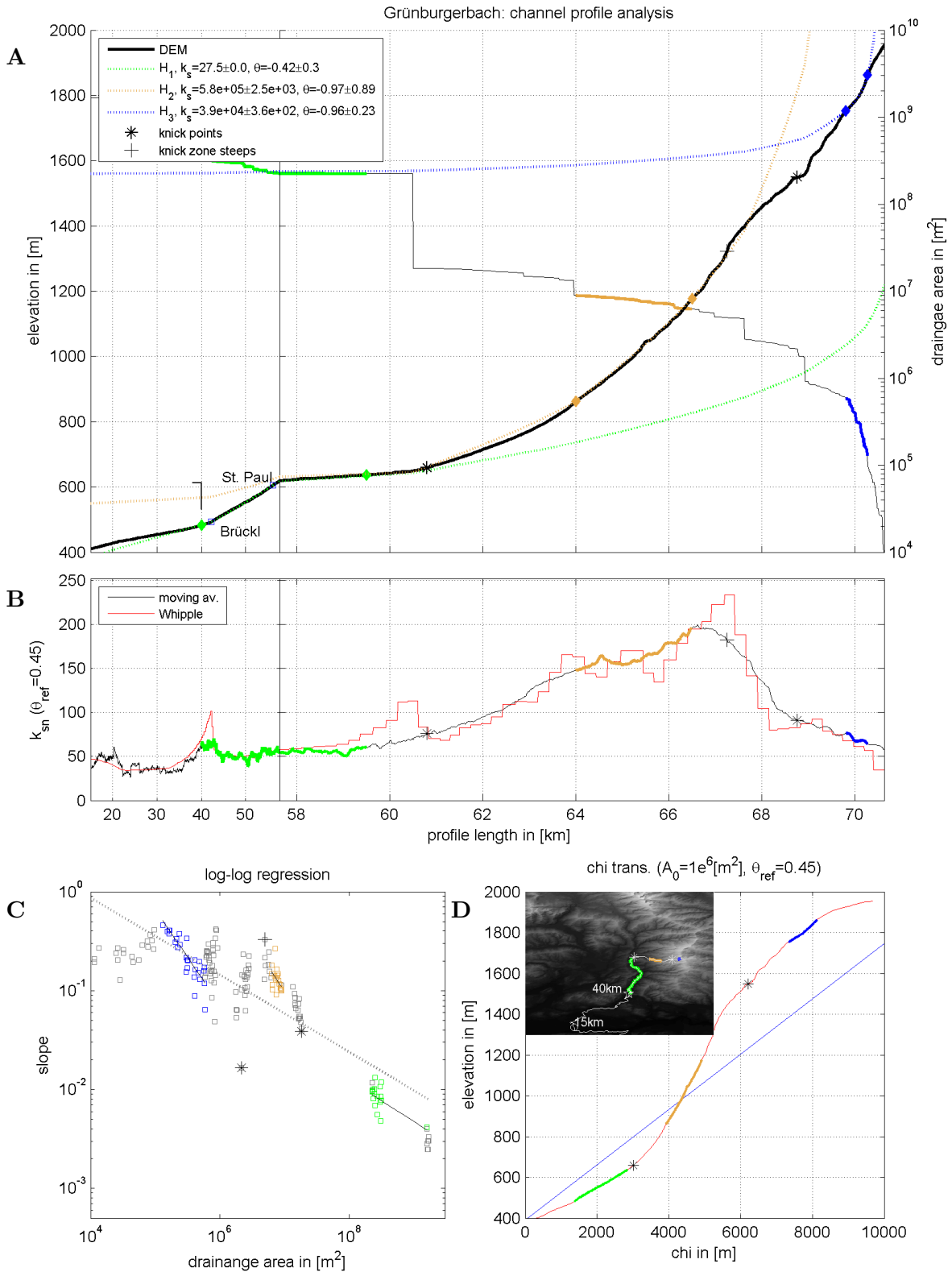

Figure 3.37.: The Grünburgerbach is an example of a fluvial channel coming down from the Saualpe. A top height planation surface is identified and highest k_{sn} values in the region are found here. **A**: Elevation and drainage profile, brackets indicate LGM extent, **B**: k_{sn} plot, **C**: log(S)-log(A) plot and **D**: χ-transformed elevation plot. Colours relate to k_s, θ regression sections.

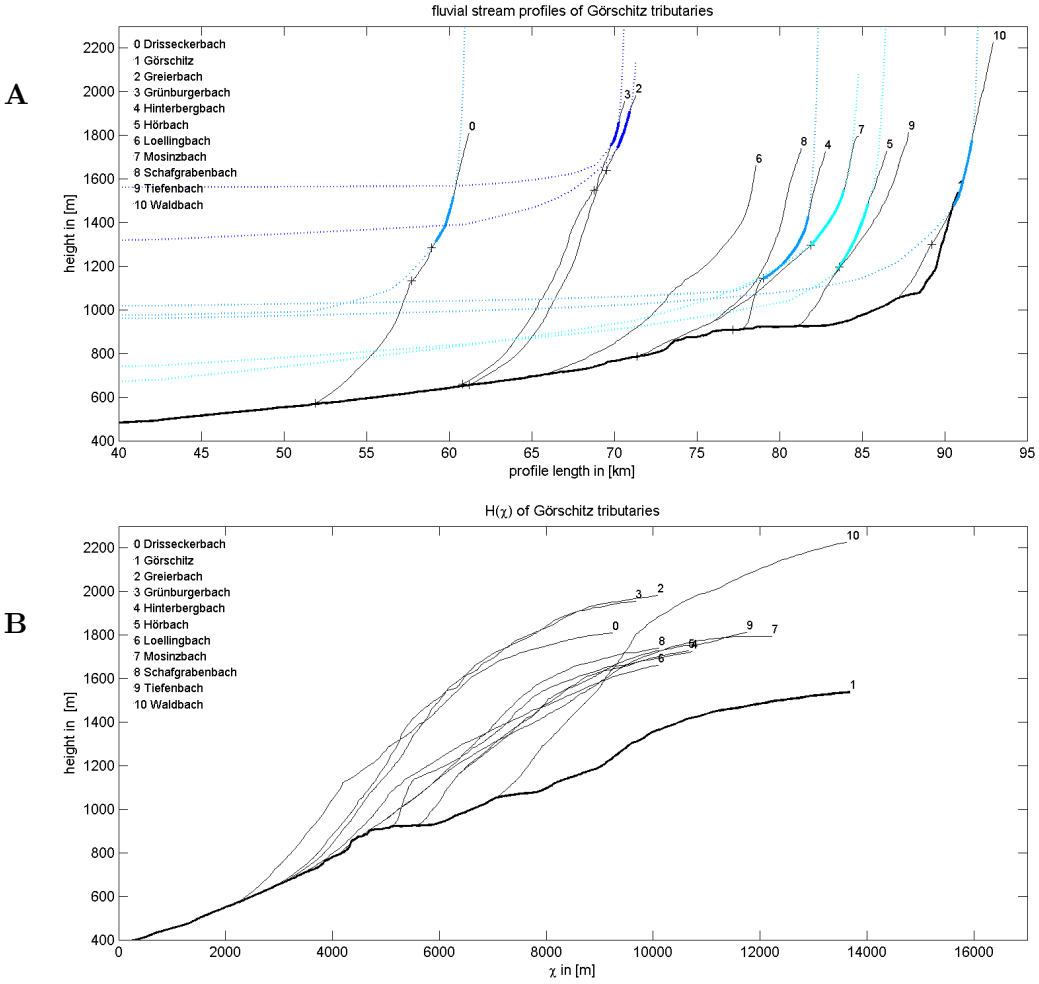

Figure 3.38.: **A**: Overview of prolonged Görschitz river tributaries regression segments, which identifies three planation surfaces at 770 m, 1000 m and 1460 m. **B**: Shows the elevation model $H(\chi)$. A strong spread between main trunk and tributaries is observed.

quite well with the planation surfaces toward the west. In particular, for the southern Saualpe tributaries the incision depth of the top surface reaches the highest values for the whole region with up to 800 m incision depth.

The $H(\chi)$ plot (Fig. 3.38B) shows very pronounced differences between the Görschitz main trunk and all tributaries, indicating different genesis of the rivers (see also Wimitz River). This separation might be explained with the Görschitz directly on-top of the fault, while all tributaries are located on the eastern side of the fault.

3.2.5.2. Görschitztal Fault Activity

From the above findings together with high k_{sn} values for all tributaries upstream of the Görschitztal fault (Fig. 3.35) it can be concluded that this fault is still active. The high incision depth of up to 800 m indicates the strongest uplift in this region. In particular, for the southern Saualpe massif. In Fig. 3.35 the Görschitz fault separates into a system of faults toward the south. The $H(\chi)$ analysis suggests that the westernmost part of the fault system seems to be the active fault line.

4. Discussion and Conclusion

4.1. Planation Surfaces within the Gurktaler Alps

Within this work, the existence of planation levels between the Klagenfurter Basin and the well-known Nockfläche in the Murtal catchment to the south of the Tamsweger Basin is suggested by morphometric analysis. An approximate location with respect to the Nockfläche and Saualpe planation surfaces is given in Fig. 4.1. Therefore, the data represented above support Aigner (1922); Spreitzer (1932), who asserted several Piedmont-steps to be still existent toward the south of the Nockfläche. Furthermore, the data set of uplift proxies within the Eastern Alps, e.g. Legrain et al. (2014, 2015); Wagner et al. (2011) was considerably prolonged to the west.

In total 4 planation levels were resolved between the Hochterrasse level (650 m) at the western banks of the lower Gurk River and the Nockfläche around 1700-2200 m. In general, most of these surfaces show a tilting tendency. Toward the NW about 50-100 m higher altitudes are reached. This is one reason why the level of planation surfaces are defined as broader intervals. The EW fraction of this tilting also correlates with the profile elevation of the main river trunks in the region. In a profile in NS direction close to Althofen all three river system of the Wimitz, the Gurk and the Metnitz show comparable heights of 630-640 m. In the NS profile through Weitenfeld the elevations of the main trunks already raised up to 740 m and 710 m for the Wimitz and the Gurktal and already about 850 m in the Metnitztal.

L1 - Palaeo-surface 750-850 m (cyan): The biggest fractions of this palaeo-surface is grouped to the W, NW and N margin of the Hochterrasse in the lower Gurk River area. A good viewpoint for this terrace in the field is given on top of the Hochterrasse close to Eixendorf. Many river regression segments in the middle Gurk valley also align with this surface level.

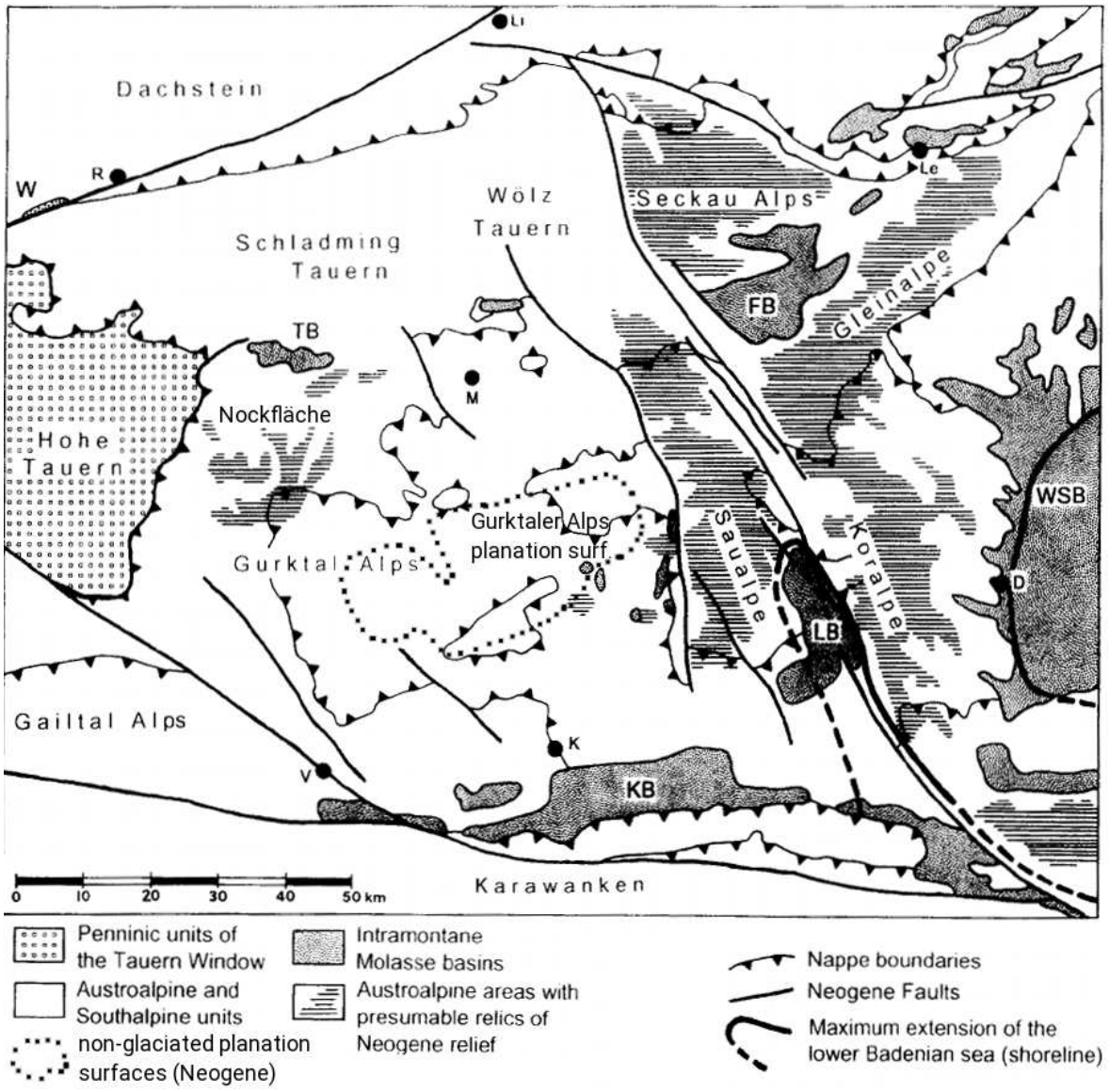

Figure 4.1.: Shows the distribution of relict landscapes within the Eastern Alps to the east of the Tauern window (Hejl, 1997). The approximate location of found non-glaciated planation surfaces out of the present work are outlined by dotted lines.

L2 - Palaeo-surface 800-950 m (light blue): This lower intermediate level mostly maps within the Wimitz valley and the middle Gurk valley. It correlates with the Severgraben bridge altitude. Therefore, it is only present in the Nockberge Senke region.

L3 - Palaeo-surface 900-1300 m (magenta): This upper intermediate level is the most widespread surface within the Nockberge Senke. It is not completely bounded within the rim structure, because a small fraction was also mapped within the Görzbach tributary. The

border between the upper and the lower intermediate level is difficult to define. At some map locations, no geomorphological evidence for a separation was found. Therefore, both levels contact each other. From the geomorphological viewpoint, it is likely, that both levels are identical.

L4 - Palaeo-surface >1200 m (blue): The uppermost planation surface is not restricted in height within the investigation area. But it is supposed to be constraint by the Nockfläche to the north, with a starting height of about 1700 m (Exner, 1949). The uppermost surface P4 was mainly defined by river profile analysis. All river systems, which touch the outer boundary of the Nockberge Senke rim exhibit this highest level. Namely, these are the upper Gurk, the western tributaries of the middle Gurk, the Metnitz and the Görschitz River system. This level was also mapped for highest mountains within the Nockberge Senke based on morphological reasons. Only two knick points within the Mödringberge at the Feistritz and the Zweinitzenbach are found to support P4 in the area. But on the other hand, no stable channel segments within this level were found. For the Wimitzer Berge, no evidence from river profile analysis is found. Therefore, the uppermost level is uncertain within the Nockberge Senke.

To the east of the Gurktaler Alps within the Styrian Basin and Palaeozoic of Graz, additional planation surfaces were investigated, e.g. Wagner et al. (2011); Legrain et al. (2014, 2015). The Gurktaler Alps are separated from these regions by at least two active fault systems, namely the Pöls-Lavanttal and the already discussed Görschitztal fault system. Due to unknown thrust or normal faulting dip, it is likely, that altitudes of relict surfaces do not correlate across these fault systems. But on the other hand, Wagner et al. (2011) mapped several planation surfaces relative to the Mur level and thereby, also regarded the Hochterrasse level, which is well-known in both regions. Therefore, a relative comparison with respect to the Hochterrasse is used in order to correlate the levels between both locations, using the Pleistocene terrasse as a base level marker in both regions.

A series of planation surfaces have been recognised in the Styrian basin by Wagner et al. (2011). This data is re-levelled (Tab. 4.1) with respect to the Mindl/Riß Middle Terrace Group (40-60 m $\approx$ 50 m). On the right-hand side, the planation levels L1-L4 from the Gurktaler Alps are re-levelled based on the Hochterrasse at 650 m altitude, where a Rißian age was assumed only based on terrace designation.

Styrian Basin	altitude rel. [m]	age	Gurktaler Alps	altitude rel. [m]	remark
Kor level	1150-1450	Upper Sarmatian	-	-	Nockfläche (1050-1550 m)
Wolscheneck	850-950	Lower Pannonian	-	-	
Hubenhalt	650-750	Late Pannonian (5.1-7.4 Ma)	L4	>550	correlation ?
Trahütten	450-550	Early Pliocene (4-5 Ma)	L3	250-650	correlation given but width misalignment
Hochstraden (Kalkleiten)	275-400	Pliocene (3.4-4 Ma)	L2	150-300	correlation OK
Stadelberg/ Zahrerberg	130-250	Pliocene (≈3 Ma)	L1	100-200	correlation OK

Table 4.1.: Correlation of planation surfaces between the Styrian Basin, Palaeozoic of Graz (Wagner et al., 2011) and the Gurktaler Alps. The relative altitude means the difference between the actual level and the Hochterrasse level in the region.

The comparison shows a reasonable correlation of the L1 level in the Gurktaler Alps with the well-known Stadelberg level at the eastern end of the Alps. Based on this conjunction the Stadelberg planation age of approximately 3 Ma can be assigned to the L1 level. In this way, the L2 level can be assigned with the Hochstraden level with an origin age of 3.4-4 Ma. Finally, a reasonable correlation for the L3 level with the Trahütten planation surface with an origin age of 4-5 Ma is found. The latter correlation needs to be questioned due to a mismatch of the width between the levels. In the Gurktaler Alps, this surface is four times broader distributed in altitude compared to the Styrian Basin. For the Gurktaler Alps, the level L4 relates to altitudes above 1200 m, which easily also reaches heights above 1600 m to the east of the upper Gurk region. Therefore, a correlation is possible, but the available data is not sufficient enough for a statement. The higher Kor level (Middle Miocene) might correlate with the Nockfläche planation surface, which would be in agreement with age assumptions from Exner (1949); Hejl (1997, 1998).

At first sight, for the Wolscheneck level, there does not exist a corresponding planation surface

within the Gurktaler Alps. But on the other hand, a potential for an additional level between P4 and the Nockfläche is existent. As mentioned in chapter 3, further palaeo-surfaces exist to the north and north-west of the Metnitz valley. But they were not investigated within this work.

4.2. Uplift in the Gurktaler Alps

Stream power analysis in the region showed for all investigated river systems a local disequilibrium condition in the upper channel heads of almost all tributaries. In particular, this was expressed by a k_{sn} peak below the channel head. This phenomenon was explained by an erodibility inhomogeneity for the upper channel segments, which was taken as a criterion for a relict landscape. Therefore, it was assumed, that palaeo-surfaces consist of a top layer out of unconsolidated sediments, which locally increases the erodibility. In consequence the k_{sn} values are decreasing. On the other hand, hard-rock incision for the lower altitudes of slopes of the tributaries might be responsible for an erodibility decrease, which in turn increases the k_{sn} values. The knick point between both regimes is still heading toward the channel head. This finding is seen as a proxy for an insufficient time period until the latest change in uplift rate. Because of this, the local k_{sn} peaks, which are often found within the knick point zone cannot be interpreted for a proxy of uplift rate directly but for a proxy, that uplift rate increased recently within the last few million years.

This finding supports the apatite fission-track cooling path modelling studies of Hejl (1997, 1998). He showed for the Gurktaler Alps - no samples within the target region of this study - a Miocene build up age for the planation surface and modelled a recent uplift event starting about four million years ago based on assumptions.

In comparison, Reinecker (2000) defused the younger cooling path history modelling and indicated more gentle exhumation spread over several phases within an extended time range since the Pannonian (Late Miocene).

On the other hand, Wagner et al. (2010) revealed about 500 m Mur River incision during the last four million years within the Palaeozoic of Graz, which is in good agreement to the Hejl

river system	level	mean alt. [m]	mean incision [m]	profile pos. [km]
Upper Gurk	L2	959	19 (?)	131
	L3	1222	282±55	131
	L4	1460	520±98	131
Middle Gurk	L1	780	172±36	82
	L2	900	293±20	82
	L3	1015	408±110	82
Metnitz	L2	887	277±51	81
	L3	1183	573	81
	L4	1286	676±39	81
Wimitz	L1	771	168±30	60
Görschitz	L1	760	204±29	50
	L2	996	440±28	50
	L4	1456	901±153	50
remark	level	mean alt. [m]	mean incision [m]	difference [m]
glob. average	L1	776	181	181 (fr. trunk lev.)
glob. average	L2	935	337	156
glob. average	L3	1140	421	84
glob. average	L4	1401	699	278

Table 4.2.: Mean altitude, incision depth ($\pm 1\sigma$) of relict landscapes measured approximately above the main trunks at the given profile length.

(1997, 1998). He accounted this incision mostly to uplift. In Wagner et al. (2011) this total incision was resolved into separate levels (Tab. 4.1), which were used as the time base for uplift rate estimations in the sequel.

In Tab. 4.2 the statistics of level altitudes and incision depth of all regression segments of the river profile analysis of the tributaries in the investigation area are given. The data for the mean altitude of the planation surfaces and its mean incisions are taken from the profile position length given in the last column of the table. The mean altitudes fit quite well with the above discussed values for L1-L4.

In addition, the statistics at the bottom table shows that the mean value of all surfaces within the region also fit well into the defined intervals of L1 - L4. One can see the increase of incision

between the successive levels of the whole region between 180 up to 700 m. These data can be interpreted as an uplift history for the Gurktaler Alps within four steps of strong uplift according to the given difference of incision depth with intermediate periods of stasis, which would allow for building up each level as a Piedmont-step in the base position.

With Hejl (1997, 1998) assumption, that the recent period of uplift started about four million years ago, an average uplift rate of 700/4 Ma = 175 m/Ma can be estimated (assuming negligible exhumation on-top of relict landscapes). Just for comparison Hejl (1997, 1998) provided Early Miocene measured exhumation rates of 89 m/Ma, which also implies an uplift rate higher than this because the area was morphologically elevated since the Eocene (Linzer et al., 2002).

On the other hand, Wagner et al. (2011) provided slightly different timings for successfully correlated surfaces, which range from 1-2 Ma for L1 surface and up to 5 Ma for L3 the surface. An average uplift rate of the Gurktaler Alps is calculated by 421/5 Ma = 84 m/Ma, which appears to be plausible. Interestingly this uplift rate equals the measured Early Miocene exhumation rates for the Gurktaler Alps given by Hejl (1997, 1998).

4.3. Evolution of Valley Incisions

Within the Metnitz valley, a cross profile of the valley was found, where several stages of landscape evolution are becoming apparent. See section 3.1.3 for a description and in particular, see. Fig. 3.10A for a picture of the valley profile. Several landscape evolution models (Fig. 4.2) are discussed in the following. All models suggest the top level to exhibit a Miocene planation surface.

Model A: Fluvial incision is assumed to have acted for a very long time period. This resulted in the erosion of a large V-shaped valley, which was broadened in the Pleistocene by glacial processes. On the other hand, the model requires the existence of an inner gorge for the protection of the V-shaped valley bottom, which was not observed in the field

Model B: This model represents an intermediate model, which concludes all major younger landscape evolution processes into the Pleistocene. The varying interplay between glaciation

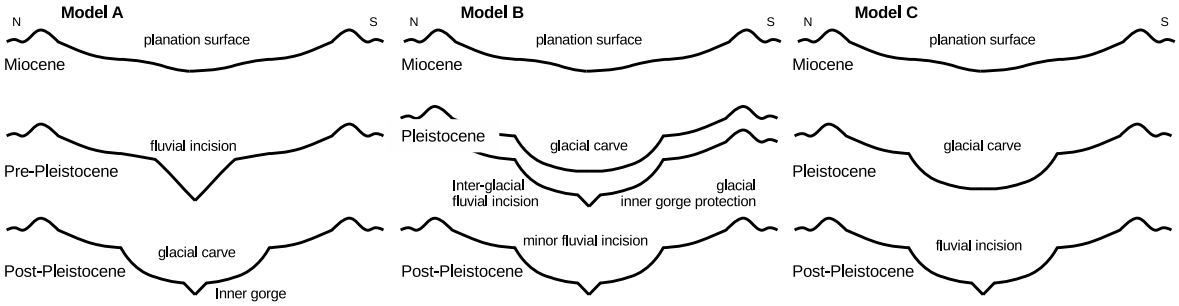

Figure 4.2.: Shows three landscape evolution models for the explanation of the Metnitz valley profile between Mt. Grebenzen and Mt. Eggerhöhe.

periods with glacial buzz-saw and wet inter-glacial periods with fluvial incisions would allow a prolonged time frame up to two million years for the landscape evolution. In particular, for the incision of a deep V-valley. On the other hand, also the concept of an inner gorge is required to protect the V-valley bottom from glacial advances.

Model C: In this model all fluvial erosion is supposed to be Post-Pleistocene. Therefore, this implies a fast evolution of the fluvial V-shaped valley bottom. The drawback of model C can be seen in the fact, that the time period of about 20.000 a afterwards the LGM might have been not long enough to erode this 100-150 m deep valley within this limited time period.

In total several proxies were found, which limit the latest phase of uplift into a short period of time probably not older than Late Pliocene to Pleistocene. These proxies are:

- Evolution model B in the Metnitz valley indicates Pleistocene erosion and is judged to be most plausible. For the lower V-valley, no planation surface was observed, probably due to glacial overprint.

- The strong V-valley incision of 170-200 m in the Wimitz valley (L1 surface) correlates with the incision depths of the Metnitz valley. For the Wimitz valley, it was concluded, that this channel is not equilibrated and therefore probably not older than Pleistocene.

- Un-equilibrated channel profiles close to the channel head are found in the whole area, indicating recent uplift not older than a few Ma.

- The correlation of L1 with Stadelber / Zahrerberg level suggest an age of three million years, which is slightly older compared to the above given rough estimates.

Appendix A.

Appendix

A.1. Paleo-geographic Evolution of the Eastern Alps

During the Cadomian orogeny (Von Raumer et al., 2015), Apulia was part of a promontory attached to Africa. The Austroalpine and South-alpine (realms within Apulia) have been part of the Hun super-terrane, which separated from the northern margin of Gondwana in Early Palaeozoic times (ca. 435 Ma) closing up the northern Rheic Ocean toward Gondwana and opening up the Palaeotethys in the back-arc (Schuster et al., 2001).

The opening of the Palaeotethys in the Ordovician to Silurian is supposed to be the origin of protoliths found in the Palaeozoic zones in the Eastern Alps Stampfli (1996). In particular, these are the Carnic Alps, the Greywacke zone, the Gurktaler nappes and the Palaeozoic of Graz, showing rock types from shallow marine sediments, volcanism, rifting and subduction within the Hochwipfelflysch in the Anisian in the Carnic Alps (Neubauer and Pistotnik, 1984; Stampfli, 1996).

During the Variscan collisional event (380 - 300 Ma) this Hun super-terrane (including the western parts of the Alpine terrain) was squeezed between former accreted Baltica, Laurentia and Avalonia in the north and the Gondwana continent in the south forming Pangaea (Schuster et al., 2001). But the south-eastern border of the Variscan orogen was an active continental margin below, which the westernmost part of the Palaeotethyan ocean was subducted Stampfli (1996). In the Permian (290 – 249 Ma) slab roll-back of the western Palaeotethys induced

extension on the southern margin of Laurasia forming small back-arc basins. One of these triggered the opening of the Meliata - Hallstatt ocean.

In the Anisian (240 Ma) the northward Palaeotethys subduction already finished in its western gulf. The deposition of evaporites in the former back-arc basin indicate the start of rifting in the Western Carpathians, and magmatism also followed by evaporites (Haselgebirge) in the Austroalpine (Greywacke Zone) (Kozur, 1991). The Meliata-Hallstatt ocean now evolved within the Apulian plate with a connection to the Neotethys (Schuster et al., 2001; Stampfli et al., 1998). In the Early Triassic widespread shallow shelf siliciclastic rocks of the Werfen Fm. and from Middle Triassic times onward carbonate sedimentation of Guttenberg limestones are present in most of the NCA nappe (Mandl, 2000). After the Anisian Reiffling event (rapid deepening and block-faulting) the basin differentiated into a shallow marine facies (Wetterstein Fm.) interrupted by the Reiffling/Partnach Basin and the Hallstatt basin within the deeper shelf bordering the open Tethys ocean (Mandl, 2000). From Late Carnian (220 Ma) onward carbonate production increased onto the whole shallow water platform (Hauptdolomit and Dachstein Fm.) due to sea level rise and a transgressive pulse at the Norian/Rhaetian boundary (Mandl, 2000). The intra-oceanic subduction of the Meliata - Hallstatt ocean was already in progress.

In the Callovian (upper Middle Jurassic) the platforms drowned (Mandl, 2000; Gawlick et al., 1999) and radiolarites and turbidites were sedimented (Strubberg, and Ruhpolding Fm.) due to the approaching south-eastward subduction front. In the Oxfordian (162 Ma, Upper Jurassic) the siliciclastic sedimentation abruptly finished, which is interpreted as the final E to SE subduction of the MH ocean beneath the intra-oceanic Vardar subduction zone. Obduction halted along the distal eastern continental margins of Adria before the onset of the eo-alpine orogeny in Early Cretaceous time.

The Barremian - Cerremanian (145-94Ma) eo-alpine orogeny is correlated with uplift and subsequent gravitational nappe sliding of the Juvavic nappe into a northward adjacent trough in the Tirolikum (Gawlick et al., 1999). This early orogeny started within the eastern part of the Austroalpine plate and is interpreted to relate to an oblique continent-continent collision zone, resulting in a complex internal structure of nappe stacking and folding, which starts with a W to NNW directed thrusting in the Upper Cretaceous, followed by an E directed

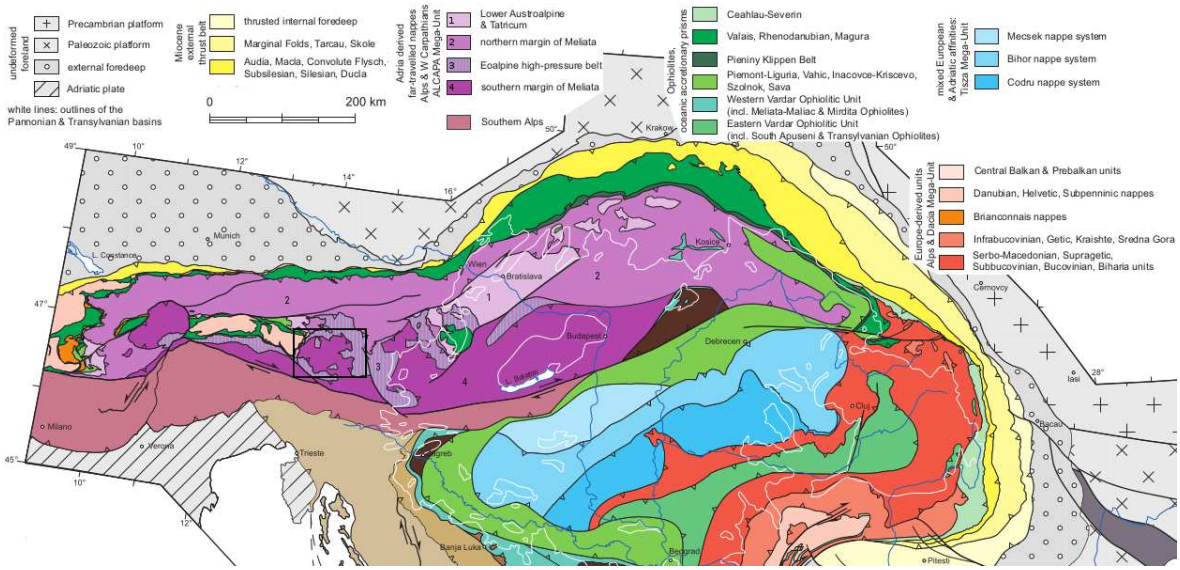

Figure A.1.: Depicts the Austroalpine units of the Eastern Alps according to (Schmid et al., 2008). The map identified Lower Austroalpine (light violet colour) and upper Austroalpine tectonic units (darker violet colours). Furthermore, palaeo-geographic heritage to facies of e.g. the Meliata-Hallstatt Ocean is given. Within the black box the location of the Gurktaler nappe is marked.

extension event, which is interpreted as a gravitational collapse (Froitzheim et al., 1994). The geographical position of this suture between the Periadriatic line and the southern edge of the NCA is still debated. A belt of high metamorphic rocks up to ecologist facies with the Koralpe-Wölz and Saualpe crystalline is discussed to constitute this S to SE directed continent-continent collision zone Froitzheim et al. (1996); Stüwe and Schuster (2010); Handy et al. (2010). In the Palaeocene to Eocene the direction of thrusting changed to top N to NNW, which Froitzheim et al. (1994, 1996) related to subduction of the Alpine Tethys to the north.

The opening of eastern part of the Alpine Tethys (Piemont–Ligurian Ocean basin) stated in parallel to the Meliata-Hallstatt subduction (200–170 Ma). While the oblique opening of the northern Valais ocean basin began from 131 to 93 Ma and was linked to the opening of the Bay of Biscay and to intra-continental subduction and nappe stacking in the Eastern Alps, referred to as the eo-alpine Orogeny (Faupl and Wagreich, 2000).

The closure of Alpine Tethys occurred in three stages and started from (131-118 Ma) in the Western part where the Ligurian ocean basin was involved in eastward intra-oceanic sub-

duction, e.g. (Handy et al., 2010). A second stage (84–35 Ma) entailed southeast-directed subduction, initially of the Piemont Ocean and the western part of the Ligurian Ocean, and finally of the Valais Ocean and the distal European continental margin. The third and final stage (35 Ma–recent) involved continent-continent collision and orogen build up in the Alps and roll-back subduction of most of the remaining eastern Ligurian Ocean.

The map in Fig. A.1 (Schmid et al., 2008) shows both the palaeogeogenetic origin of rocks in the Meliata-Hallstatt ocean and tectonic units. The Austroalpine Adria derived nappe constitutes the upper plate (Neubauer et al., 2000) and is divided into the stacked Upper and Lower Austroalpine units. In the Eastern Alps, the crystalline basement of the later is exhumed at sparse locations, which are the Radstädter Tauern to the north of the Gurktaler nappes. An eo-alpine high-pressure belt (Koralpe-Wölz nappes) separates the northern and southern margin of Meliata facies in EW direction. Kozur (1991) assumed an initial southward sliding of the northern carbonate platform into the Meliata-Hallstatt basin, resulting in a stacking of Juvavic carbonate nappes on-top of Permian evaporites during the intra-oceanic subduction but did not give an explanation for the fare transport of cover nappes to the north. On the other hand, Gawlick et al. (1999) discussed northward gravitational sliding of the northern NCA into an adjacent northern oceanic tough caused by subduction independent tectonics.

The Eastern Alps wedge is composed out of several tectonostratigraphic units, which are shortly described in the following. In the under-plate position these are the stable European continental lithosphere, followed by the Helvetic zone, a thin-skinned thrust-belts formed out of detached continental cover sequences, which was trusted on-top of the European margin. In the Eastern Alps, the Alpine Tethys developed within the European continental margin consisting basically out of the Valais unit (North Peninnic oceanic nappes), which separates the stable European foreland from the Sub-Peninnic. Remnants of this north-Peninnic flysch in-fillings of the Valais unit can be observed as the Rhenodanubic Flyschzone at the north of NCA and on-top of the exhumed nappe stack of the Tauern Window as the Obere Schieferhülle above the Helvetian nappes and the Sub-Peninnic gneisses of the Lepontian dome.

A.2. Regression Results of Stream Profile Analysis

The following collection of tables in Tab. A.1-A.8 shows the regression results of all investigated river systems. Within the tables the segments are identified by a label, the minimum height H and the related drainage area A of each segment at the outlet point. The *lgm* flag identifies the segment to be glacially or fluvial overprinted. The last two columns are displaying the regression results of the steepness index k_s and the concavity index θ together with the confidence intervals.

River	seg	H_{out} [m]	A_{out} [km^2]	lgm	$k_s \pm 2\sigma_{ks}$	$\theta \pm 2\sigma_\theta$
Andertalbach	H1	552	1.58e+03	0	3.84e+02 ±4.53e-01	-0.58 ±0.40
	H2	937	2.30e+03	1	2.35e-02 ±8.31e-05	-0.08 ±0.55
	H3	1458	2.55e+03	0	1.29e+07 ±1.61e+05	-1.33 ±0.17
Gurk	H1	552	1.24e+03	0	3.84e+02 ±4.53e-01	-0.58 ±0.40
	H2	937	1.68e+03	1	2.35e-02 ±8.31e-05	-0.08 ±0.55
	H3	1330	2.30e+03	0	7.94e+04 ±1.38e+02	-0.91 ±0.05
	H4	1620	2.55e+03	0	5.59e+04 ±3.51e+02	-0.93 ±0.14
Holzbodenbach	H1	552	1.58e+03	0	3.84e+02 ±4.53e-01	-0.58 ±0.40
	H2	937	2.29e+03	1	2.35e-02 ±8.31e-05	-0.08 ±0.55
Neuwirtalmbach	H1	552	1.25e+03	0	3.84e+02 ±4.53e-01	-0.58 ±0.40
	H2	937	1.71e+03	1	2.35e-02 ±8.31e-05	-0.08 ±0.55
	H3	1330	2.55e+03	0	4.77e+04 ±4.28e+02	-0.89 ±0.05
	H4	1809	2.55e+03	0	1.53e+05 ±1.34e+03	-1.02 ±0.34
Saureggenbach	H1	552	1.26e+03	0	3.84e+02 ±4.53e-01	-0.58 ±0.40
	H2	937	2.29e+03	1	2.35e-02 ±8.31e-05	-0.08 ±0.55
	H3	1538	2.30e+03	1	4.59e+04 ±8.56e+02	-0.89 ±0.52
Stoicharthüttenbach	H1	552	1.26e+03	0	3.84e+02 ±4.53e-01	-0.58 ±0.40
	H2	937	1.71e+03	1	2.35e-02 ±8.31e-05	-0.08 ±0.55
	H3	1330	2.55e+03	0	3.16e+02 ±1.93e+00	-0.60 ±0.07
Winklbach	H1	552	1.26e+03	0	3.84e+02 ±4.53e-01	-0.58 ±0.40
	H2	937	1.71e+03	1	2.35e-02 ±8.31e-05	-0.08 ±0.55
	H3	1276	2.30e+03	1	1.83e+10 ±2.40e+08	-1.61 ±0.49
Ursulabach	H1	552	1.58e+03	0	3.84e+02 ±4.53e-01	-0.58 ±0.40
	H2	937	2.29e+03	1	2.35e-02 ±8.31e-05	-0.08 ±0.55
	H3	1335	2.55e+03	0	5.73e+01 ±9.40e-02	-0.48 ±0.03
Görzbach	H1	552	1.62e+03	0	3.84e+02 ±4.53e-01	-0.58 ±0.40
	H2	1045	2.30e+03	0	1.30e+04 ±7.91e+01	-0.76 ±0.25
	H3	1452	2.55e+03	0	4.53e+03 ±2.13e+01	-0.76 ±0.12
Peiningbach	H1	552	1.67e+03	0	3.84e+02 ±4.53e-01	-0.58 ±0.40
	H2	1437	2.55e+03	0	6.09e+02 ±3.68e+00	-0.65 ±0.16

Table A.1.: Upper Gurk River channel-profile regression data. H_{out}, A_{out} means the elevation and catchment size of the outlet of the segment H_i, while k_s, θ are the regressed steepness and concavity index including a 2σ confidence interval. The *lgm* flag indicates if the segment was glaciated or not.

River	seg	H_{out} [m]	A_{out} [km^2]	lgm	$k_s \pm 2\sigma_{ks}$	$\theta \pm 2\sigma_\theta$
Mühlbachgraben	H1	552	2.30e+03	0	2.67e+02 ±2.96e-01	-0.55 ±0.19
	H2	682	2.30e+03	0	4.09e+06 ±1.35e+04	-1.19 ±0.17
	H3	942	2.55e+03	0	1.15e+04 ±7.01e+01	-0.84 ±0.14
Olschnöggbach	H1	552	2.30e+03	0	1.86e+01 ±4.12e-02	-0.42 ±0.40
	H2	639	2.30e+03	0	1.41e+07 ±5.76e+04	-1.29 ±0.16
	H3	836	2.55e+03	0	1.94e+07 ±3.89e+05	-1.37 ±0.48
Albeck_schattseite	H1	552	2.30e+03	0	1.82e+01 ±1.41e-02	-0.42 ±0.37
	H2	752	2.55e+03	0	7.06e+06 ±3.53e+04	-1.24 ±0.33
	H3	919	2.55e+03	0	1.43e+07 ±1.66e+05	-1.41 ±0.41
Pirkerkogelbach	H1	552	2.30e+03	0	8.67e+01 ±1.46e-01	-0.50 ±0.27
	H2	725	2.55e+03	0	3.69e+05 ±2.55e+03	-1.06 ±0.67
	H3	868	2.55e+03	0	2.13e+04 ±2.63e+02	-0.93 ±0.32
Plötschgrabenbach	H1	552	2.29e+03	0	8.16e+01 ±7.70e-02	-0.50 ±0.21
	H2	745	2.30e+03	0	1.37e+09 ±9.18e+06	-1.57 ±1.01
	H3	1027	2.55e+03	0	1.42e+02 ±1.41e+00	-0.51 ±0.13
Draschelbach	H1	552	2.30e+03	0	2.32e+02 ±2.52e-01	-0.55 ±0.18
	H2	682	2.33e+03	0	3.73e+03 ±1.91e+01	-0.76 ±0.10
	H3	987	2.55e+03	0	1.20e+01 ±8.88e-02	-0.40 ±0.19
Ratschachbach	H1	552	2.29e+03	0	5.98e+01 ±1.35e-01	-0.48 ±0.39
	H2	646	2.30e+03	0	1.31e+14 ±6.99e+11	-2.26 ±0.68
	H3	794	2.55e+03	0	1.87e+06 ±4.82e+03	-1.14 ±0.21
Glödnitz	H1	552	1.67e+03	0	1.89e-01 ±1.78e-04	-0.20 ±0.44
	H2	736	2.30e+03	1	6.93e+03 ±3.86e+01	-0.80 ±0.97
Sirnitz	H1	552	2.29e+03	0	1.00e+02 ±9.41e-02	-0.51 ±0.34
	H2	810	2.30e+03	0	1.21e+06 ±8.89e+03	-1.08 ±0.22
	H3	1205	2.55e+03	0	8.23e+03 ±1.10e+02	-0.79 ±0.19
Griffenbach	H1	552	1.71e+03	0	3.48e+00 ±2.46e-03	-0.34 ±0.42
	H2	769	2.30e+03	0	1.92e+05 ±4.95e+02	-0.93 ±0.11
	H3	1240	2.55e+03	1	4.64e+01 ±7.65e-01	-0.39 ±0.15
Stronbach	H1	552	2.29e+03	0	1.00e+02 ±9.41e-02	-0.51 ±0.34
	H2	810	2.30e+03	0	1.99e+04 ±8.83e+01	-0.84 ±0.31
	H3	971	2.54e+03	0	3.44e+10 ±5.55e+08	-1.76 ±0.51
	H4	1300	2.55e+03	0	4.93e+02 ±9.50e+00	-0.59 ±0.36
Hafendorfbach	H1	552	2.55e+03	0	6.59e+00 ±5.88e-03	-0.37 ±0.27
	H2	727	2.55e+03	0	1.21e+09 ±9.77e+06	-1.72 ±0.66
	H3	892	2.55e+03	0	2.90e+07 ±1.61e+06	-1.47 ±1.59
Hochrindlbach	H1	552	1.71e+03	0	3.48e+00 ±2.46e-03	-0.34 ±0.42
	H2	804	2.30e+03	0	1.87e+09 ±6.33e+06	-1.55 ±0.41
	H3	1241	2.55e+03	0	2.26e+04 ±2.80e+02	-0.86 ±0.35
Wildbachgraben	H1	552	2.30e+03	0	1.21e+01 ±2.69e-02	-0.40 ±0.41
	H2	635	2.30e+03	0	1.43e+05 ±4.04e+02	-1.00 ±0.11
Höllgrabenbach	H1	552	2.30e+03	0	1.17e+02 ±3.10e-01	-0.51 ±0.57
	H2	720	2.55e+03	0	1.41e+03 ±7.21e+00	-0.68 ±0.09
	H3	946	2.55e+03	0	1.16e+04 ±3.31e+02	-0.89 ±0.59
Zammelsbergbach	H1	552	2.55e+03	0	1.09e-01 ±1.28e-04	-0.17 ±0.45
	H2	771	2.55e+03	0	1.96e+05 ±2.04e+03	-1.08 ±0.66
Krassnitzbach	H1	552	2.30e+03	0	8.16e+01 ±7.70e-02	-0.50 ±0.21
	H2	706	2.30e+03	0	9.86e+09 ±3.65e+07	-1.68 ±0.47
	H3	1037	2.55e+03	0	2.65e+02 ±2.76e+00	-0.57 ±0.19
Zweinitzenbach	H1	552	2.29e+03	0	8.16e+01 ±7.70e-02	-0.50 ±0.21
	H2	709	2.30e+03	0	3.50e+06 ±9.45e+03	-1.15 ±0.13
	H3	1203	2.55e+03	0	3.13e+05 ±3.74e+03	-1.05 ±0.55
Langwiesenbach	H1	552	2.30e+03	0	1.42e+02 ±2.26e-01	-0.52 ±0.27
	H2	645	2.30e+03	0	1.40e+08 ±6.77e+05	-1.37 ±0.25
	H3	1031	2.55e+03	0	3.92e+03 ±3.27e+01	-0.82 ±0.22
Leonhardsbach	H1	552	2.29e+03	0	1.99e+01 ±1.57e-02	-0.43 ±0.37
	H2	829	2.30e+03	0	2.11e+10 ±7.05e+07	-1.75 ±0.29
	H3	1153	2.55e+03	0	1.66e+06 ±2.96e+04	-1.19 ±0.75
Mödringbach	H1	552	1.67e+03	0	5.46e+01 ±5.02e-02	-0.48 ±0.20
	H2	770	2.54e+03	0	6.77e+04 ±1.46e+02	-0.92 ±0.08
	H3	1027	2.55e+03	0	8.19e+04 ±9.11e+02	-0.95 ±0.24
Kainzbach	H1	552	2.33e+03	0	1.07e+02 ±2.28e-01	-0.51 ±0.31
	H2	634	2.55e+03	0	2.22e+04 ±2.99e+02	-0.84 ±1.19
	H3	957	2.55e+03	0	7.74e+01 ±9.78e-01	-0.54 ±0.22

Table A.2.: Middle Gurk River channel-profile regression data. H_{out}, A_{out} means the elevation and catchment size of the outlet of the segment H_i, while k_s, θ are the regressed steepness and concavity index including a 2σ confidence interval. The *lgm* flag indicates if the segment was glaciated or not.

River	seg	H_{out} [m]	A_{out} [km^2]	lgm	$k_s \pm 2\sigma_{ks}$	$\theta \pm 2\sigma_\theta$
Rabingbach	H1	638	2.55e+03	0	3.15e+12 ±6.11e+10	-2.13 ±1.24
	H2	957	2.55e+03	0	8.07e+01 ±1.54e+00	-0.60 ±0.37
Watteinbach	H1	657	2.55e+03	0	6.82e+05 ±2.83e+03	-1.11 ±0.39
	H2	871	2.55e+03	0	2.70e+03 ±4.38e+01	-0.81 ±0.32
Zabersdorfbach	H1	619	2.30e+03	0	6.24e+06 ±2.34e+04	-1.21 ±0.28
	H2	776	2.55e+03	0	7.13e+02 ±2.30e+00	-0.66 ±0.17

Table A.3.: Lower Gurk River channel-profile regression data. H_{out}, A_{out} means the elevation and catchment size of the outlet of the segment H_i, while k_s, θ are the regressed steepness and concavity index including a 2σ confidence interval. The *lgm* flag indicates if the segment was glaciated or not.

River	seg	H_{out} [m]	A_{out} [km^2]	lgm	$k_s \pm 2\sigma_{ks}$	$\theta \pm 2\sigma_\theta$
Metnitz	H1	552	1.64e+03	1	2.74e+03 ±4.08e+00	-0.67 ±0.18
	H2	793	2.30e+03	1	1.58e+00 ±4.79e-03	-0.26 ±0.09
	H3	1231	2.55e+03	1	4.55e+02 ±9.50e+00	-0.61 ±0.20
Mödringbach2	H1	552	1.67e+03	1	2.74e+03 ±4.08e+00	-0.67 ±0.18
	H2	793	2.30e+03	1	1.11e+02 ±1.76e-01	-0.49 ±0.21
	H3	1200	2.55e+03	0	5.93e+02 ±3.44e+00	-0.61 ±0.07
Pöllauerbach	H1	552	1.70e+03	0	7.65e+00 ±1.51e-02	-0.38 ±0.20
	H2	963	2.55e+03	0	5.35e+02 ±2.97e+00	-0.56 ±0.09
	H3	1683	2.55e+03	0	6.98e+01 ±8.33e-01	-0.49 ±0.32
Moserwinkelbach	H1	552	2.30e+03	1	4.11e+03 ±8.65e+00	-0.69 ±0.24
	H2	730	2.30e+03	1	6.33e+11 ±1.48e+09	-1.88 ±0.65
	H3	1021	2.55e+03	0	1.05e+05 ±4.34e+02	-0.99 ±0.10
Schranzbach	H1	552	1.71e+03	0	1.03e+01 ±2.55e-02	-0.40 ±0.36
	H2	670	2.30e+03	1	1.03e+08 ±2.38e+05	-1.33 ±0.23
	H3	1029	2.55e+03	0	2.88e+09 ±3.69e+07	-1.64 ±0.19
	H4	1536	2.55e+03	0	4.41e+03 ±4.54e+01	-0.81 ±0.22
Röttingbach	H1	552	1.64e+03	1	2.74e+03 ±4.08e+00	-0.67 ±0.18
	H2	792	2.29e+03	1	2.47e+03 ±9.24e+00	-0.67 ±0.15
	H3	1305	2.55e+03	1	7.44e+01 ±2.95e-01	-0.44 ±0.12
Timrianbach	H1	552	2.30e+03	0	1.16e+03 ±2.95e+00	-0.63 ±0.32
	H2	808	2.33e+03	0	6.54e+02 ±3.03e+00	-0.59 ±0.19
Rossbach	H1	552	2.29e+03	1	1.48e+03 ±2.73e+00	-0.64 ±0.24
	H2	756	2.30e+03	1	1.16e+04 ±7.58e+01	-0.78 ±0.13
Schwarzenbach	H1	552	1.67e+03	1	2.74e+03 ±4.08e+00	-0.67 ±0.18
	H2	788	2.30e+03	1	2.38e+02 ±3.55e-01	-0.54 ±0.22
	H3	1017	2.30e+03	1	7.53e+03 ±3.98e+01	-0.74 ±0.22
	H4	1217	2.55e+03	0	1.64e+11 ±1.44e+09	-1.97 ±0.52
Feistritz	H1	552	1.71e+03	1	2.92e+03 ±4.99e+00	-0.67 ±0.21
	H2	910	2.55e+03	0	4.34e+02 ±8.00e-01	-0.59 ±0.08
	H3	1246	2.55e+03	0	5.07e+02 ±5.10e+00	-0.61 ±0.22
Teichlbach	H1	552	1.71e+03	1	2.74e+03 ±4.08e+00	-0.67 ±0.18
	H2	809	2.54e+03	1	1.38e+04 ±9.45e+01	-0.81 ±0.25
Ulsbach	H1	552	1.67e+03	1	2.74e+03 ±4.08e+00	-0.67 ±0.18
	H2	793	2.30e+03	1	1.33e-01 ±3.59e-04	-0.12 ±0.12
Gwerzbach	H1	552	2.29e+03	1	1.48e+03 ±2.73e+00	-0.64 ±0.24
	H2	754	2.54e+03	1	1.69e+04 ±3.14e+01	-0.79 ±0.06
	H3	1329	2.55e+03	1	1.79e+02 ±2.46e+00	-0.51 ±0.14
Vellachbach	H1	552	2.29e+03	1	2.74e+03 ±4.08e+00	-0.67 ±0.18
	H2	818	2.30e+03	1	9.38e+14 ±8.42e+12	-2.28 ±4.57
	H3	1021	2.55e+03	0	1.52e+03 ±6.02e+00	-0.70 ±0.05
Zienitzenbach	H1	552	2.30e+03	0	6.76e+03 ±1.74e+01	-0.72 ±0.26
	H2	705	2.55e+03	1	1.07e+04 ±7.65e+01	-0.79 ±0.15
	H3	1088	2.55e+03	0	1.29e+04 ±7.50e+01	-0.89 ±0.15

Table A.4.: Metnitz River channel-profile regression data. H_{out}, A_{out} means the elevation and catchment size of the outlet of the segment H_i, while k_s, θ are the regressed steepness and concavity index including a 2σ confidence interval. The *lgm* flag indicates if the segment was glaciated or not.

River	seg	H_{out} [m]	A_{out} [km^2]	lgm	$k_s \pm 2\sigma_{ks}$	$\theta \pm 2\sigma_\theta$
Frischengraben	H1	466	5.42e+02	1	3.64e+13 ±2.63e+11	-1.94 ±3.41
	H2	534	2.29e+03	0	1.31e-02 ±4.42e-05	-0.01 ±1.15
	H3	861	2.55e+03	0	1.57e+02 ±1.22e+00	-0.57 ±0.11
Pitschgraben	H1	466	5.52e+02	1	3.64e+13 ±2.63e+11	-1.94 ±3.41
	H2	534	2.30e+03	0	2.57e-05 ±9.62e-08	0.33 ±1.39
	H3	825	2.55e+03	0	1.29e+06 ±1.20e+04	-1.21 ±0.45
Schwarzenbach2	H1	466	5.77e+02	1	3.64e+13 ±2.63e+11	-1.94 ±3.41
	H2	897	2.55e+03	0	4.57e+01 ±2.54e-01	-0.51 ±0.07
Wimitz	H1	466	4.54e+02	1	3.64e+13 ±2.63e+11	-1.94 ±3.41
	H2	534	5.77e+02	0	1.31e-02 ±4.42e-05	-0.01 ±1.15
	H3	737	2.30e+03	0	7.50e+11 ±9.85e+09	-1.96 ±1.13
	H4	879	2.55e+03	0	2.70e+02 ±1.49e+00	-0.59 ±0.06
Steinbichelbach	H1	466	5.51e+02	1	3.64e+13 ±2.63e+11	-1.94 ±3.41
	H2	528	2.30e+03	0	1.23e-01 ±4.00e-04	-0.13 ±1.16
	H3	770	2.55e+03	0	1.88e+04 ±1.88e+02	-0.84 ±0.28
	H4	948	2.55e+03	0	3.77e+03 ±3.75e+01	-0.74 ±0.16
Goschenbach	H1	466	5.69e+02	1	3.64e+13 ±2.63e+11	-1.94 ±3.41
	H2	534	2.30e+03	0	1.31e-07 ±8.36e-10	0.62 ±2.53
	H3	865	2.55e+03	0	1.76e+02 ±1.30e+00	-0.53 ±0.09
Graibach	H1	466	4.63e+02	1	3.64e+13 ±2.63e+11	-1.94 ±3.41
	H2	534	2.29e+03	0	1.31e-02 ±4.42e-05	-0.01 ±1.15
	H3	738	2.30e+03	0	5.49e+06 ±8.19e+04	-1.25 ±0.63
	H4	919	2.55e+03	0	6.86e+06 ±6.15e+04	-1.26 ±0.25
Gritschgrabenbach	H1	466	5.73e+02	1	3.64e+13 ±2.63e+11	-1.94 ±3.41
	H2	782	2.55e+03	0	1.48e+03 ±1.34e+01	-0.66 ±0.11

Table A.5.: Wimitz River channel-profile regression data. H_{out}, A_{out} means the elevation and catchment size of the outlet of the segment H_i, while k_s, θ are the regressed steepness and concavity index including a 2σ confidence interval. The *lgm* flag indicates if the segment was glaciated or not.

River	seg	H_{out} [m]	A_{out} [km^2]	lgm	$k_s \pm 2\sigma_{ks}$	$\theta \pm 2\sigma_\theta$
Drisseckerbach	H1	484	2.29e+03	0	6.62e+00 ±1.79e-02	-0.35 ±0.46
	H2	570	2.30e+03	0	5.35e+14 ±1.62e+12	-2.21 ±0.74
	H3	1310	2.55e+03	0	2.24e+04 ±2.88e+02	-0.84 ±0.23
Görschitz	H1	484	1.67e+03	0	1.20e+02 ±2.13e-01	-0.49 ±0.18
	H2	1077	2.55e+03	1	5.31e+05 ±1.18e+04	-1.15 ±0.28
Greierbach	H1	484	2.29e+03	0	4.11e+01 ±5.64e-02	-0.44 ±0.29
	H2	827	2.30e+03	0	3.09e+02 ±1.17e+00	-0.49 ±0.10
	H3	1739	2.55e+03	0	3.32e+02 ±5.51e+00	-0.59 ±0.33
Grünburgerbach	H1	484	2.29e+03	0	2.75e+01 ±3.76e-02	-0.42 ±0.30
	H2	863	2.30e+03	0	5.80e+05 ±2.54e+03	-0.97 ±0.89
	H3	1753	2.55e+03	0	3.91e+04 ±3.56e+02	-0.96 ±0.23
Hinterbergbach	H1	484	2.29e+03	1	1.20e+02 ±2.13e-01	-0.49 ±0.18
	H2	1144	2.55e+03	0	1.05e+05 ±3.94e+02	-0.94 ±0.12
Hörbach	H1	484	1.70e+03	1	1.20e+02 ±2.13e-01	-0.49 ±0.18
	H2	1182	2.55e+03	0	2.19e+03 ±1.27e+01	-0.67 ±0.23
Loellingbach	H1	484	1.71e+03	1	4.77e+01 ±5.63e-02	-0.45 ±0.23
	H2	751	2.30e+03	1	2.66e+07 ±7.60e+04	-1.17 ±0.63
	H3	1299	2.55e+03	1	3.57e+01 ±9.87e-02	-0.41 ±0.04
Mosinzbach	H1	484	1.70e+03	0	5.30e+02 ±6.65e-01	-0.57 ±0.21
	H2	790	2.30e+03	0	5.31e+01 ±1.28e-01	-0.42 ±0.10
	H3	1298	2.55e+03	0	1.28e+02 ±8.66e-01	-0.50 ±0.15
Schafgrabenbach	H1	484	2.29e+03	0	5.30e+02 ±6.65e-01	-0.57 ±0.21
	H2	790	2.55e+03	0	2.91e+02 ±7.62e-01	-0.52 ±0.04
Tiefenbach	H1	484	1.67e+03	1	1.20e+02 ±2.13e-01	-0.49 ±0.18
Waldbach	H1	484	1.66e+03	0	1.20e+02 ±2.13e-01	-0.49 ±0.18
	H2	1477	2.55e+03	0	2.02e+05 ±1.31e+03	-0.96 ±0.19

Table A.6.: Görschitz River channel-profile regression data. H_{out}, A_{out} means the elevation and catchment size of the outlet of the segment H_i, while k_s, θ are the regressed steepness and concavity index including a 2σ confidence interval. The *lgm* flag indicates if the segment was glaciated or not.

River	seg	H_{out} [m]	A_{out} [km^2]	lgm	$k_s \pm 2\sigma_{ks}$	$\theta \pm 2\sigma_\theta$
Silberbach	H1	540	1.70e+03	0	3.92e+01 ±1.43e-01	-0.48 ±0.81
	H2	1164	2.55e+03	0	7.87e+03 ±7.50e+01	-0.81 ±0.29
Dobritschergrabenbach	H1	540	2.30e+03	1	3.92e+01 ±1.43e-01	-0.48 ±0.81
	H2	664	2.30e+03	1	4.36e+04 ±1.24e+02	-0.85 ±0.16
	H3	1153	2.55e+03	1	1.66e+01 ±4.87e-01	-0.46 ±0.11

Table A.7.: Silberbach River channel-profile regression data. H_{out}, A_{out} means the elevation and catchment size of the outlet of the segment H_i, while k_s, θ are the regressed steepness and concavity index including a 2σ confidence interval. The *lgm* flag indicates if the segment was glaciated or not.

River	seg	H_{out} [m]	A_{out} [km^2]	lgm	$k_s \pm 2\sigma_{ks}$	$\theta \pm 2\sigma_\theta$
Glan	H1	450	5.66e+02	1	8.76e+02 ±3.34e+00	-0.70 ±0.38
	H2	531	2.30e+03	1	1.08e+07 ±6.16e+04	-1.25 ±0.57
	H3	610	2.55e+03	1	1.68e+09 ±4.48e+07	-1.75 ±0.43
Bachergrabenbach	H1	450	5.73e+02	1	8.76e+02 ±3.34e+00	-0.70 ±0.38
	H2	953	2.55e+03	0	2.58e+04 ±1.55e+02	-0.95 ±0.10
Roggbach	H1	450	5.50e+02	1	8.76e+02 ±3.34e+00	-0.70 ±0.38
	H2	780	2.30e+03	1	3.33e+09 ±4.59e+07	-1.66 ±1.17
	H3	880	2.55e+03	1	1.76e+02 ±5.25e+00	-0.72 ±0.29
Feistritz2	H1	450	2.29e+03	1	4.18e+05 ±2.84e+03	-1.01 ±0.51
	H2	570	2.29e+03	1	5.36e+08 ±7.49e+06	-1.38 ±1.21
	H3	893	2.55e+03	0	6.26e+05 ±1.77e+03	-1.15 ±0.12
Liembergbach	H1	450	5.70e+02	1	4.71e+02 ±2.22e+00	-0.66 ±0.57
	H2	570	2.29e+03	1	1.56e+05 ±2.31e+03	-0.91 ±1.38
	H3	661	2.30e+03	1	3.29e+06 ±3.63e+04	-1.24 ±0.85
	H4	740	2.55e+03	1	2.20e+08 ±1.17e+07	-1.72 ±2.58
Harterbach	H1	450	2.29e+03	1	2.42e+05 ±1.57e+03	-0.98 ±0.50
	H2	880	2.55e+03	0	7.24e+03 ±4.00e+01	-0.84 ±0.16
Mühlbach	H1	450	2.29e+03	1	1.12e+06 ±6.70e+03	-1.06 ±0.21
	H2	816	2.55e+03	0	1.85e+04 ±1.98e+02	-0.89 ±0.22
Kraigerbach	H1	450	2.30e+03	1	5.05e+09 ±1.67e+07	-1.47 ±0.26
	H2	594	2.54e+03	0	1.51e+05 ±2.24e+03	-0.97 ±0.24
	H3	970	2.55e+03	0	1.64e+03 ±1.80e+01	-0.74 ±0.11

Table A.8.: Glan River channel-profile regression data. H_{out}, A_{out} means the elevation and catchment size of the outlet of the segment H_i, while k_s, θ are the regressed steepness and concavity index including a 2σ confidence interval. The *lgm* flag indicates if the segment was glaciated or not.

A.3. Geomorphological Map of the Gurktaler Alps and Outcrop Overview

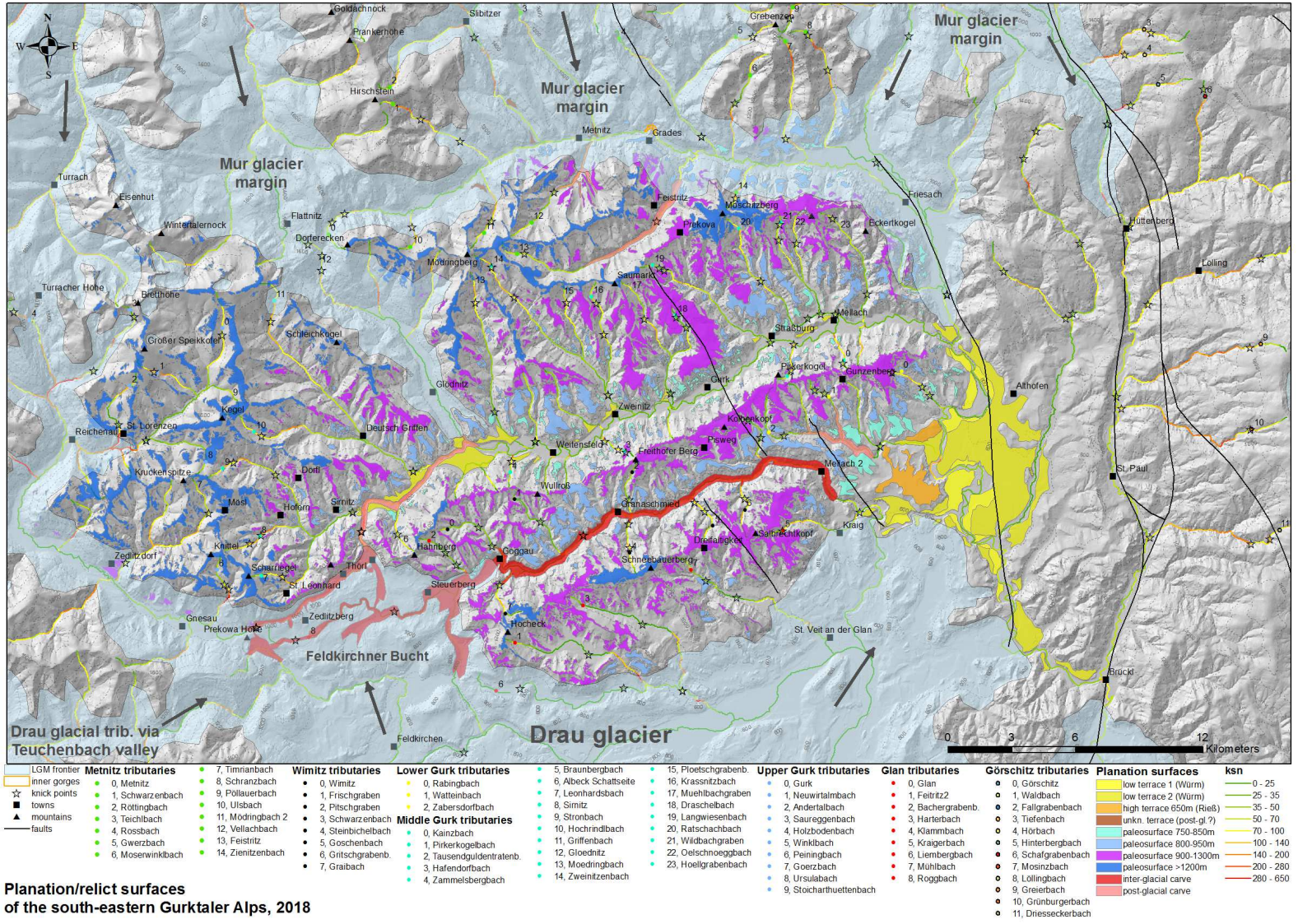

Figure A.2.: Geomorphological map of the Gurktaler Alps with mapped palaeo-surfaces.

ref.	date	lon.	lat.	outcrop description	lithology	structures	hydrology
OCa1	23.07.2016	14,298040	46,905605	Langwiesental bridge north of Straßburg	Qtz-phyllite		50l/s
OCa2	23.07.2016	14,269572	46,956170	Feistritztal, last serpentine before valley floor	Qtz-phyllite		
OCa3	23.07.2016	14,263408	46,973314	300m long lateral moraine E of Grades at southern valley side			
OCa4	24.07.2016	14,180529	46,850480	bridge over Gurk 600m W of Weitenfeld			7000l/s, D < cobbles
OCa5	24.07.2016	14,143678	46,850739	Gurk bridge at foot of Braunsberg terrace			7000l/s, D < boulders, bed-rock incision
OCa6	24.07.2016	14,139814	46,852103	Gurk knick point 150m downstream of Glödnitztal junction			7000l/s, bed-rock
OCa7	24.07.2016	14,073772	46,824212	Sirnitz knick point, 100m upstream from Gurk	phyllitic hard-rock channel	(220/45) sf	200l/s, river bed: medium gravels - boulders
OCa8	24.07.2016	14,075116	46,816769	Enge Gurk knick point at tunnel, steep river slope, gorge		(245/40) sf	hard-rock channel
OCa9	24.07.2016	14,160414	46,858052	Mödringbach valley, very low slope, wavy surface			50l/s
OCa10	24.07.2016	14,23391	46,866235	Zweinitzenbach valley, low slope			60l/s
OCb1	31.09.2016	14,264138	46,977862	block (in-situ?) at road, 600m E of inner gorge near Grades		(348/31) sf	
OCb2	31.09.2016	14,189080	46,955363	fluviale cross-bedded sediments at S slope in upper Vellach valley			
OCc1	14.04.2017	14,640431	46,927330	Löllinggrabenbach, 5km W of Klippitztörl, outcrop 70x10m, EW	Qtz-mica-schist (70% Qtz, 30% Biotit), roofing 1-2m thick marble banks	(33,5/26) sf, (52/25) sf	
OCc2	14.04.2017	14,618107	46,921360	Löllinggrabenbach, 1km E of Lölling, steep knick point		downst. valley broad.	160l/s
OCc3	15.04.2017	14,341231	46,890446	Pirkerkogelbach, at knick point terrace remnants, which correlation with N Gurk valley side			1-1.5l/s, 70% gravel-cobble, 30% silt
OCc4	15.04.2017	14,340980	46,881229	Pirkerkogelbach upper valley, outcrop 1x1m outcrop (in-situ?)	Qtz-phyllite, strongly altered + foliated	(160/31) sf	
OCc5	15.04.2017	14,314239	46,903118	road outcrop Straßburg-Prekowa, 400m N of Herd, 5x2m, NW-SE	Qtz-phyllite, strongly altered + foliated	(252/15) sf	
OCc6	15.04.2017	14,296509	46,920430	road outcrop Straßburg-Prekowa, house Winklern, 3x1m	Qtz-phyllite	(336/15) sf	
OCc7	15.04.2017	14,313087	46,903522	50m S of OCc5	Qtz-phyllite	(346/15) sf	
OCc8	15.04.2017	14,317119	46,899109	road outcrop Straßburg-Prekowa, 150m downwards of Herd, NS	Qtz-phyllite, NB7	(242/15) sf	
OCc9	15.04.2017	14,250027	46,865089	2km downstream of Zweinitzen, fluviale sediments at construction side	strongly rounded, coarse sand to pebble, un-consolidated, un-sorted, Qtz, phyllites		
OCc10	15.04.2017	14,034173	46,793751	Leonhardsbach upper knick point, relief flattens remarkably	Qtz-phyllite		24l/s
OCc11	15.04.2017	14,027032	46,790020	Leonhardsbach 50m below Alpenbad St. Leonard, above kick point further flattening			
OCc12	15.04.2017	14,024233	46,789307	upper Leonhardsbach above Alpenbad, low relief and low slope			3l/s
OCc13	15.04.2017	14,029222	46,819595	road outcrop at junction Sirnitz-Stronbach east of a farm	Qtz-phyllite	(156/23) sf	

Table A.9.: Synopsis of field work data - part 1.

ref.	date	lon.	lat.	outcrop description	lithology	structures	hydrology
OCc13a	15.04.2017	14,035612	46,817261	Sirnitz valley, bridge at last farm, flat valley floor, upstream steep rise			15l/s
OCc14	15.04.2017	14,195690	46,850188	Weitenfeld Hauptstr., 5mx100m long, N-side	phyllite	(305/24) sf	
OCc15	16.04.2017	14,143470	46,850709	bridge at Braunsberg terrace foot, massive base with gravel-cobble terrace on top	green-schist, strongly foliated, 100m E, fluv. rounded cobbles	(234/35) sf	
OCc15a	16.04.2017	14,137807	46,839523	Braunsberg terrace at village	rounded, coarse sand – coarse gavel, green-schist, phyllites		
OCc15b	16.04.2017	14,135007	46,843895	Braunsberg terrace scarp			no permanent drainage visible
OCc16	16.04.2017	14,075022	46,816968	Enge Gurk knick point at tunnel, steep slope, gorge – revisited			
OCc17	16.04.2017	14,079465	46,802683	Severgraben bridge across Gurk, „Severgraben Naturdenkmal“			4800l/s
OCc18	16.04.2017	14,082292	46,778835	Fuchsgruben village, potential old Gurk river bed when Gurk drained through Wimitz valley			5-8l/s
OCc19	16.04.2017	14,037934	46,748942	Himmelberg, bridge across Peiningbach, deeply incised			100l/s
OCc20	16.04.2017	13,922292	46,795273	Zedlitz village, bridge across Görzbach			20l/s
OCc21	16.04.2017	13,945547	46,809803	Görzbach road leaves valley floor, parking lot, below knick point			steep slope at lower valley compared to Sirnitz side
OCc22	16.04.2017	13,948245	46,809963	Görzbach valley floor 100m to the E from parking lot			slope decreases, steep V-valley
OCc23	16.04.2017	13,951165	46,809608	Görzbach valley floor 200m to the E from parking lot			steep V-valley
OCc24	16.04.2017	13,953493	46,809662	road above Görzbach in Görzwinkel, close to last houses			steep V-valley but low slope
OCc25	16.04.2017	13,959013	46,809895	road 100m past last houses, outcrop 2x5m, EW	phyllite, strongly altered, foliated and faulted, NB1	(30/40) sf, (23/15) sf	
OCc26	16.04.2017	13,973909	46,818971	road 100m uphill after N-turn, outcrop 2x5m at sideway to E	porphyry (basaltic?) material, weakly foliated, strongly faulted, black-grey colour (100m uphill to pass green-schist cobbles), NB2	(64/60) fp?, (280/20) fp?	
OCc27	16.04.2017	14,028985	46,790791	Leonhardsbach revisited (in-situ?)	phyllite, strongly folded, NB3, NB4	(10/30) sf?, (145/45) sf	
OCc28	16.04.2017	14,043926	46,813095	road at junction Leonhardsbach-Sirnitz, outcrop 20x3m, EW	phyllite, fine grained weakly metamorphic but strongly folded, NB5		
OCc29	16.04.2017	14,032634	46,831463	Hochrindlbach lower, 200m below Unterdörfl, road dead end	leucocratic phyllite, strongly deformed, NB6	(165/45) sf?	
OCc30	17.04.2017	14,392524	46,846397	Zabersdorfbach at Unterburg	sand-pebbles with soil fraction		70l/s, low slope

Table A.10.: Synopsis of field work data - part 2.

ref.	date	lon.	lat.	outcrop description	lithology	structures	hydrology
OCc31	17.04.2017	14,371218	46,877063	panorama view at St. Florian church			high altitude palaeo-surface at Wimitz valley
OCc32	17.04.2017	14,379398	46,820563	Wimitz at power station, Spitz village			70l/s?? dam area
OCc33	17.04.2017	14,340139	46,841530	Wimitz upstream of large moraine, gorge, vertical side valley slope	phyllite, foliated, NB8	(262/24) sf	320l/s
OCc34	17.04.2017	14,291176	46,837871	Wimitz to Pisweg connection road, 20-50x4m, EW, 50m above valley floor	phyllite + marble banks	(335/15) sf, (332/34) sf	
OCc35	17.04.2017	14,258135	46,820889	4km upstream of Wimitz from junction with Pisweg side-road, 2 farms	compact foliated phyllite, some faults	(106/33) sf, (82/35) sf, (112/28) sf	
OCc36	17.04.2017	14,231457	46,821598	Wimitz knick point at Granaschmied bridge, steep rock wall to the S, 100m long section			60l/s
OCc37	17.04.2017	14,211517	46,812465	Wimitz 1km upstream of Steinbichl junction, outcrop N of road, 15x5-8m, EW	phyllite, strongly folded and deformed	(302/26) sf, (283/21) sf	
OCc38	17.04.2017	14,197988	46,804198	junction Wimitz-Frischengraben			15l/s, hanging valley
OCc39	17.04.2017	14,138008	46,793243	Wimitz-Bösenbach, below water barrier to the E at Niederwinklern			5-10l/s, 2 big slightly rounded rock blocks
OCc40	17.04.2017	14,141940	46,792988	lake E of Niederwinklern	strongly laminated and altered phyllites	(308/36) sf, 302/24) sf	
OCc41	17.04.2017	14,060167	46,919030	Glödnitz-Metnitz road, 1km S of junction to Flattnitz, high above valley floor	phyllite - mica-schist, Qtz-lenses, strongly foliated and altered, NB9	(245/21) sf, (243/28) sf	
OCc42	17.04.2017	14,033005	46,942680	Flattnitz main road, 50x10m, EW	mica-schist, bituminous smell, NB10	small drag folds l 5cm E vergent, sigma clasts → top E	
OCc43	17.04.2017	14,173950	46,976940	main road 600m to the E of Metnitz, northern side	phyllite, strongly deformed and altered, NB11	(48/20) sf, (55/28) sf	
OCc44	17.04.2017	14,156217	47,001175	road 200m upstream of Wöbring in Röttingbachgraben, 30x3m, NW-SO	phyllite	(290/16) sf, (332/22) sf, ecc with top SE n.faults	
OCc45	17.04.2017	14,147721	47,022737	bridge over Roettingbach 500m before pass			50l/s
OCc46	17.04.2017	14,154123	47,043640	1.5km downstream of pass			no visible surface flow
OCc47	17.04.2017	14,164667	47,055347	200m NE of Ortner farm, rock wall 30x10m in 20m above road to NW	phyllite, strongly folded and partly altered, NB13, NB14	(0/25) sf, (308/25) sf	

Table A.11.: Synopsis of field work data - part 3.

ref.	date	lon.	lat.	outcrop description	lithology	structures	hydrology
OCc48	17.04.2017	14,200338	47,074649	road outcrop 50x3m, NS, 50m upstream before junction with Lassnitzbach	phyllite, strongly folded, NB15	(312/45) sf, (325/40) sf	
OCc49	17.04.2017	14,179054	47,106468	road outcrop 6x1m, SW-NE at N side	Qtz-phyllite, slightly deformed	(180/25) sf, (190/20) sf	
OCd1	06.06.2017	14,271530	46,803900		thin section 1		
OCd2	06.06.2017	14,292530	46,806370		thin section 2		
OCd3	06.06.2017	14,297650	46,810680		thin section 3		
OCd4	06.06.2017	14,299977	46,816291		thin section 4		
OCd5	06.06.2017	14,298425	46,825308		thin section 5		
OCd6	06.06.2017	14,299635	46,818443		thin section 6		
OCd7	06.06.2017	14,305170	46,818658		thin section 7		
OCd8	06.06.2017	14,317670	46,818400		thin section 8		
OCd9	06.06.2017	14,326080	46,811520		thin section 9		
OCd10	06.06.2017	14,32619	46,797300		thin section 10		
OCe1	25.06.2017	14,159470	46,800189	Goggau, 50m into small side road to S, 8x1m, EW	Qtz-phyllite, orientated sample, WT1	(308/27) sf	
OCe3	25.06.2017	14,211274	46,812588	see OC37	phyllite, orientated sample, WT3	(302/35) sf	
OCe4	25.06.2017	14,288608	46,837373	see OC34	phyllite, orientated sample, WT4		
OCe5	25.06.2017	14,241500	46,802752	road outcrop 600m uphill of Steinbichl, 30x2m, NS, before pass	phyllite, orientated sample, WT5		
OCe6	25.06.2017	14,280480	46,803835	road outcrop at junction to side road to Dreifaltigkeit, 10x3m, NW-SE	phyllite, orientated sample, WT6		
OCf1	03.09.2017	14,076140	46,854401	first bridge (upstream direction) in Deutsch-Griffen town			1000-2000l/s
OCf2	03.09.2017	14,045892	46,877220	Griffenbach 100m before Sand, outcrop 30x15m, NS, 30m W of road	phyllite, strongly folded	(250/46) sf, (280/59) h, (235/35) L	
OCf3	03.09.2017	14,050932	46,874191	further 300m downhill at small house (Sandschmid), outcrop 10m above road	phyllite, strongly folded, fault systems parallel sf	(150/38) sf	
OCf4	03.09.2017	14,056895	46,871035	Tenzenberg 300m downhill, outcrop 20m above road,6x5m SW-NE	phyllite	(140/25) sf, (150/55) sf	
OCf5	03.09.2017	14,070788	46,855488	Deutsch-Griffen at side road junction to church, northern slope	phyllite, laminated in cm scale	(180/36) sf	
OCf6	03.09.2017	14,030430	46,869533	Rauschenenneggen 7, kick-turn to E, small outcrop 2x1m, uphill	phyllite	(155/32/ sf	
OCf7	03.09.2017	14,096079	46,847198	1.9km downhill from Deutsch-Griffen, outcrop E of road 150x5m, SO-NW	Qtz-phyllite, strongly foliated	(230/44) sf, (248/38) sf, (260/42) sf	

Table A.12.: Synopsis of field work data - part 4.

Bibliography

Aigner, A. (1922). Geomorphologische Beobachtungen in den Gurktaler Alpen. *Sb. Akad. Wiss. Wien, math.-nat. KI. A. I*, 131:243–278.

Aigner, A. (1924). Über tertiäre und diluviale Ablagerungen am Südfuße der Niederen Tauern. *Jahrbuch Geologische Bundesanstalt*, 74:179–196.

Appold, T. (1989). Tektonisch-metamorphe Entwicklung der Glimmerschiefergruppe auf ÖK-Blatt 186 St. Veit/Glan. *Arbeitstagung Geol. B.-A.*, pages 14–30.

Bartosch, T., Stüwe, K., and Robl, J. (2017). Topographic evolution of the Eastern Alps: The influence of strike-slip faulting activity. *Lithosphere*, 9(3):384–398.

Eaton, B. (2013). Hydraulic geometry: Empirical investigations and theoretical approaches. In Schroder, J. and Wolf, E., editors, *Treatise on Geomorphology*, 9, chapter 9.18, pages 313–329. Academic Press, San Diego, CA.

Ebner, F. and Sachsenhofer, R. F. (1995). Palaeogeography, subsidence and thermal history of the Neogene Styrian Basin (Pannonian basin system, Austria). *Tectonophysics*, 242:133–150.

Egholm, D., Nielsen, S., Pedersen, V., and Lesemann, J.-E. (2009). Glacial effects limiting mountain height. *Nature*, 460:884–887.

England, P. and Houseman, G. (1986). Finite strain calculations of continental deformation 2. comparison with the India-Asia collision zone. *Journal of Geophysical Research Atmospheres*, 91(B3):3664–3676.

England, P. and McKenzie, D. (1983). Correction to: a thin viscous sheet model for continental deformation. *Geophysical Journal of the Royal Astronomical Society*, 73:523–532.

Exner, C. (1949). Beitrag zur Kenntnis der jungen Hebung der östlichen Hohen Tauern. *Mitt. geograph. Ges. Wien*, 91.

Exner, C. (1989). Geologie des mittleren Lungaus. *Jahrbuch Geologische Bundesanstalt*, 132(1):7–103.

Exner, C., Hejl, E., and Mandl, G. W. (2005). Geologische Karte der Republik Österreich: 157 - Tamsweg. *GBA, ÖK 1:50.000*.

Faupl, P. and Wagreich, M. (2000). Late Jurassic to Eocene palaeogeography and geodynamic evolution of the Eastern Alps. *Mitt. Österr. Geol. Ges.*, 92.

Flügel, H. and Neubauer, F. R. (1984). Geologische Karte der Steiermark 1:200.000. *GBA*.

Frisch, W., Kuhlemann, J., and Dunkl, I. (2001). The Dachstein paleosurface and the Augenstein Formation in the Northern Calcareous Alps - a mosaic stone in the geomorphological evolution of the Eastern Alps. *Int. J. Earth Sci.*, 90:500–518.

Frisch, W., Kuhlemann, J., Dunkl, I., and Brügel, A. (1998). Palinspastic reconstruction and topographic evolution of the Eastern Alps during late Tertiary tectonic extrusion. *Tectonophysics*, 297:1–15.

Froitzheim, N., Schmid, S. M., and Conti, P. (1994). Repeated change from crustal shortening to orogen-parallel extension in the Austroalpine units of Graubünden. *Eclogae Geologicae Helvetiae*, 87:559–612.

Froitzheim, N., Schmid, S. M., and Frey, M. (1996). Mesozoic paleogeography and the timing of eclogite- facies metamorphism in the Alps: A working hypothesis. *Eclogae Geologicae Helvetiae*, 89(1):81–110.

Gawlick, H.-J., Frisch, W., Vecsei, A., Steiger, T., and Böhme, F. (1999). The change from rifting to thrusting in the Northern Calcareous Alps as recorded in Jurassic sediments. *Geologische Rundschau*, 87:644–657.

Genser, J., Cloetingh, S. A., and Neubauer, F. (2007). Late orogenic rebound and oblique Alpine convergence: New constraints from subsidence analysis of the Austrian Molasse basin. *Global and Planetary Change*, 58(1-4):214–223.

GeoServies-KAGIS (2015). Digitales 10m - Geländemodell aus Airborne ... http://gis.ktn.gv.at/OGD/Geographie_Planung/ogd-10m-at.zip.

GeoServies-KAGIS (2017). ArcGIS shapefiles of the 1:200.000 geological map of Carinthia. ArcGIS shapefiles. https://gis.ktn.gv.at.

Hack, J. (1957). Studies of longitudinal profiles in Virginia and Maryland. *U. S. Geol. Surv. Prof. Pap.*, 294-B.

Handy, M. R., Schmid, S. M., Bousquet, R., Kissling, E., and Bernoulli, D. (2010). Reconciling plate-tectonic reconstructions of Alpine Tethys with the geological–geophysical record of spreading and subduction in the Alps. *Earth-Science Review*, 102:121–158.

Hejl, E. (1997). 'Cold spots' during the Cenozoic evolution of the Eastern Alps: thermochronological interpretation of apatite fission-track data. *Tectonophysics*, 272:159–173.

Hejl, E. (1998). Über die känozoische Abkühlung und Denudation der Zentralalpen östlich der Hohen Tauern - eine Apatit-Spaltspuranalyse. *Mitteilungen Österreichische Geologische Gesellschaft*, 89:179–199.

Hergarten, S., Robl, J., and Stüwe, K. (2016). Tectonic geomorphology at small catchment sizes – extensions of the stream-power approach and the χ method. *Earth Surface Dynamics*, 4:1–9.

Hergarten, S., Wagner, T., and Stüwe, K. (2010). Age and Prematurity of the Alps Derived from Topography. *Earth and Planetary Science Letters*, 297:453–460.

Howard, A. D. and Kerby, G. (1983). Channel changes in badlands. *Geological Society of America*, 94:739–752.

Keil, M. and Neubauer, F. (2011). The Miocene Enns Valley basin (Austria) and the North Enns Valley fault. *Austrian Journal of Earth Sciences*, 104(1):49–65.

Kirby, E. and Whipple, K. (2001). Quantifying differential rock-uplift rates via stream profile analysis. *Geology*, 29(5):415–418.

Kirby, E., Whipple, K. X., Tang, W., and Chen, Z. (2003). Distribution of active rock uplift along the eastern margin of the Tibetan Plateau: Inferences from bedrock channel longitudinal profiles. *Journal of Geophysical Research*, 108(B4).

Kozur, H. (1991). The evolution of the Meliata-Hallstatt ocean and its significance for the early evolution of the Eastern Alps and Western Carpathians. *Palaeogeography, Palaeoclimatology, Palaeoecology*, 87:109–135.

Krenmayr, H., Pavlik, W., Bayer, I., and Schiegl, M. (2014). Geologische Karte der Republik Österreich: 185 - Straßburg. *GBA, GEOFAST 1:50.000*.

Kuhlemann, J., Dunkl, I., Brügel, A., Spiegel, C., and Frisch, W. (2006). From source terrains of the Eastern Alps to the Molasse Basin: Detrital record of non-steady-state exhumation. *Tectonophysics*, 413:301–316.

Kuhlemann, J. and Kempf, O. (2002). Post-Eocene evolution of the North Alpine Foreland Basin and its response to Alpine tectonics. *Geology*, 152:45–78.

Lacey, G. (1930). Stable channels in alluvium. *Inst. Civil Eng. Proc.*, 229:359–384.

Legrain, N., Dixon, J., Stüwe, K., von Blanckenburg, F., and Kubik, P. (2015). Post-Miocene landscape rejuvenation at the eastern end of the Alps. *Lithosphere*, 7(1):3–13.

Legrain, N., Stüwe, K., and Wölfer, A. (2014). Incised relict landscapes in the eastern Alps. *Geomorphology*, 221:124–138.

Leopold, L. B. and Maddock, T. (1953). The hydraulic geometry of stream channels and some physiographic implications. *US Geological Survey Professional Paper*, 252.

Linzer, H.-G., Decker, K., Peresson, H., Dell'Mour, R., and Frisch, W. (2002). Balancing lateral orogenic float of the Eastern Alps. *Tectonophysics*, 354:211–237.

Mandl, G. W. (2000). The Alpine sector of the Tethyan shelf - Examples of Triassic to Jurassic sedimentation and deformation from the Northern Calcareous Alps. *Mitt. Österr. Geol. Ges.*, 92:61–77.

Montgomery, D. R. and Korup, O. (2010). Preservation of inner gorges through repeated Alpine glaciations. *Nature Geoscience*, 4:62–67.

Neubauer, F., Cloetingh, S., Dinu, C., and Mocanu, V. (1997). Tectonics of the Alpine-Carpathian-Pannonian region: introduction. *Tectonophysics*, 272:93–96.

Neubauer, F. and Genser, J. (1990). Architektur und Kinematik der östlichen Zentralalpen - eine Übersicht. *Mitt. naturwiss. Ver. Steiermark*, 120:203–219.

Neubauer, F., Genser, J., and Handler, R. (2000). The Eastern Alps: Results of a two-stage collision process. *Mitt. Österr. Geol. Ges.*, 92:117–134.

Neubauer, F. and Pistotnik, J. (1984). Das Altpaläozoikum und Unterkarbon des Gurktaler Deckensystems (Ostalpen) und ihre paläogeographischen Beziehungen. *Geologische Rundschau*, 73(1):149–174.

Neumann, H. H. (1989). Die Oberkreide des Krappfeldes. *Arbeitstagung Geol. B.-A.*, pages 70–79.

Perron, J. T. and Royden, L. (2012). An integral approach to bedrock river profile analysis. *Earth Surface Processes and Landforms*, 38(6):570–576.

Pestal, G., Hejl, E., Egger, H., and Husen, D. V. (2005). Geologische Karte von Salzburg 1:200.000. *GBA*.

Pilger, A., Schönenberg, R., Fritsch, W., and Meixner, H. (1978). Geologische Karte der Republik Österreich: Saualpe. *GBA, ÖK 1:25.000*.

Pistotnik, J. (1976). Ein Transgressionskontakt des Stangalm-Mesozoikums. *Carinthia II*, 166(86):127–131.

Rantitsch, G. and Russegger, B. (2000). Thrust-related very low grade metamorphism within the Gurktal Nappe Complex (Eastern Alps). *Jahrbuch Geologische Bundesanstalt*, 142(2):219–225.

Ratschbacher, L., Frisch, W., and Linzer, H.-G. (1991). Lateral extrusion in the Eastern Alps, part 2: Structural analysis. *Tectonics*, 10(2):257–271.

Reinecker, J. (2000). Stress and deformation: Miocene to present-day tectonics in the Eastern Alps. *Tübinger Geowissenschafliche Arbeiten, Reihe A*, 55.

Robl, J., Heberer, B., Prasicek, G., Neubauer, F., and Hergarten, S. (2017). The topography of a continental indenter: The interplay between crustal deformation, erosion, and base level changes in the eastern Southern Alps. *Journal of Geophysical Research: Earth Surface*, 122:1–25.

Robl, J., Prasicek, G., Hergarten, S., and Stüwe, K. (2015). Alpine topography in the light of tectonic uplift and glaciation. *Global and Planetary Change*, 127:34–49.

Robl, J., Stüwe, K., Hergarten, S., and Evans, L. (2008). Extension during continental convergence in the Eastern Alps: The influence of orogen-scale strike-slip faults. *Geology*, 36(12):963–966.

Rocky Austria, Geologische Bundesanstalt (2013). Der Alpenraum zum Höhepunkt der letzten Eiszeit - Posterkarte.

Royden, L. and Perron, J. T. (2013). Solutions of the stream power equation and application to the evolution of river longitudinal profiles. *Journal of Geophysical Research: Earth Surface*, 118:497–518.

Schmid, S. M., Bernoulli, D., Fügenschuh, B., Matenco, L., Schefer, S., Schuster, R., Tischler, M., and Ustaszewski, K. (2008). The Alpine-Carpathian-Dinaridic orogenic system: correlation and evolution of tectonic units. *Swiss J. Geosci.*, 101:139–183.

Schmid, S. M., Fügenschuh, B., Kissling, E., and Schuster, R. (2004). Tectonic map and overall architecture of the Alpine orogen tectonic map and overall architecture of the Alpine orogen. *Eclogae geol. Helv.*, 97:93–117.

Schuster, R., Scharbert, S., Abart, R., and Frank, W. (2001). Permo-Triassic extension and related HT/LP metamorphism in the Austroalpine - Southalpine realm. *Mitt. Ges. Geol. Bergbaustud. Österr.*, 45:111–141.

Schwanghart, W. and Kuhn, N. J. (2010). Topotoolbox: A set of Matlab functions for topographic analysis. *Environmental Modelling & Software*, 25:770–781.

Spiegel, C., Kuhlemann, J., Dunkl, I., and Frisch, W. (2001). Paleogeography and catchment evolution in a mobile orogenic belt: the Central Alps in Oligo–Miocene times. *Tectonophysics*, 341:33–47.

Spreitzer, H. (1932). Zum Problem der Piedmonttreppe. *Mitt. Geograph. Ges. Wien*, 75:327–364.

Stampfli, G. M. (1996). The Intra-Alpine terrain: A Paleotethyan remnant in the Alpine Variscides. *Eclogae geol. Helv.*, 89(1):13–42.

Stampfli, G. M., Mosar, J., Marquer, D., Marchant, R., Baudin, T., and Borel, G. (1998). Subduction and obduction processes in the Swiss Alps. *Tectonophysics*, 296:159–204.

Stüwe, K. (2007). *Geodynamics of the Lithosphere*. Springer-Verlag, 2 edition.

Stüwe, K. and Schuster, R. (2010). Initiation of subduction in the Alps: Continent or ocean? *Geological Society of America*, 32(2):175–178.

Thiedig, F., Husen, D. V., and Pistotnik, J. (1999). Geologische Karte der Republik Österreich: 186 - Sankt Veit an der Glan. *GBA, ÖK 1:50.000*.

Van Husen, D. (1987). Die Ostalpen in den Eiszeiten. Geologische Bundesanstalt, Wien.

Van Husen, D. (2011). Quaternary glaciations in Austria. In Ehlers, J., Gibbard, P. L., and Hughes, P. D., editors, *Development in Quarternary Sciences*, 15, chapter 2, pages 15–28. Elsevier.

Van Husen, D. (2012). Zur glazialen Entwicklung des oberen Gurktales. *Jb. Geol. B.-A.*, 152(1-4):39–56.

Von Gosen, W., Haiges, K.-H., Neubauer, F., Pistotnik, J., and Thiedig, F. (1985). Die tektonischen Baueinheiten am Nord- und Westrand der Gurktaler Decke (Österreich). *Jahrbuch Geologische Bundesanstalt*, 127(4):693–699.

Von Gosen, W., Pistotnik, J., and Schramm, J.-M. (1987). Schwache Metamorphose in Gesteinsserien des Nockgebietes und im Postvariszikum des Karawankenvorlandes (Ostalpen, Kärnten). *Jb. Geol. B.-A.*, 130(1):31–36.

Von Raumer, J. F., Stampfli, G. M., Arenas, R., and Martinez, S. S. (22015). Ediacaran to Cambrian oceanic rocks of the Gondwana margin and their tectonic interpretation. *Int. J. Earth Sci.*, 104:1107–1121.

Wagner, T., Fabel, D., Fiebig, M., Häuselmann, P., Sahy, D., Xu, S., and Stüwe, K. (2010). Young uplift in the non-glaciated parts of the Eastern Alps. *Earth and Planetary Science Letters*, 295:159–169.

Wagner, T., Fritz, H., Stüwe, K., Nestroy, O., Rodnight, H., Hellstrom, J., and Benischke, R. (2011). Correlations of cave levels, stream terraces and planation surfaces along the river Mur—Timing of landscape evolution along the eastern margin of the Alps. *Geomorphology*, 134:62–78.

Weiss, E. H. (1977). Zur Hydrogeologie des Grundwasseraustrittes der Gurk unterhalb der Prekowa (Tiebelursprung). *Carinthia II*, 167(87):95–104.

Whipple, K. X., Snyder, N. P., and Dollenmayer, K. (2000). Rates and processes of bedrock incision by the Upper Ukak River since the 1912 Novarupta ash flow in the Valley of Ten Thousand Smokes, Alaska. *Geology*, 28(9):835–838.

Whipple, K. X. and Tucker, G. E. (1999). Dynamics of the stream-power river incision model: Implications for height limits of mountain ranges, landscape response timescales, and research needs. *Journal of Geophysical Research: Earth Surface*, 104(B8):17,661–17,674.

Whipple, K. X., Wobus, C., Kirby, E., Crosby, B., and Sheehan, D. (2007). New tools for quantitative geomorphology: Extraction and interpretation of stream profiles from digital topographic data. *topographic data; Short Course presented at the Geological Society of America Annual Meeting, Denver, CO.*

WMS Service, Geologische Bundesanstalt (2017). Projekte onegeology, 1ge_gba_500k_surface_geology.

Wobus, C., Whipple, K. X., Kirby, E., Snyder, N., Johnson, J., Spyropolou, K., Crosby, B., and Sheehan, D. (2006). Tectonics from topography: Procedures, promise, and pitfalls. *Geological Society of America*, Special Paper 398:55–74.

Wölfler, A., Kurz, W., Fritz, H., and Stüwe, K. (2011). Lateral extrusion in the Eastern Alps revisited: Refining the model by thermochronological, sedimentary, and seismic data. *Tectonics*, 30:1–15.

Wölfler, A., Stüwe, K., Danisik, M., and Evans, N. J. (2012). Low temperature thermochronology in the Eastern Alps: Implications for structural and topographic evolution. *Tectonophysics*, 541-543:1–18.

Zeilinger, G., Kuhlemann, J., Reinecker, J., Kazmer, M., and Frisch, W. (1999). Das Tamsweger Tertiär im Lungau (Österreich): Fazies und Deformation eines intramontanen Beckens. *N. Jb. Geol. Paläont. Abh.*, 214(3):537–569.